TESIS DE LA UNIVERSIDAD DE ZARAGOZA

2024

121

Francisco Javier Esteras Saz

Destilación osmótica con membranas para una desalcoholización parcial de vino y cerveza más eficiente y sostenible

Director/es

Coronas Ceresuela, Joaquín Juan

De La Iglesia Pedraza, Óscar

ISSN 2254-7606

Prensas de la Universidad Universidad Zaragoza

Universidad de Zaragoza
Servicio de Publicaciones

ISSN 2254-7606

Universidad Zaragoza
1542

Tesis Doctoral

DESTILACIÓN OSMÓTICA CON MEMBRANAS PARA UNA DESALCOHOLIZACIÓN PARCIAL DE VINO Y CERVEZA MÁS EFICIENTE Y SOSTENIBLE

Autor

Francisco Javier Esteras Saz

Director/es

Coronas Ceresuela, Joaquín Juan
De La Iglesia Pedraza, Óscar

UNIVERSIDAD DE ZARAGOZA
Escuela de Doctorado

Programa de Doctorado en Ingeniería Química y del Medio Ambiente

2023

UNIVERSIDAD DE ZARAGOZA

Escuela de Ingeniería y Arquitectura

Área de Ingeniería Química

Departamento de Ingeniería Química y Tecnologías del Medio Ambiente

TESIS DOCTORAL

Destilación osmótica con membranas para una desalcoholización parcial de vino y cerveza más eficiente y sostenible

Memoria presentada por

Francisco Javier Esteras Saz

Graduado en Química, para optar al título de Doctor por la Universidad de Zaragoza

Febrero 2023

D. Joaquín Coronas Ceresuela, Catedrático de Universidad del Departamento de Ingeniería Química y Tecnologías del Medio Ambiente de la Universidad de Zaragoza, y D. Óscar de la Iglesia Pedraza, Profesor Contratado Doctor del Centro Universitario de la Defensa, centro adscrito a la Universidad de Zaragoza,

CERTIFICAN:

Que la Memoria de Tesis Doctoral titulada "Destilación osmótica con membranas para una desalcoholización parcial de vino y cerveza más eficiente y sostenible", presentada por D. Francisco Javier Esteras Saz, ha sido realizada bajo su dirección en el mencionado departamento y reúne los requisitos para ser presentada por su autor para optar al Grado de Doctor por la Universidad de Zaragoza.

Para que así conste, firma, la presente en Zaragoza, a 01 de febrero de 2023,

Fdo: Dr. Joaquín Coronas Ceresuela

Fdo: Dr. Óscar de la Iglesia Pedraza

A trasegar

Agradecimientos

El vino se trasiega durante su maduración para que evolucione potenciando aquellos matices que hacen de él un producto fresco, complejo y equilibrado. Como el vino, he trasegado por aquí y por allá en el límite entre la responsabilidad, el interés y la improvisación. Desde la química elemental de la interacción molecular hasta la más ingenieril de los procesos de separación. Con sinceridad admito que el trasiego que ahora me ahora da la oportunidad de escribir estos agradecimientos no estaba premeditado, ni siquiera soñado. Pero alguien se acordó de mí. Cuatro años después, echo la vista atrás con la ilusión de poder reconocer la importancia de las personas que me han acompañado en la persecución de mis propios matices.

Gracias a mis directores, por confiar en mí y darme la oportunidad de realizar esta Tesis Doctoral en su grupo de investigación; por vuestra dedicación y apoyo durante estos años, así como por todos los conocimientos transmitidos. Gracias Joaquín por mostrarme el nivel de auto-exigencia y capacidad con el que siempre se debería abordar la investigación, una valiosa visión de la ciencia que me llevo conmigo. Gracias además por darme la oportunidad de aprender y crecer más allá de lo que recojo en este trabajo. A Óscar, creo que un mero agradecimiento como director no alcanza para describir la paciencia, la entrega y la cercanía que has tenido conmigo. Muchas gracias por demostrar con hechos tu implicación, tanto personal como profesional, conmigo y mi trabajo.

A Carlos Téllez por su involucración durante todo este tiempo. Gracias por tu paciencia conmigo para discutir los resultados de este trabajo.

Gracias al grupo de investigación CREG, y a todas las personas que han pasado por él durante estos años. Marta y Cristina, empezamos a la vez este camino, y juntos poco a poco hemos crecido, cada uno con sus virtudes y sus peculiaridades. Con vosotras, el día a día se alargó más allá del laboratorio. Muchas gracias por vuestra compañía lejos de la investigación. A Lucas e Iñigo, gracias por alentarme a mejorar y seguir aprendiendo. Jose, muchas gracias por querer que los demás aprendamos, por tu apoyo y por tu ayuda más allá de este trabajo. Gracias al CREG de abajo. Esta historia se inició allí con el apoyo y la ayuda de Patricia y Javi, y, por supuesto, mi agradecimiento por su paciencia y disposición aún perdura. Gracias a todos, nos vemos en el próximo partido.

Un pequeño reconocimiento a cada una de las personas que, entre tiras y aflojas, han coincidido conmigo y forman también parte de esta historia.

Gracias por tu confianza en los matices que este trasiego podía potenciar en mí y no dejar que yo mismo la perdiera. Con cariño y paciencia, me has acompañado cada día

haciendo este camino algo más sencillo. Tu pasión por la ciencia me empujó a no dejar pasar la oportunidad de investigar, pero es la valentía que demuestras con tu ilusión, sin reservas, la que quiero destacar aquí. Cristina, haces mejor a la gente que tienes alrededor, y este trabajo es un ejemplo de ello. Gracias por ayudarme a ser un mejor investigador. Aguantamos estoicos ayudándonos a caminar, para volar sin ataduras.

A mi familia. Gracias por ofrecerme siempre la mejor versión de vosotros mismos. Un esfuerzo que no siempre he valorado como merece. Gracias por animarme a seguir, por confiar en mí, y por demostrarme una y otra vez que estáis a mi lado.

Índice

Índice de figuras

Índice de tablas

Abreviaturas y acrónimos

A	Membrane area (m^2)
C	Concentration ($g \cdot kg^{-1}$)
d	Diameter (m)
D	Effective diffusion ($m^2 \cdot s^{-1}$)
G	Mass of component (g)
Gz	Graetz number: $Gz = ReScd_h/L$ (dimensionless)
H	Henry Constant ($mol \cdot m^{-3} \cdot Pa^{-1}$)
HSP	Hansen solubility parameter ($MPa^{0.5}$)
J	Flux ($g \cdot s^{-1} \cdot m^{-2}$)
K	Mass transfer coefficient
K_f	Feed mass transfer coefficient ($m \cdot s^{-1}$)
K_G	Global mass transfer coefficient ($g \cdot m^{-2} \cdot s^{-1} \cdot Pa^{-1}$)
K_s	Stripping mass transfer coefficient ($m \cdot s^{-1}$)
K_m	Membrane mass transfer coefficient ($g \cdot m^{-2} \cdot s^{-1} \cdot Pa^{-1}$)
L	Effective length of module (m)
M	Molar weight ($g \cdot mol^{-1}$)
n	Number of hollow fibers
P	Pressure (bar)
Q	Flow rate ($mL \cdot min^{-1}$)
R_f	Feed mass transfer resistance ($s \cdot Pa \cdot g^{-1}$)
R_m	Membrane mass transfer resistance ($s \cdot Pa \cdot g^{-1}$)
R_s	Stripping mass transfer resistance ($s \cdot Pa \cdot g^{-1}$)
Re	Shell side Reynolds number: $Re = 4Q_i/\mu_i n\pi d_i$ (dimensionless)
R_g	Ideal gas constant (8.314 $J \cdot mol \cdot K^{-1}$)
Sc	Schmidt number: $Sc = D_i/v$ (dimensionless)
Sh	Sherwood number (dimensionless)
T	Temperature (K)
t	Time (s)
v	Molar volume ($cm^3 \cdot mol^{-1}$)
V	Volume (mL)
W	Weight (g)

Greek letters

$\boldsymbol{\delta}$	Membrane thickness (m)
$\boldsymbol{\delta_d}$	Dispersion force of Hansen solubility parameters ($MPa^{0.5}$)
$\boldsymbol{\delta_h}$	Specific interaction of Hansen solubility parameters ($MPa^{0.5}$)
$\boldsymbol{\delta_p}$	Polar interaction of Hansen solubility parameters ($MPa^{0.5}$)
$\boldsymbol{\varepsilon}$	Membrane porosity (dimensionless)
$\boldsymbol{\mu}$	Fluid viscosity (Pa·s)
$\boldsymbol{v}$	Kinematic viscosity: $v = \mu/\rho$ ($m^2 \cdot s^{-1}$)
$\boldsymbol{\rho}$	Fluid density ($kg \cdot m^{-3}$)
$\boldsymbol{\tau}$	Membrane tortuosity (dimensionless)
$\boldsymbol{v}$	Fluid velocity ($m \cdot s^{-1}$)
$\boldsymbol{\varphi}$	Variable in Eq. (3.13)
$\boldsymbol{\phi}$	Packing density (dimensionless)

Subscripts

a	Inner of the module
e	Effective
ex	External
Exp	Experimental
f	Feed phase
G	Global
h	Hydraulic
in	Inner
k	Knudsen
ln	Logarithm mean
m-air	Molecular in air
p	Pore membrane
s	Stripping phase
Theo	Theoretical

Superscripts

EtOH	Ethanol
i	Component
w	Water

Acronym

DPPH	2,2-Diphenyl-1-picrylhydrazyl
EBC	European Brewing Convention
EBC	European Brewing Convention
GHG	Greenhouse gases
IBU	International Bitterness Units
IWSR	International Wine and Spirits Research
OD	Osmotic distillation
OIV	Organización Internacional de la Viña y el Vino
PP	Polypropylene
PVDF	Polyvinylidene fluoride
PP	Polypropylene
PV	Pervaporación
RO	Reverse osmosis
SCC	Spinning cone column
SEM	Scanning electron microscopy
STM	Standard temperature and pressure
WCA	Water contact angle
YAN	Yeast assimilable nitrogen

Prólogo

La presente tesis doctoral que lleva por título “Destilación osmótica con membranas para una desalcoholización parcial de vino y cerveza más eficiente y sostenible” se ha desarrollado en el marco definido por el proyecto titulado “Aumento de la competitividad en el sector vitivinícola español mediante el diseño de nuevas técnicas de desalcoholización” con acrónimo ALCOHOLESS, proyecto financiado por: FEDER/Ministerio de Ciencia, Innovación y Universidades – Agencia Estatal de Investigación/ Proyecto (RTC-2017-6360, MCIN/AEI/10.13039/501100011033), entre cuyos objetivos principales se encuentra el desarrollo de una herramienta tecnológica de separación de etanol basada en el uso de membranas. Esto supone el desarrollo de un sistema de desalcoholización novedoso que permita responder a los retos derivados del procesado de vinos con altas graduaciones alcohólicas. Con este propósito, se ha llevado a cabo el diseño y montaje de dos plantas de separación por membranas a escala de laboratorio: una de destilación osmótica (OD) para reducir el grado alcohólico de los vinos, y otra de pervaporación (PV) para mejorar el rendimiento económico del proceso de desalcoholización. Este proyecto se enmarca dentro del reto R2 “Seguridad y calidad alimentarias; actividad agraria productiva y sostenible, recursos naturales, investigación marina y marítima”, integrado en el conjunto de retos globales establecidos del programa marco de i+D+i europeo HORIZON 2020. En el proyecto intervienen la entidad empresarial BODEGA MATARROMERA S.L., y la Universidad de Zaragoza (UZ), como centro de investigación pública. A su vez UZ está representada por dos grupos de investigación: el Laboratorio de Análisis de Aroma y Enología (LAAE) y el Grupo Catálisis, Membranas e Ingeniería del Reactor (CREG), donde se ha llevado a cabo esta tesis doctoral.

El grupo CREG se integra en el Departamento de Ingeniería Química y Tecnologías del Medio Ambiente (IQTMA) de la UZ y en Instituto de Nanociencia y Materiales de Aragón (INMA). Entre otras actividades, el CREG ha desarrollado su investigación en el campo de las membranas selectivas desde 1991, especializándose en la preparación y caracterización de membranas tanto inorgánicas como poliméricas, así como en su aplicación a separaciones en fase gas, reactores de membrana, nanofiltración y pervaporación, entre otros. En este contexto, el presente trabajo, apoyándose en la experiencia mencionada del grupo CREG en el campo de las membranas, ha facilitado el desarrollo de la destilación osmótica con membranas. Esto ha permitido abrir una nueva línea de investigación en el grupo, estudiando la aplicación de las membranas en la desalcoholización de bebidas (vino y cerveza) bajo condiciones suaves de presión y temperatura.

Resumen

La industria enológica ha observado en los últimos años cómo el cambio climático repercute en el ciclo fenológico de la vid y consecuentemente en la maduración de la uva, provocando en último término un aumento del grado alcohólico del vino. Un mayor grado alcohólico en el vino repercute negativamente en su aroma equilibrio e implica un mayor coste de exportación debido a las elevadas tasas impuestas sobre el etanol en muchos países. Además, se opone frontalmente a la creciente preocupación de los consumidores por cuidar sus hábitos alimentarios y por llevar un estilo de vida más saludable, dificultando su incorporación al mercado. Como respuesta, en los últimos años, se han desarrollado distintas estrategias que, para obtener un vino final con menor grado alcohólico, pueden llevarse a cabo durante cada una de sus etapas de producción: etapa pre-fermentativa, durante la fermentación y etapa pos-fermentativa. En fase de desarrollo, es la última estrategia la más estudiada, habiéndose evaluado diferentes tecnologías sobre el vino en su etapa pos-fermentativa, destacando la destilación, la evaporación, y la separación con membranas.

Una de las estrategias más prometedoras para la desalcoholización del vino es el uso de membranas para la retirada selectiva del etanol. Estas membranas se diferencian entre sí en la presión requerida para su funcionamiento y presentan la ventaja de operar eficientemente a temperatura ambiente, lo que minimiza el impacto sobre aquellos componentes del vino asociados con su perfil organoléptico, además de exigir un menor consumo de energía en comparación con otras tecnologías. En este sentido, la destilación osmótica (OD, de *osmotic distillation*) presenta la ventaja adicional de trabajar eficientemente a presión atmosférica gracias a que es la diferencia de presiones parciales entre las dos disoluciones separadas por una membrana hidrófoba la que define su capacidad de separación. Sin embargo, la alta volatilidad y el carácter poco polar de parte de los aromas del vino hacen que la OD presente, en ciertos aspectos, un impacto negativo sobre el vino. Además, desde el punto de vista industrial, su consumo de agua es considerado un inconveniente. En este trabajo se ha estudiado el potencial de la OD como técnica de desalcoholización parcial de vino, abarcando desde el conocimiento y desarrollo de sus fundamentos teóricos hasta el análisis de la influencia de las principales condiciones de operación. Asimismo, se ha propuesto una intensificación del proceso desde un punto de vista económico a través de la valorización por pervaporación con membranas de los residuos de la OD. Asimismo, se ha extendido la OD como técnica de desalcoholización a la industria cervecera.

Resumen

Se han identificado los fenómenos de transporte clásicos que intervienen en la trasferencia de componentes a través de la membrana, estudiando además la posible interacción componente-membrana. En conjunto, se ha desarrollado un modelo teórico-empírico capaz de predecir la influencia experimental de las condiciones de operación, como la relación de volumen y caudal de ambas fases o el grado de desalcoholización, sobre determinados componentes del vino. Este modelo incorpora un algoritmo de cálculo basado en el uso de los llamados parámetros de solubilidad de Hansen.

El estudio experimental de las variables de operación, incluyendo la temperatura y la composición inicial del vino, ha permitido optimar el tiempo experimental requerido y disminuir la pérdida de aromas durante el proceso de OD, especialmente de aquellos más volátiles y menos polares. Se ha visto que una mayor fuerza impulsora inicial para los aromas no se traduce en mayores porcentajes de pérdida, facilitando la selección de aquellos vinos más idóneos de ser tratados por OD. En relación al papel de las membranas, los resultados han demostrado que sus características estructurales tienen una influencia limitada sobre la eficiencia del proceso. Sin embargo, se ha obtenido vino parcialmente desalcoholizado con un perfil organoléptico muy similar al original al cambiar la composición de membrana. En concreto, una membrana de PVDF con tratamiento superficial para incrementar su carácter hidrófobo, con efecto “lotus”, preservó mejor su capacidad selectiva, manteniendo la diferencia de presión parcial como única fuerza impulsora, y favoreciendo la retención de aquellos componentes menos concentrados.

En referencia al consumo de agua, se ha desarrollado una solución que combina la OD con otra tecnología de membrana: la pervaporación (PV). La PV se focaliza en el tratamiento de la corriente de extracción que se genera en el proceso de desalcoholización (considerada generalmente como un residuo), con una concentración insuficiente de etanol para alcanzar cierto valor añadido (en función del grado alcohólico objetivo), pero suficiente para impedir su reutilización. El doble tratamiento de la corriente hidroalcohólica por PV, hidrófoba e hidrófila de manera consecutiva, ha permitido reutilizar la corriente de extracción en desalcoholizaciones posteriores sin repercusión negativa añadida sobre el vino, a la par que el etanol extraído del vino se concentra hasta generar bioetanol (>99 % en peso) de alto valor añadido.

El estudio de la capacidad de desalcoholización de la OD se ha completado con otra matriz alcohólica, la cerveza, y otro grado de desalcoholización, -50 % del grado alcohólico inicial, obteniendo una cerveza parcialmente desalcoholizada con un grado alcohólico de 2.5 v/v%. Esta graduación la define en el mercado americano como *una light beer*, y su interés radica en el esperado aumento de la preservación de los

compuestos de la cerveza original como consecuencia del menor gradiente de presiones parciales necesario para alcanzar ese grado de desalcoholización, en comparación con el exigido para la desalcoholización total del producto. Asimismo, las variables de operación previamente establecidas se han re-evaluado en base a esta nueva matriz y grado de desalcoholización, estudiando su influencia sobre los parámetros de calidad típicamente utilizados en la industria cervecera. Estos parámetros, que aseguran unos atributos específicos de calidad, han permitido una comparación cualitativa de la *light beer* obtenida en esta Tesis Doctoral frente al conjunto de cervezas totalmente desalcoholizadas cuyos parámetros de calidad se recogen en literatura.

CAPÍTULO 1

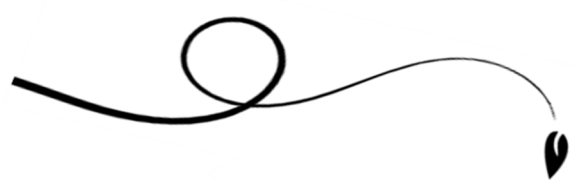

INTRODUCCIÓN

1.1 SITUACIÓN ACTUAL DE LA VITICULTURA

1.2 ESTRATEGIAS DE DESALCOHOLIZACIÓN

1.3 DESALCOHOLIZACIÓN PARCIAL DE BEBIDAS ALCOHÓLICAS

1 Introducción

1.1 Situación actual de la viticultura

1.1.1 Cambio climático

El crecimiento de la población y de los niveles promedio de consumo social han conducido a un incremento en la necesidad de recursos, causando impactos globales sobre el planeta. Uno de estos impactos es el incremento de las emisiones de los gases de efecto invernadero (GHG, de *greenhouse gases*), que contribuyen al calentamiento de la Tierra [1–4]. Este proceso, conocido como cambio climático, se define como la variación en el clima a consecuencia directa o indirecta de la actividad humana, que resulta en la variación de la composición atmosférica en diversos gases, pero que sobre todo se centra en el CO_2, cuya concentración se prevé que alcance las 500 ppm antes de final de siglo [5]. La relación de las emisiones de GHG con el cambio climático, y a su vez a con alteraciones en el clima de la Tierra, se acepta por la mayor parte de la comunidad internacional [6–8], evidenciándose en el incremento de la temperatura del aire y de los océanos, en el deshielo de los casquetes polares, así como en la variación del ciclo hidrológico [9]. Además, se espera un agravamiento de la situación con incrementos de la temperatura media de 1 °C cada 20 años, el doble de lo aumentado los últimos 100 años [10]. Estos datos corresponden al promedio obtenido en el conjunto del planeta, pero el efecto del cambio climático no es homogéneo en toda su superficie, siendo en las regiones cálidas donde se registran o podrán registrarse incrementos de temperatura más acusadas [11].

Al ser una de las zonas europeas más cálidas, no sorprende que España se encuentre entre las regiones que pude sufrir un mayor impacto en lo que se refiere a incremento de temperatura y escasez de agua [12], habiendo presentado un aumento medio en 1,5 °C en su temperatura media durante en el siglo XX [13]. Esto supone que el impacto del cambio climático sobre la agricultura sea una de las mayores preocupaciones de los productores españoles, entre los que destacan los vinicultores [14,15].

El clima influye notablemente en la fisiología de la vid, y factores como la temperatura y la lluvia determinan la calidad de la cosecha y la productividad del viñedo. Por ejemplo, las cosechas de 2018 y 2019 se caracterizaron por una temperatura elevada y prolongadas sequías, provocando en la uva una disminución de nitrógeno asimilable por las levaduras durante la posterior fermentación (YAN, de *yeast assimilable nitrogen*) y un aumento de azucares y pH, repercutiendo en la calidad final de los vinos [16]. Además, el incremento de la temperatura influye en el crecimiento de la vegetación, cuyas consecuencias más evidentes son la diminución del peso de la baya

y del racimo ya que se detiene el crecimiento de la superficie foliar, aumentando la sobreexposición de los racimos, así como la respiración y evapotranspiración [17]. Sin embargo, es el efecto del cambio climático sobre el ciclo vegetativo de la vid el mayor responsable de las alteraciones observadas en las cosechas de los últimos años y, por tanto, en las características de lo los vinos resultantes. El ciclo vegetativo de la vid se muestra en la Fig. 1.1.

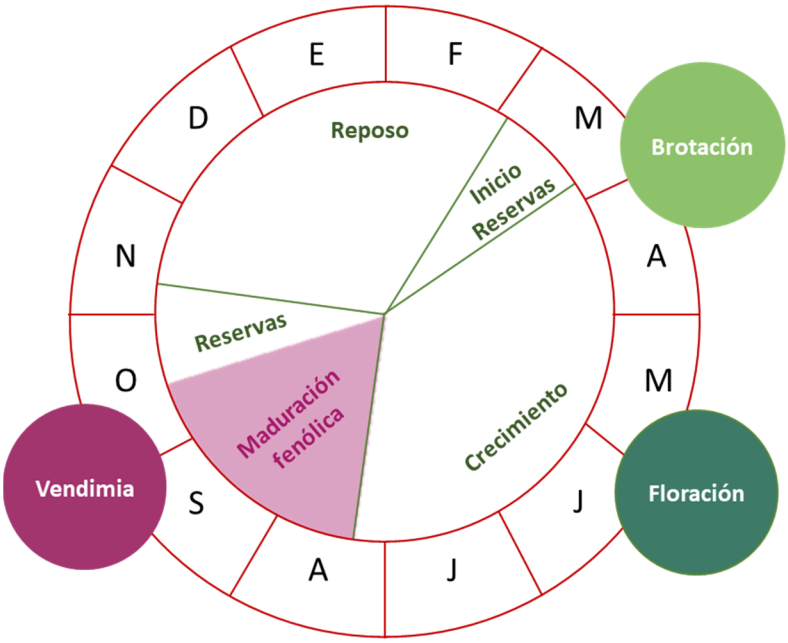

Fig. 1.1 Ciclo vegetativo de la vid.

El incremento de la temperatura induce el adelanto de la fecha de brotación y la ampliación del periodo activo de crecimiento de la vid, lo que provoca a su vez el adelanto de las diferentes fases de su ciclo biológico. Este desajuste se traduce en un inicio cada vez más precoz de la maduración fenólica, lo que determina la composición de la uva y, por extensión, de los vinos resultantes.

Durante la maduración fenólica se incrementa la cantidad de agua y de azucares, sales minerales, aminoácidos (YAN, mencionados previamente) y compuestos fenólicos (como taninos y antonianos). Además, decae la concentración de aminas y de ácidos orgánicos debido a su combustión durante la respiración de la uva. Cuando la concentración de azúcares en la uva es máxima se considera que se ha alcanzado la madurez industrial. Este es el momento que históricamente se ha considerado como idóneo para vendimiar (ver Fig. 1.2). Sin embargo, el adelanto de la maduración fenólica produce un desajuste con la madurez industrial, lo que se traduce en la obtención de mostos con características no deseables para la producción de vinos.

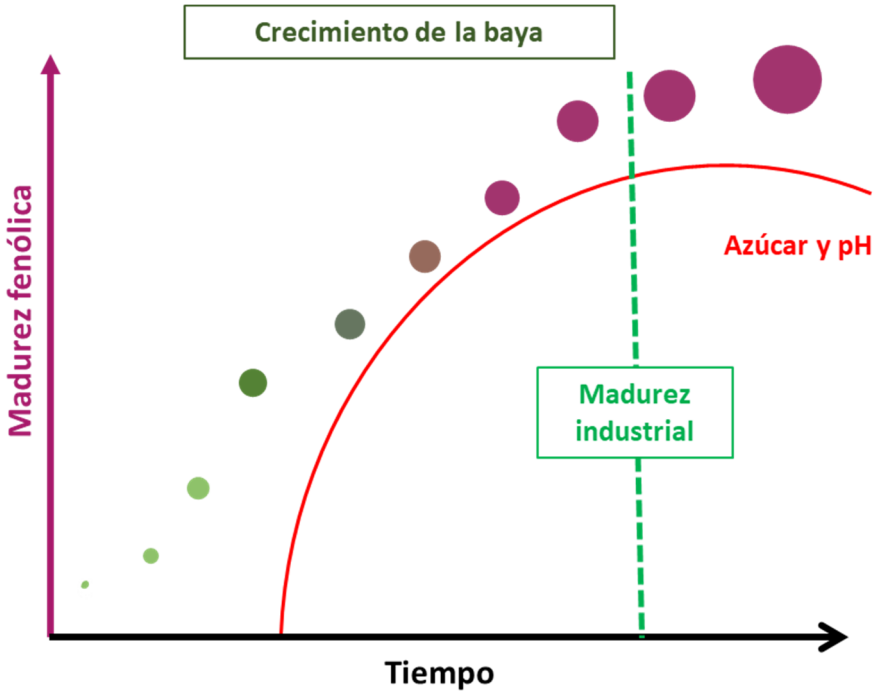

Fig. 1.2 Madurez fenólica e industrial de la uva.

En las condiciones mencionadas, las uvas vendimiadas presentan una elevada concentración de azucares y una baja acidez. Además, estas variaciones en los tiempos de maduración pueden disminuir el desarrollo de compuestos fenólicos, bien por influir sobre el proceso de síntesis durante la maduración, bien por no alcanzarse la maduración suficiente de los mismos. Todo esto se traduce en vinos con un contenido alcohólico mayor, más inconsistentes y susceptibles de sufrir fenómenos de oxidación y con menor aroma y color [18,19].

1.1.2 Tendencia actual de consumo

Históricamente, el vino, especialmente el tinto, se ha relacionado con un consumo selecto y un producto de calidad, proporcionándole un alto valor mercantil. Vinos de gran concentración y armonía se han valorado positivamente, siendo para ello indispensable que la uva alcance un grado de madurez aromática y fenólica óptimo [20].

Con la prioridad de mantener su alto perfil organoléptico, no es de extrañar que el grado alcohólico medio de los vinos tintos españoles se haya incrementado en los últimos años, sobrepasando en la mayoría de ellos los 14 grados de alcohol. Este incremento en el grado repercute negativamente en el producto final, ya que disminuye su calidad al afectar a la percepción de atributos como acidez, dulzor, astringencia, aroma y sabor, dando lugar a sensaciones más cálidas y pesadas [21–23]. Además, el

mayor contenido en etanol incrementa la solubilidad de los compuestos volátiles en el vino [22,24], lo que enmascara el propio perfil especifico de cada variedad de vino.

Por otro lado, la industria vinícola se enfrenta a la creciente preocupación por parte del consumidor de cuidar sus hábitos alimentarios y llevar una vida más saludable. Por todo ello, no es extraño que los consumidores se vean desalentados a adquirir estos vinos de mayor graduación, y demanden un producto equilibrado que se alinee con esta tendencia. No sorprende, por tanto, que entre las 5 predicciones formuladas para 2022 por la prestigiosa compañía Wine Intelligence (www.wineintelligence.com, accedido el 26 de enero de 2023) se incluyera el desarrollo de una nueva subcategoría de vino servido en un formato portátil (en lata) y de formulación baja en etanol, transformando el concepto de vino tradicional hacia una bebida espumosa a base de vino, denominada Wine seltzer, cuyo crecimiento en el mercado se prevé exponencial para 2023 según International Wine and Spirits Research (IWSR), la principal base de datos de bebidas alcohólicas (IWSR, 2022).

Por último, es evidente que el vino no está exento de los impuestos aplicados sobre las bebidas alcohólicas, cuya recaudación media en Europa se encuentra cerca del 1 % del total de ingresos tributarios (Taxes in Europe, Database), y que un incremento del grado alcohólico se traduce en una mayor presión fiscal. Por ejemplo, el tipo impositivo en España queda fijado en 38,48 € por hectolitro/grado alcohólico si la bebida no supera los 15 grados de alcohol, mientras que en caso contrario asciende a 64,13 €.

Para afrontar este nuevo escenario producido por el cambio climático, el surgimiento de nuevos mercados y el cambio de preferencias de los consumidores, el sector enológico demanda estrategias de desalcoholización capaces de responder en tiempo y forma, sin devaluar la imagen del vino de producto de calidad, alejándose del concepto de "*ready to drink*" [25].

1.2 Estrategias de desalcoholización

En los últimos años se han desarrollado distintas estrategias enológicas para obtener un vino que cumpla las expectativas de calidad esperadas con un menor grado alcohólico. Estas técnicas pueden clasificarse de acuerdo a la etapa de producción del vino sobre la que pueden actuar: reduciendo la acumulación de azúcar en la uva durante su crecimiento (pre-fermentativa), limitando el rendimiento de la conversión de azúcar en etanol (durante la fermentación) y separando el etanol del resto del vino ya acabado (pos-fermentativa). En la Fig. 1.3 se muestra una clasificación general de las estrategias según dicho criterio.

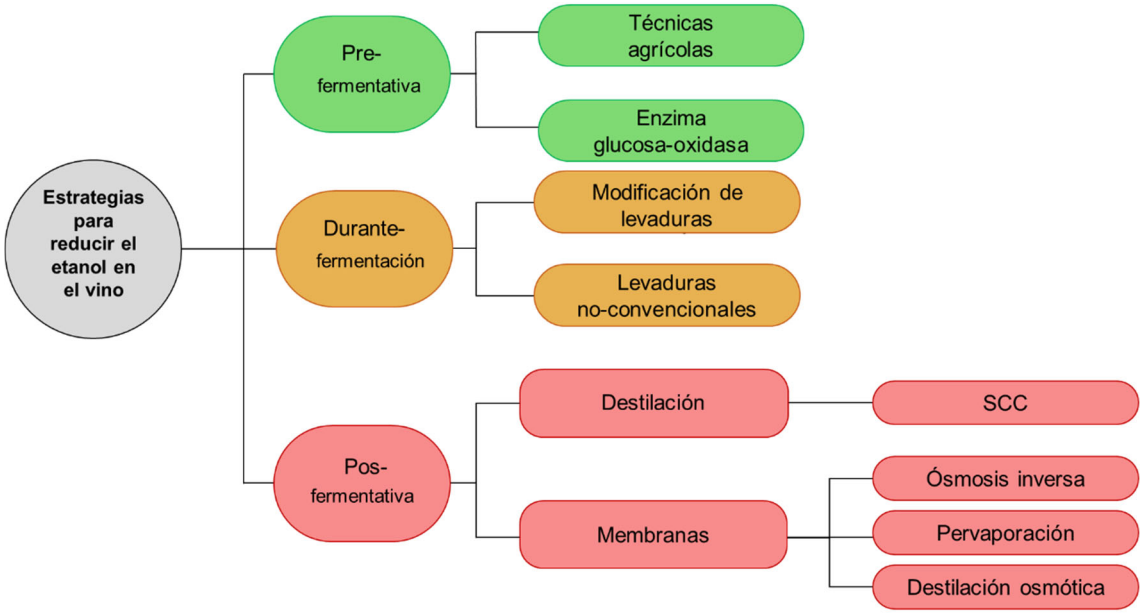

Fig. 1.3 Estrategias para reducir el contenido de etanol en la industria vinícola.

Las estrategias pre-fermentativas son muy variadas e incluyen desde aquellas que se basan en el uso de las técnicas de cultivo, como sistemas de poda o técnica de riego [26–35] hasta la adicción de enzimas para disminuir la conversión de glucosa a etanol durante la fermentación alcohólica [36–38]. Sin embargo, hasta ahora este tipo de estrategias han presentado diferentes inconvenientes que frenan su implantación industrial. Por ejemplo, si bien es cierto que las técnicas de poda influyen notoriamente en la acumulación de glucosa en la uva, y por extensión de etanol en el vino, también disminuyen la aparición de compuestos fenólicos deseados, además de afectar, generalmente de forma negativa, a la calidad de la uva [39–41]. Por otro lado, se ha reportado que la adicción de enzimas como la glucosa oxidasa, que permite alcanzar reducciones significativas de la contracción de etanol en vino, resulta en vinos más ácidos y menos afrutados [19,42,43].

El uso de levaduras modificadas genéticamente para reducir el contenido de alcohol en el vino o para favorecer el metabolismo del carbono hacia otros productos. disminuyendo la concentración de etanol, se engloban dentro de las estrategias que se aplican durante la fermentación de la uva. Sin embargo, el efecto de estas levaduras no convencionales parece estar lejos de controlarse completamente, dando lugar en muchas ocasiones a compuestos no deseados, como acetatos, acetaldehído y acetoína [44,45].

Finalmente, las estrategias pos-fermentativas son aquellas que permiten reducir el contenido de etanol en los vinos mediante procesos de transferencia de materia y, sin

duda, son las más estudiadas hasta ahora. De hecho, algunas tecnologías, como las columnas de conos rotatorios o la ósmosis inversa, ya se han implementado a nivel industrial y su uso está regulado de acuerdo a las normas de la Organización Internacional de la Viña y el Vino (OIV) (OIV-OENO-373-B-2010).

1.2.1 Tecnologías de destilación

Las columnas de conos rotatorios (SCC, de *spinning cone column*) se han probado en procesos de desalcoholización por bodegas como Bodega Torres, Freixenet o Codorníu. Consisten fundamentalmente en una columna de acero inoxidable con un eje central giratorio al que está soldada una serie de conos invertidos, mientras que en la pared del recipiente hay a su vez soldados otros conos estáticos superpuestos. El vino se alimenta por la parte superior del recipiente que contiene la columna de conos mojando las superficies cónicas, lo que aumenta la superficie de contacto y facilita la evaporación de los aromas y del etanol, favorecida por las condiciones de vacío y temperatura a las que se lleva a cabo el proceso [46–48]. En la desalcoholización por SCC se suelen distinguir dos etapas de trabajo. Inicialmente se obtiene un concentrado de los aromas del vino alimentado que evaporan en la superficie de los conos (más volátiles que el etanol) y el consecuente vino desaromatizado. Este vino pobre en aromas se somete a una segunda etapa a mayor temperatura para evaporar, de manera análoga a los aromas, el etanol. El vino desalcoholizado que se obtiene es el resultado de mezclar el concentrado en aromas y el vino desaromatizado y posteriormente desalcoholizado, y puede alcanzar un grado alcohólico muy bajo (menos de 0,5 % en volumen) (Ver Fig. 1.4).

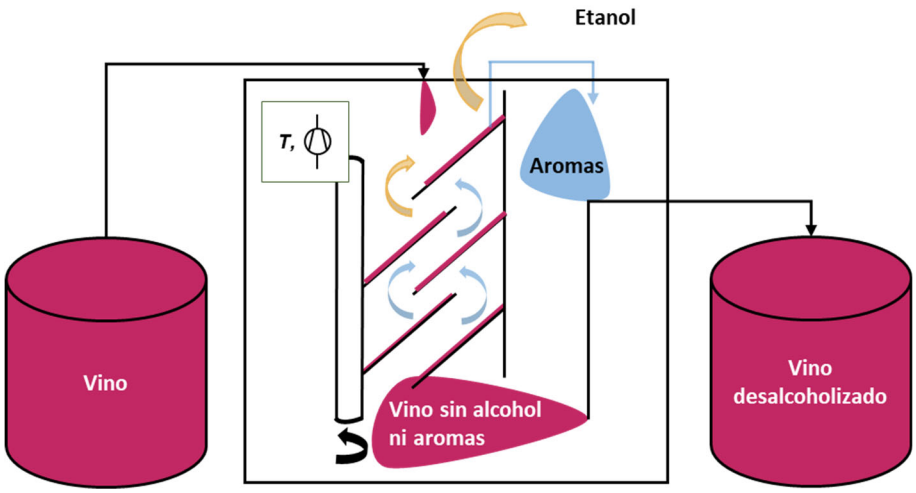

Fig. 1.4 Esquema de un proceso de desalcoholización con una columna de conos rotatorios.

Sin embargo, las condiciones de temperatura y presión de vacío requeridas para desalcoholizar por SCC repercuten negativamente en la calidad organoléptica del vino y encarecen los costes de operación [49–51].

1.2.2 Tecnologías de membrana

Las membranas aparecen como estrategia de desalcoholización en los años 80 [52–54] como posible solución a los problemas derivados de la desalcoholización mediante procesos térmicos, ya que las membranas tienen la ventaja de ofrecer unas buenas propiedades selectivas a temperatura ambiente, siendo capaces de separar eficientemente el etanol del vino sin necesidad de incrementar la temperatura de trabajo. Esta propiedad les permite minimizar su impacto sobre los componentes del vino ligados a su aroma y sabor, con un bajo consumo energético respecto a las tecnologías de destilación, como las SCC.

La tecnología de membranas es aquella que se sirve de una membrana para, a partir de una corriente de alimentación, generar dos corrientes de salida: permeado, aquella que atraviesa la membrana selectivamente, y retenido, compuesta por el resto de la composición alimentada (Fig. 1.5).

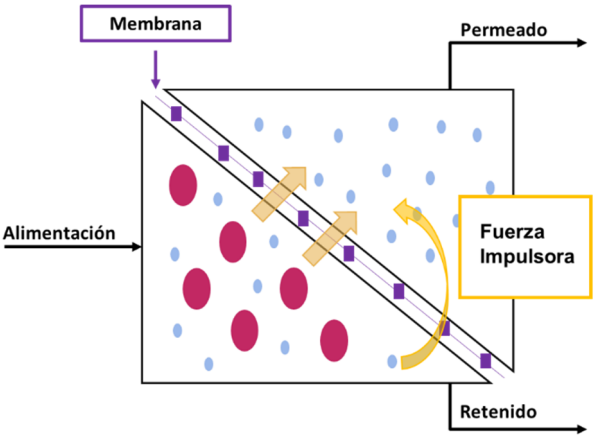

Fig. 1.5 Esquema de un proceso de separación por membrana.

En general, la membrana actúa como una barrera física semipermeable capaz de separar dos corrientes de forma selectiva aplicando una fuerza impulsora como puede ser un gradiente de presión o de concentración.

1.2.2.1. Módulos de membrana

Para maximizar su superficie de contacto, las membranas se empaquetan en módulos de membrana, cuyas características dependen de la geometría de las membranas que contienen; básicamente planas o tubulares [55].El empaquetamiento de membranas planas da lugar a módulos planos o en espiral ("*spiral wound*") mientras que los módulos de membrana tubulares y de fibra hueca requieren membranas con geometría tubular. Además de maximizar la relación de la superficie de contacto de la membrana por volumen ocupado, los módulos de membrana buscan ofrecer una baja pérdida de carga asociada a la corriente de alimentación (disminuyendo el gasto energético requerido por el proceso) y una distribución homogénea de la misma. También es recomendable que presenten procesos de limpieza y de mantenimiento sencillos [56].

Los módulos planos se basan en un apilamiento de dos o más membranas planas a través de las cuales se conduce la alimentación, de manera que el permeado se recoge en los extremos de las membranas. (Fig. 1.6A) Pese al bajo grado de empaquetamiento que presenta, su uso está extendido en el tratamiento de aguas residuales, fundamentalmente en instalaciones de pequeña capacidad, debido a su sencillo mantenimiento y escaso ensuciamiento ("*fouling*") [57,58]. Una estrategia para aumentar el grado de empaquetamiento de estos módulos, a costa de un mayor ensuciamiento, es disponer las membranas planas enrolladas alrededor de un tubo central por el cual se introduce la alimentación (Fig. 1.6B) [59].

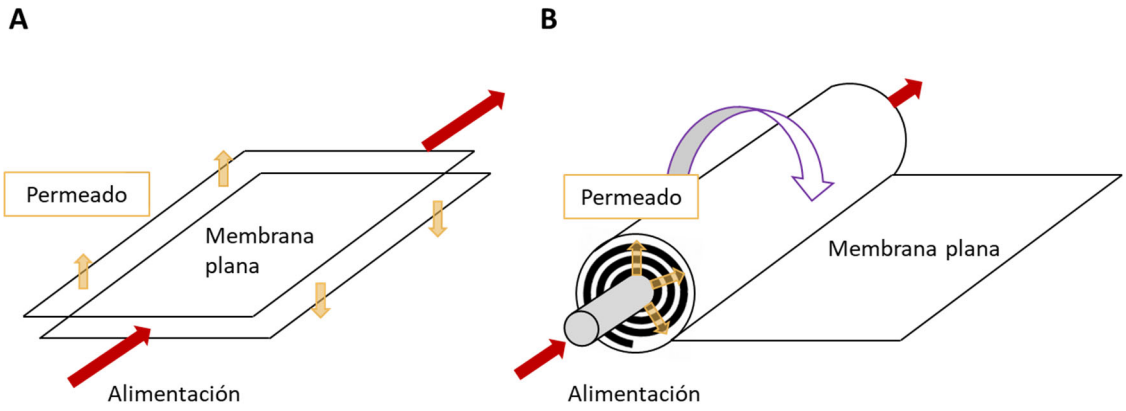

Fig. 1.6 Representación esquemática de dos módulos de membrana equipados con membranas planas. A) Modulo plano; B) módulo en espiral ("*spiral wound*").

Por otro lado, los módulos tubulares presentan una estructura similar a la de un intercambiador de calor en el que la alimentación se conduce por el interior de los tubos

mientras que el permeado se recoge en la carcasa que los rodea (ver Fig. 1.7A). Esta configuración les permite operar a elevados caudales de alimentación sin dañar la membrana, por lo que su uso es especialmente recomendable en aplicaciones cuya alimentación presente sólidos en suspensión. Además, los módulos tubulares presentan la ventaja de poder alimentarse también por la carcasa (invirtiendo así el sentido del flujo a través de la membrana) lo que, junto al diámetro relativamente elevado de los tubos, permite un mantenimiento relativamente sencillo [60].

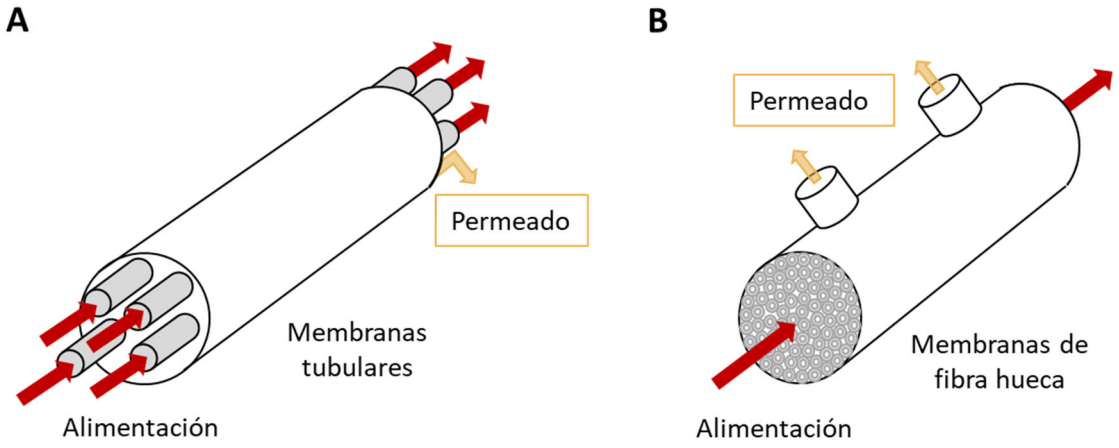

Fig. 1.7 Representación esquemática de dos módulos de membrana equipados con membranas tubulares. A) Modulo tubular; B) módulo de fibras huecas.

Finalmente, los módulos de fibras huecas están constituidos por haces de fibras empaquetadas en una carcasa a presión, lo que les otorga una alta densidad de empaquetamiento. Comparten con los módulos tubulares la versatilidad de poder conducir la alimentación por el interior o por el exterior de las fibras huecas (Fig. 1.7B), aunque en este caso las fibras huecas soportan presiones más elevadas desde fuera hacia dentro, por lo que en tecnologías de membrana a alta presión (como la ósmosis inversa) la alimentación está limitada a circular por el interior de las fibras huecas, incrementando el ensuciamiento de las mismas [61]. En cualquier caso, su mayor grado de empaquetamiento convierte a los módulos de fibra hueca en aquellos que mayor interés despiertan a nivel industrial [62].

En cuanto a su naturaleza, las membranas se clasifican en naturales o sintéticas, y estas a su vez pueden ser inorgánicas, poliméricas o mixtas [63], siendo las membranas poliméricas las más utilizadas en aplicaciones industriales debido a factores como precio, flexibilidad o facilidad de fabricación [64]. Sin embargo, es su versatilidad la que les permite trabajar eficientemente en las diferentes aplicaciones, la gran mayoría ya implementadas a escala industrial, recogidas en la Tabla 1.1.

Tabla 1.1 Procesos de separación de membranas en fase líquida.

Proceso de separación	Fuerza impulsora	Tamaño de sustancias retenidas	Aplicación habitual
Ósmosis inversa	Presión (40-80 bar)	0,1-1 nm	Desalinización
Pervaporación	Presión de vapor	< 1nm	Deshidratación, desalcoholización
Nanofiltración	Presión (5-40 bar)	0,5-2 nm	Separación de compuestos orgánicos y sales
Destilación osmótica	Presión de vapor	-	Desalinización, desalcoholización

La separación por ósmosis inversa (RO, de *reverse osmosis*) puede entenderse como la transferencia de compuestos de bajo peso molecular, como el etanol, a través de una membrana hidrófila semipermeable, cuya fuerza impulsora, superada la presión osmótica de la disolución a tratar, es la diferencia de presión a ambos lados de la membrana. Debido al muy pequeño tamaño de poro que presentan las membranas destinadas a RO, entre 0,1 y 1 nm, es necesario aplicar una presión elevada sobre la alimentación para favorecer el gradiente a través de la membrana. La

Fig. 1.8 muestra como la RO es capaz de desalcoholizar vino (retenido) eficientemente sin necesidad de incrementar la temperatura, generando a su vez una disolución hidroalcohólica (permeado). Sin embargo, durante la desalcoholización, otras sustancias de bajo peso molecular atraviesan la membrana junto con el etanol y el agua, lo que se traduce en vinos con menor concentración de aromas, similares a los obtenidos por SCC [65,66].

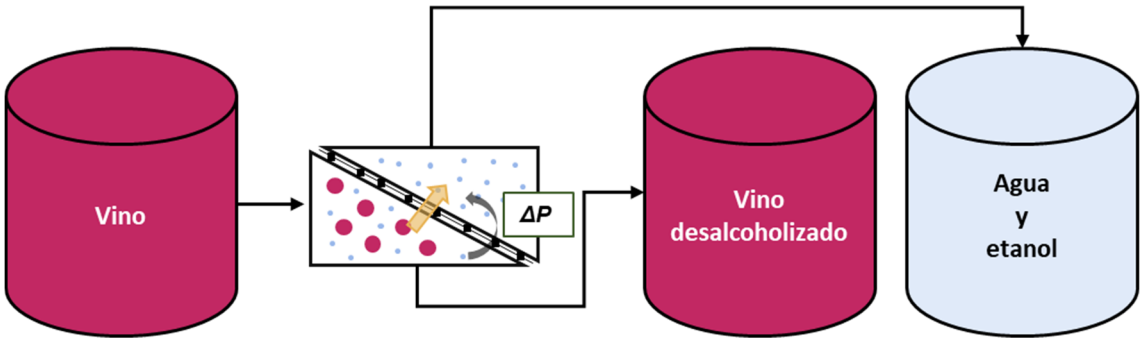

Fig. 1.8 Esquema de un proceso de separación por ósmosis inversa.

El principal inconveniente de la técnica de RO reside en la alta transferencia de agua hacia el permeado, que atraviesa la membrana selectivamente respecto al etanol dando lugar a permeados de tan solo un grado alcohólico. Como consecuencia, una vez finalizada la desalcoholización es necesario añadir agua al vino obtenido para alcanzar un producto óptimo, práctica ilegal en muchos países productores de vino y que impide la denominación de estos productos bajo el término de "vino" [67–69]. Además, la elevada presión de trabajo requerida (hasta 80 bar) encarece el coste operación.

Por otro lado, la pervaporación (PV) es una tecnología de membranas cuya fuerza impulsora es una diferencia de presión de vapor (para ello se aplica vacío en el lado del permeado), pero está estrechamente condicionada por el mecanismo de transporte que domina la transferencia de componentes debido al uso generalizado de membranas poliméricas densas [70–72]. Este mecanismo, conocido como modelo de solución-difusión, se divide en tres etapas: adsorción del componente objeto de separación en la membrana polimérica (alcanzando previamente una fase vapor), difusión del componente a través de la membrana como consecuencia de la fuerza impulsora mencionada, y desorción del componente en el otro lado de la membrana [73,74]. Así, la capacidad selectiva de la PV viene dada principalmente por dos factores: la afinidad del compuesto objetivo con el polímero y la capacidad de difusión de tal compuesto dentro del mismo.

Este mecanismo de separación explica el interés que ha generado la PV como técnica alternativa a la destilación tradicional para separar mezclas de líquidos con puntos de ebullición similares y también mezclas azeotrópicas [75,76]. Además, aunque la difusión a través de la membrana es en fase gas y es necesario alcanzar una cierta temperatura, esta es mucho menor que la requerida por un proceso destilación tradicional, reduciendo el gasto energético requerido [77–79]. Por lo tanto, no es de extrañar que el sector vinícola también haya contemplado su aplicación; existen numerosos estudios en la literatura no solo para retirar etanol sino también para la obtención de corrientes enriquecidas en aromas [80–84]. Pese a ello, su aplicación a nivel industrial aún es limitada por la lenta transferencia de componentes a través de la membrana que tiene lugar a baja temperatura, cuyo incremento queda sujeto a la propia preservación del vino alimentado [85,86].

La nanofiltración (NF) presenta la ventaja de poder separar eficientemente la glucosa del mosto de la uva y el etanol del vino ya fermentado, lo que le confiere una mayor versatilidad que otras técnicas de membrana. Además, al utilizar membranas con mayor tamaño de poro con respecto a RO, entre 0,5 y 2 nm, no requiere presiones tan altas de trabajo (5-40 bar) abaratando el proceso. Aunque se han reportado estudios de desalcoholización llevados a cabo por NF, es la separación selectiva de azucares la que

ha despertado mayor interés [87–90], por lo que la NF podría englobarse dentro de las estrategias pre-fermentativas (la Fig. 1.3 no se duplica por simplificación). Los resultados reportados de NF como técnica de desalcoholización revelan una pérdida prácticamente total de los componentes volátiles del vino [91–94].

Como alternativa a las tecnologías ya mencionadas, la destilación osmótica (OD, de *osmotic distillation*) es una técnica de membrana que, al contrario que las anteriores, es capaz de trabajar eficientemente a temperatura ambiente y presión atmosférica [95]. Estos factores la convierten en una alternativa viable, abaratando los costes de producción y, potencialmente, minimizando el impacto sobre la matriz del vino [96]. Al igual que en PV, la fuerza impulsora que lidera el transporte a través de la membrana es el gradiente de presión de vapor de cada componente entre las corrientes de alimentación y barrido, que quedan separadas por dicha membrana, tal como se puede ver en la .

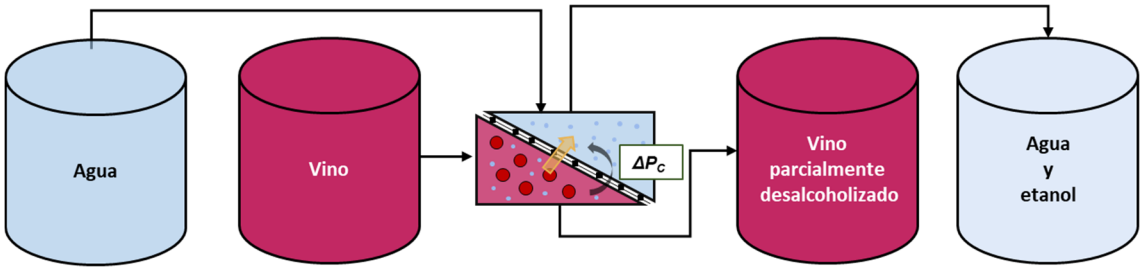

Fig. 1.9.

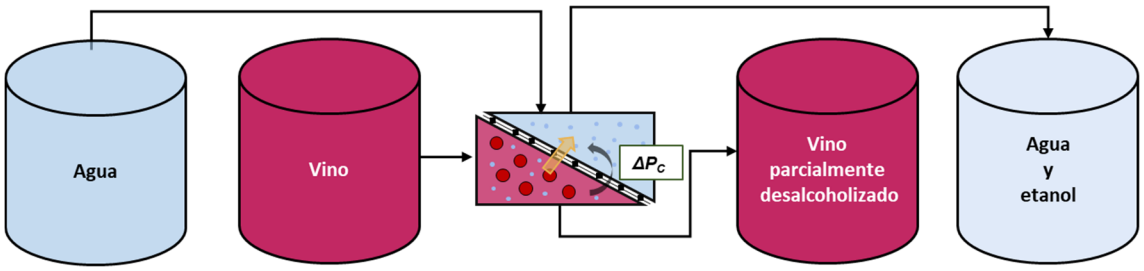

Fig. 1.9 Esquema de un proceso de separación por destilación osmótica.

La OD se equipa con membranas poliméricas porosas, que permiten trabajar bajo condiciones más inocuas para el producto tratado y, en vez de por difusión como era el caso de la técnica anterior, el transporte ocurre en este caso a través de los poros de la membrana. Este mecanismo, representado a través del llamado modelo *Dusty-Gas Model*, queda definido por las colisiones entre las moléculas transportadas (difusión molecular) y entre estas moléculas con las propias paredes de los poros (difusión de Knudsen) [97].

Teniendo en cuenta el tamaño de poro típico utilizado en OD, de alrededor de 30-100 nm, la interacción componente-membrana parece jugar también un papel fundamental en la capacidad selectiva de estas membranas, aunque el estudio de su influencia aún no ha sido abordado. Una herramienta práctica para evaluar esta interacción pueden ser los parámetros de solubilidad de Hansen (HSP) [98–100] cuya eficacia ha sido previamente demostrada en la industria de pinturas y recubrimientos, y que permiten cuantificar la interacción (por ejemplo, en términos de solubilidad) de un cierto compuesto o material (por ejemplo, un polímero) en cierto disolvente [101,102].

Como se ha mencionado, la OD requiere una corriente de barrido que se enfrente a la corriente de alimentación al otro lado de la membrana. Trabajando en recirculación continua, algo necesario a nivel industrial, esta corriente limita el grado de desalcoholización que se puede alcanzar por OD, ya que este queda fijado por el gradiente de concentración (presión parcial) establecido a través de la membrana. Por ello, la OD es una técnica fundamentalmente orientada hacia la desalcoholización parcial de vinos.

El etanol es el compuesto de mayor concentración en el vino, a excepción del agua, y por ello cabe esperar mayores transferencias para él que para el resto de componentes. Sin embargo, aunque se han reportado resultados prometedores [103–105], la tendencia general es una transferencia experimental para los aromas mayor de la esperada, alcanzando en la mayoría de los casos valores muy cercanos a la situación de equilibrio mencionaba previamente [106–108]. Una posible explicación reside en que la mayor volatilidad e hidrofobia (apolaridad) que presentan estos componentes reduce el rendimiento de las membranas de polipropileno, el material más ampliamente utilizado para construir membranas de OD [109,110], para retener los aromas en el vino. En este sentido, aunque actualmente se encuentren pocas alternativas en la bibliografía, fenómenos como el ensuciamiento de la membrana [111] o la adsorción de componentes en la membrana [103] se han estudiado ya, sentando las bases para el desarrollo de una membrana que mejore las prestaciones de la OD como técnica de desalcoholización.

Finalmente, hay que tener en cuenta que la OD es la única técnica que requiere de una corriente de agua (barrido) auxiliar a la corriente de alimentación, lo que resulta en un importante inconveniente a nivel industrial, ya que el elevado gasto de agua por unidad de vino tratado se prevé insostenible (estudio del ciclo de vida 2015). Además, la corriente de barrido resultante al final del proceso es esencialmente una disolución hidroalcohólica pobre en etanol, por tanto, con muy poco valor añadido, y no puede ser reutilizada en posteriores desalcoholizaciones por el gradiente de concentración necesario entre ambas corrientes.

Hoy en día se está planteando la combinación de dos o más de las técnicas mencionadas para corregir de manera conjunta las desventajas específicas, asociadas a SCC, RO, NF y OD, avalada por estudios recientes que han reportado el éxito de estas combinaciones de procesos [112–116], destacando particularmente tres de los denominados proceso multi-etapa: NF+PV; RO+OD y OD+PV. El primer proceso multi-etapa enfocado a la desalcoholización de vino fue planteado por Salgado et al. en 2017 [113], aplicado sobre mosto de uva tipo verdejo sin fermentar con el objetivo de reducir la cantidad de azucares con la mínima influencia sobre el resto de componentes. El proceso global consistía fundamentalmente en una etapa previa de NF para desaromatizar el mosto, seguida de dos etapas de NF para retirar el azúcar del mosto desaromatizado. Una vez fermentados el mosto control y el tratado se observó un perfil organoléptico muy similar en ambos vinos. Sin embargo, la reducción en etanol alcanzada fue únicamente de 1,5 grados de alcohol. En 2019 y 2020 Pham et al. [114,115] llevaron a cabo un exhaustivo estudio sobre el rendimiento del proceso multi-etapa RO-OD (ver Fig. 1.10) en la desalcoholización de diferentes variedades de vino, obteniendo resultados de retención de aromas superiores a los reportados en la literatura previa, reflejando el potencial del proceso propuesto. Sin embargo, no hay que perder de vista que la OD se llevó a cabo con una membrana diferente (no mencionada) al resto de la bibliografía.

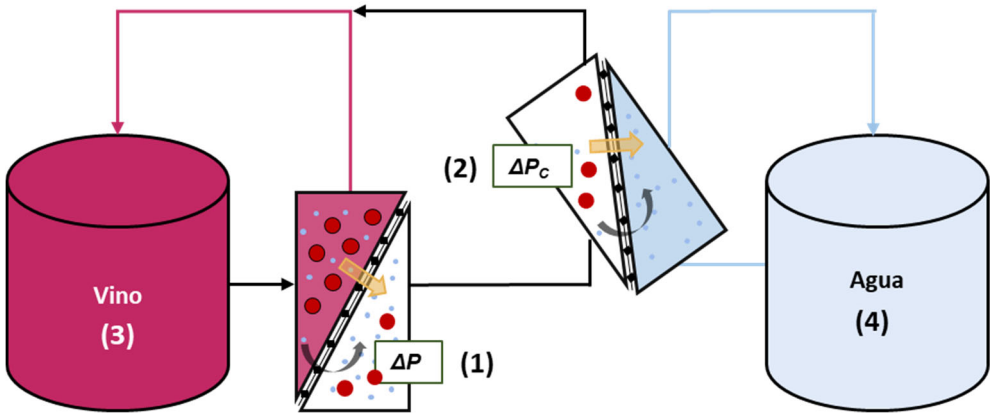

Fig. 1.10 Esquema de un proceso multi-etapa RO-OD. (1) RO; (2) OD; el vino alimentado (3) se desalcoholiza a medida que el agua (4) se enriquece en etanol.

En cualquier caso, aunque los procesos planteados permiten preservar mejor los aromas, siguen produciéndose pérdidas significativas de componentes importantes en el perfil organoléptico del vino, a la vez que se incrementa el coste energético debido fundamentalmente a la presión requerida (por ejemplo, en el caso de la RO). Otra posible aplicación de los procesos multi-etapa es la revalorización de subproductos

generados durante el proceso de desalcoholización. Por ejemplo, Kujawski et al. evaluaron el potencial de la PV como etapa de tratamiento de la corriente de barrido de un proceso de OD para secar alimentos [117], permitiendo su reutilización en ciclos de secado posteriores.

1.3 Alcance de las técnicas de desalcoholización

1.3.1 Vinos susceptibles de desalcoholización

Una variedad de uva autóctona es aquella que se origina en una región vitivinícola específica, adaptándose al terreno y al clima del entorno, lo que le confiere al vino resultante un perfil organoléptico característico y diferencial. En España se pueden encontrar Albariño, Macabeo, Xarello, Parellada y Garnacha Blanca como variedades autóctonas blancas mientras que Garnacha Tinta, Tempranillo, Cariñena y Monastrell representan las principales variedades tintas. Teniendo en cuenta el interés por someter a los vinos resultantes a un proceso de desalcoholización, son las variedades tintas las que producen vinos con mayor resistencia a los procesos mencionados anteriormente (entendiendo por esta la menor tendencia a perder, en determinadas condiciones de desalcoholización, los componentes volátiles responsables del aroma del vino), por lo que no sorprende que la mayoría de los estudios de desalcoholización recogidos en la bibliografía aborden la desalcoholización de tintos. Entre las variedades más estudiadas para su desalcoholización, incluyendo aquellas variedades no autóctonas, podemos encontrar Tempranillo, Garnacha Tinta, Merlot o Aglianico.

Dentro del abanico de variedades tintas presentado, la Tabla 1.2 resume los resultados reportados en desalcoholizaciones parciales llevadas a cabo por OD hasta el momento.

A partir de los resultados reportados en literatura se puede concluir que el grado de desalcoholización se relaciona estrechamente con la pérdida de aromas, en línea con lo mencionado anteriormente. Esto distingue a la OD como una técnica de membranas más enfocada hacia una desalcoholización parcial/ligera del producto que hacia una desalcoholización total. Por otro lado, la desalcoholización total no daría lugar a un vino propiamente dicho por las restricciones administrativas que conlleva la definición de vino, entre otros aspectos a tener en cuenta [119].

Para profundizar en los resultados recogidos en la Tabla 1.2 es importante tener en cuenta que los ésteres derivados de ácidos grasos juegan un papel clave en el perfil organoléptico de los vinos [120,121], por lo que la retención de compuestos como hexanoato de etilo, octanoato de etilo o acetato de isoamilo en los vinos

desalcoholizados puede ser una herramienta útil para comparar la resistencia de los vinos al proceso de desalcoholización.

Tabla 1.2 Desalcoholizaciones parciales llevadas a cabo por OD. Adaptada de Sam et al [118].

Variedad de vino	Grado desalcoholizado [º]	Componente volátil	Pérdida [%]
Aglianico	3	Alcoholes	8,4
		Ácidos	42,9
		Ésteres	12,5
Aglianico	2	Alcoholes	9,2
		Ácidos	33,8
		Ésteres	11,0
Aglianico	7	Alcoholes	57,9
		Ácidos	23,6
		Ésteres	12,8
Merlot	2	Acetato de etilo	37,4
		Acetato de isoamilo	34,9
		Alcohol isoamílico	13,7
		Hexanoato de etilo	33,0
		Octanoato de etilo	67,8
Barbera	9	Alcoholes	63,9
		Ácidos	17,4
		Ésteres	23,8
Tempranillo	4	Alcohol isoamílico	21,0
		Hexanoato de etilo	20,0
Garnacha	4	Acetato de isoamilo	24,0
		Hexanoato de etilo	36,0
Pelaverga	9	Alcoholes	59,9
		Ácidos	23,6
		Ésteres	45,2
Sangiovese	5	Alcoholes	56,0
		Ácidos	18,0
		Ésteres	64,0
Sangiovese	5	Alcoholes	53,6
		Ácidos	2,3
		Ésteres	19,5

La desalcoholización de vinos procedentes de la variedad Aglianico reportó un 42 % de pérdida promedio para algunos de estos compuestos volátiles como el acetato de etilo, acetato de isoamilo y hexanoato de etilo. Ligeramente mayor fue el impacto acusado por vinos de la variedad Merlot, con un vino final un 30-40 % más pobre en los aromas mencionados (70 % en el caso del octanoato de etilo). Curiosamente, han sido los vinos producidos a partir de las variedades autóctonas españolas (Tempranillo y Garnacha Tinta) los que han reportado una mayor retención de estos compuestos en el vino [104]. Tras una reducción de 4 grados, los vinos procedentes de la variedad Garnacha sufrieron unas pérdidas de acetato de isoamilo y acetato de etilo del 24 y 36 %

respectivamente, sustancialmente menores que lo reportado para otras variedades. Por otro lado, los vinos de variedad Tempranillo mostraron pérdidas aún más ajustadas de hexanoato de etilo (20 %). En este contexto, los resultados procedentes de la desalcoholización parcial (reducción de 2-3 grados de alcohol) de vinos de diferentes variedades señalan a los vinos procedentes de la uva Tempranillo como propicios para disminuir parcialmente su grado alcohólico por OD.

1.3.2 Desalcoholización parcial de cerveza: *light beer*

Junto al vino, la cerveza es una de las bebidas alcohólicas más importantes del mundo, con una producción anual cercana a los 2000 millones de hectolitros al año [122]. La cerveza es además la bebida alcohólica más consumida en la sociedad occidental (América y Europa) y sus ventas no han parado de crecer (Cerveceros de España, datos de 2021, publicados en julio de 2022). Solo en España, las ventas en 2021 alcanzaron los 40 millones de hectólitros, generando cerca de 42000 puestos de trabajo directos e indirectos [123].

Igual que ocurría con el vino, la cerveza ha evolucionado con la exigencia del consumidor y su entorno social. De hecho, la misma tendencia social por una vida más saludable que preocupaba a la industria enológica ha favorecido tradicionalmente a la cerveza frente a otras bebidas de mayor graduación como el propio vino (en países occidentales) o el sake (en Japón, también conocido como vino de arroz). Sin embargo, la exigencia comercial y legal son cada vez mayores, y la industria cervecera está respondiendo con productos más saludables y/o innovadores como la cerveza para celiacos o la cerveza sin alcohol [122,124,125].

La cerveza sin alcohol ha crecido en interés durante estos últimos años gracias al atractivo objetivo que pretende: mantener las propiedades saludables y organolépticas intrínsecas de la cerveza sin los efectos adversos del etanol. Esta popularidad sin embargo no termina de reflejarse en los mercados, donde la relación de ventas entre las cervezas con y sin alcohol se mantiene aproximadamente en una relación de 5 a 1 en miles de kilos consumidos (Ministerio de Agricultura, Pesca y Alimentación de España, datos de 2021, publicados en agosto de 2022) debido a que las características sensoriales de la cerveza sin alcohol son, en general, inferiores a aquellas ligadas a una cerveza “normal”.

Por ejemplo, la disminución del etanol por actividad enzimática genera un sabor muy dulce en la cerveza, mientras que aquellos procesos que requieren temperatura conducen a productos menos intensos y con un sabor que recuerda al caramelo [126,127]. Además, tal como ocurre con la desalcoholización del vino, el uso de

membranas para disminuir el grado alcohólico ha despertado un importante interés [128–130]. Sin embargo, las cervezas desalcoholizadas están todavía lejos de colmar las exigencias del consumidor, que las sigue encontrando pobres en cuerpo y aroma [127]. No obstante, debido a la relación que se establece entre el grado de desalcoholización y el porcentaje de pérdida de aromas, cabría esperar que una cerveza sometida a desalcoholización parcial pudiera mantener unas características sensoriales más próximas a las de una cerveza normal, tal y como se ha observado para el vino. Después de lo discutido anteriormente para el vino, este objetivo parece idóneo para la desalcoholización de la cerveza por OD.

El concepto "*light beer*" aparece en los años 2000 como respuesta a la demanda por parte del consumidor de un producto sano que pueda sustituir a la cerveza normal, e irrumpe con éxito en el mercado americano: en 2010, más de la mitad de la cerveza vendida en EEUU era *light beer* [131]. Un producto con menos hidratos de carbono y menos etanol que una cerveza normal, pero con el grado alcohólico menos condicionado (fijado en 2,5 v/v% aproximadamente) que en la cerveza sin alcohol [132].

Aunque es cierto que hasta ahora su éxito en EEUU no se ha podido replicar en Europa, donde se ha atribuido a esta *light beer* defectos similares a los asociados con la cerveza totalmente desalcoholizada, la OD podría ser la técnica de desalcoholización que tenga la llave del mercado europeo para que cervezas más sanas puedan competir comercialmente con los productos tradicionales. En otras palabras, por la propia fuerza impulsora que domina la OD mencionada anteriormente, la obtención de una *light beer* con un alto perfil sensorial puede ser el proceso idóneo para la aplicación de la OD con membranas. Esto es así porque la *light beer* no exige reducir al mínimo el grado de alcohol, lo que minimiza las posibles pérdidas en el resto de componentes y permite buscar un compromiso entre el grado alcohólico objetivo y la merma de componentes.

CAPÍTULO 2

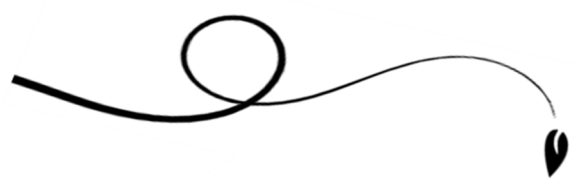

OBJETIVOS

2 Objetivos

El principal objetivo de esta Tesis Doctoral es el desarrollo de una herramienta tecnológica que permita reducir el contenido de etanol de bebidas alcohólicas mediante un proceso de destilación osmótica interfiriendo mínimamente en su composición de aromas. Este objetivo principal se sustenta en los siguientes objetivos específicos:

1. Evaluación de los fenómenos de transporte clásicos y análisis teórico-experimental de la interacción componente-membrana (basada en los parámetros de Hansen) para su uso en la predicción del rendimiento de la desalcoholización.
2. Estudio experimental de las variables estructurales (diferentes fabricantes y materiales de membrana) y de operación de la destilación osmótica.
3. Desarrollo de un proceso secuencial de tecnologías de membrana OD-PV para revalorizar el etanol retirado de las bebidas alcohólicas y minimizar el gasto de agua asociado a la OD.
4. Aplicación de la metodología desarrollada para el vino a la cerveza, estudiando el impacto de la OD en sus parámetros típicos de elaboración e identificación del grado idóneo de desalcoholización.

CHAPTER 3

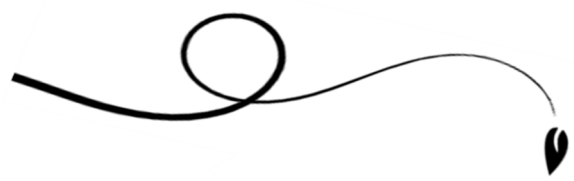

THEORETICAL AND PRACTICAL APPROACH TO THE DEALCOHOLIZATION OF WATER-ETHANOL AND RED WINE BY OSMOTIC DISTILLATION

Reproduced from Esteras-Saz, J; De la Iglesia, Ó; Peña, C; Escudero, A; Téllez, C; Coronas, J. Theoretical and practical approach to the dealcoholization of water-ethanol mixtures and red wine by osmotic distillation. Sep. Purif. Technol. 270 (2021) 118793. https://doi.org/10.1016/j.seppur.2021.118793

3 Theoretical and practical approach to the dealcoholization of water-ethanol mixtures and red wine by osmotic distillation

3.1 Introduction

There is growing evidence that a climate change is taking place, whose impact extends well beyond an increase of Earth temperature. It is also affecting the stability of ecosystems and communities around the world [6,133,134]. Viticulture has been also affected, since in recent years changes in the annual cycle of vine have been observed, which leads to a temporal mismatch between industrial and phenolic maturity [20].

The degree of ripeness conferring the optimal flavor characteristic of wine normally correlates with the highest sugar content in grapes. However, due to the global warming, the juice obtained from grapes at full phenolic maturation has an excessive concentration of sugar, resulting in wines with undesirably higher concentrations of ethanol [135]. This phenomenon is aggravated in warm climate areas such as the Mediterranean region, particularly including France, Italy and Spain as main producers of wines, and it is expected to be intensified in the next years [16,136]. Also, it has been suggested that the temperature increase (which could go from 0.3 to 1.7 ^{o}C during the next 20 years), consequence of global warming, may affect gene expression and enzymatic activity which determine grape ripening and wine characteristics [137].

At this moment, in the Mediterranean region, most of the red wines already exceed 14 v/v%, and an increment of 2 v/v% of ethanol has been detected in wines from California [138]. Furthermore, in the past twenty years, the alcoholic strength of Australian wines increased from 12.4 v/v% to 14.4 v/v% for red wines and from 12.5 v/v% to 13 v/v% for white ones [139]. As an additional example, based on the daily average air temperature data from 1981 to 2017, it was concluded that Ningxia region in China will have to change the wine grape varieties and wine types to adapt to the ongoing climate change [140].

During must fermentation, ethanol is produced with other substances such as esters, glycerol or succinic acid that confer the wine their organoleptic interest [141]. An excessive ethanol concentration is undesirable since it increases the solubility of the volatile compounds in the wine, masking the main aromas and increasing the perception of hotness on the mouth, thus reducing the wine quality [22,24]. Besides, the growing social tendency towards a healthy lifestyle, avoiding an excess of alcohol consumption,

has resulted in an increasing demand of wines with lower ethanol content, and there is no doubt that less alcoholic wines (e.g. 2-3 degrees below the current ones) would have a positive reception from markets and consumers. For this reason, decreasing the ethanol content of the current wines maintaining suitable organoleptic profiles, adequate preservation properties and healthier is currently one of the most important issues for the wine community [20,41,142].

To adapt to the above described situation of global warming in the context of wine production but also to satisfy the consumer demand and produce fresh and balanced wines with low alcoholic strength, different strategies have been studied [143,144]. Currently the most popular dealcoholization techniques are focused on the removal of ethanol from finished wines with post-fermentation separation treatments such as spinning cone columns and reverse osmosis [68,145]. However, during the separation carried out with spinning cones the wine must be slightly heated, causing an energy cost and a possible modification of its organoleptic properties. Moreover, reverse osmosis requires a relatively high energy consumption to raise the required pressure, while the installation cost can be important due the high membrane area needed to achieve a desired production. As an alternative, osmotic distillation (OD) can produce an ethanol reduction working at room temperature and with no pressure gradient thanks to the use of hydrophobic membranes. As a consequence of the low working temperature, OD has a tolerable energy demand and a low impact on the composition and sensory attributes of the processed wines. Several works have been published on the OD application for low-alcohol wine production where a partial dealcoholization did not influence significantly the color, total anthocyanins, flavonoids and contents of phenols [107,146].

In OD process, a hydrophobic porous membrane, typically of polypropylene, acts as a contactor, with the liquid mixture containing ethanol in the feed side and the extracting agent (stripper, usually liquid water) in the permeate side. The hydrophobic character of the membrane prevents water transport, while the other components of the feed that diffuse through the membrane pass from liquid to vapor phase inside the matrix pores. As a result, the gradient of partial pressures of these components between both membrane sides contributes to the driving force for the separation, meaning a reduced loss of minor components comparing to other techniques mentioned above.

The reduced loss of minority compounds during OD has been evidenced for most acids and phenolic compounds (anthocyanins and tannins) as previously reported [107,146]. However, the loss of some volatile compounds is inevitable. Lisanti et al. reported a loss of around 40 % esters with a partial (-2 v/v%) dealcoholization of wine [106]. While a loss up to 80 % was observed by Corona et al. during a dealcoholization

of 5 v/v% [146]. In fact, in dealcoholization processes where wines with an alcoholic graduation less than 1 v/v% were obtained the relative loss of volatile compounds was as high as 98 % [107].

In light of these results, the need to gain more insight into the ethanol behavior and its influence on the volatile components of wine during OD is evident. Recently, several theoretical approaches based on the classical resistance in series model [147,148] were applied [103,104,149] to describe the evolution of ethanol and aromas in the membrane contactor. However, this model, based only on the volatility to describe the liquid-gas distribution of components, was not able to predict significant differences as a function of the flow rate [104]. This may be due to the fact that the role of the membrane in the separation mechanism was not almost addressed. In this chapter, our main objective is to shred some additional light into the wine dealcoholization with hydrophobic membranes. With this purpose, first, a correlation between the OD of water-ethanol solutions and red wine will be assessed. Second, a set of experiments using wine as feed stream will be carried out to obtain the operation conditions that yield the best performance in terms on ethanol permeation and short contact time to minimize loss of aromas. Third, a mathematical model integrating the component-membrane interaction based on the application of Hansen solubility parameters will be developed, focusing on the evolution of individual wine components apart from ethanol. Finally, the experimental OD will be compared with the results generated by the proposed model at different working conditions.

3.2 Materials and methods

3.2.1 Experimental setup

Fig. 3.1 shows the schematic representation of the lab scale plant for the osmotic distillation (OD) experiments. This includes the membrane module with the feed (Q_f) and stripping (Q_s) flow systems, pressure and temperature sensors and a scale for continuous monitoring of permeation.

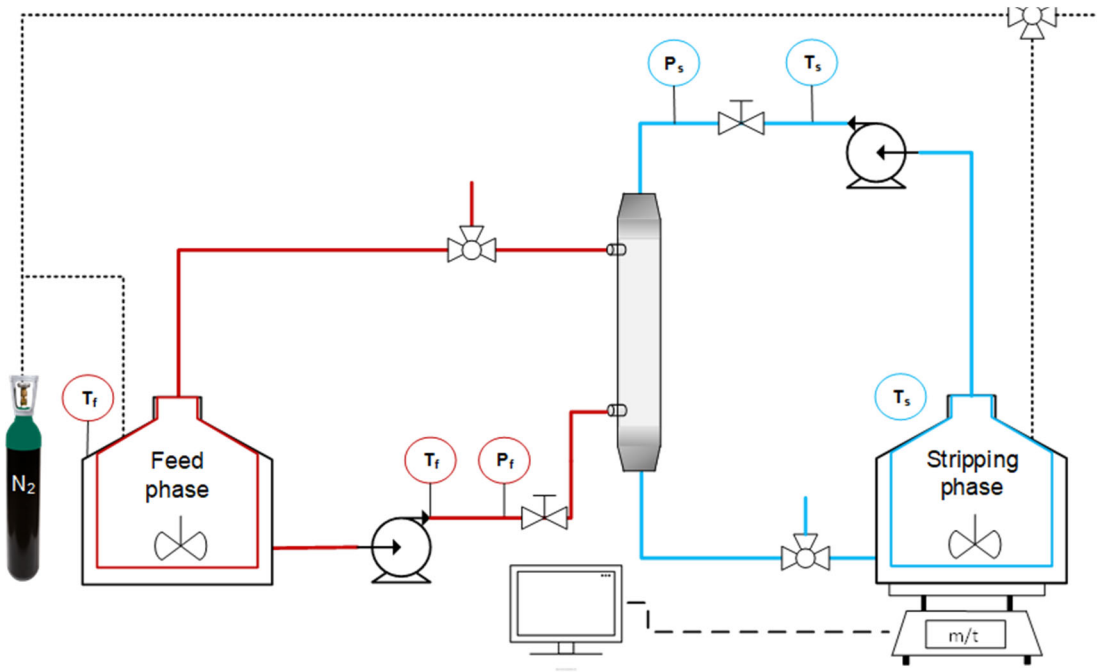

Fig. 3.1 Osmotic distillation lab scale plant scheme. T_f, T_s thermocouples, P_f, P_s manometers.

The feed tank, containing 375 mL of red wine (Tempranillo, which corresponds to a black grape variety mainly grown in Spain) that was kindly provided by Bodegas Matarromera (Valbuena del Duero, Valladolid, Spain), is connected to the shell side of the membrane module. The stripping tank, with an adjustable volume between 75 and 375 mL of water, is connected to the tube side of the membrane module and both streams circulate in a counter-current configuration. This configuration facilitates the membrane operation. The recirculated feed and stripping streams are continuously fed into the module by peristaltic pumps (DINKO, model 1.9735.15) with flows varying from 21 to 74 mL·min^{-1}.

The membrane module was equipped with Liqui-Cel^{TM} MM-1x5.5 hydrophobic porous polypropylene (PP) hollow fiber membranes from 3M. The main characteristics of the membrane module are detailed in Table 3.1.

Table 3.1 Characteristics of the hollow fiber membrane module (MM-1x5.5 x-50 Liqui-Cel™) as supplied by the manufactured 3M.

Membrane module parameter	Value
Effective membrane area (m^2)	0.18
Number of fibers	2300
Nominal pore size (μm)	0.03
Porosity (-)	0.4
Tortuosity (-) [a]	2.5
Effective fiber length (cm)	14
Membrane thickness (μm)	40
Internal fiber diameter (μm)	220
External fiber diameter (μm)	300

[a] Estimated by the following equation: $\tau = 1/\varepsilon$

The morphological characteristics of the PP hollow fibers were observed by scanning electron microscopy (SEM) using a microscope Inspect™ F50 model working at a voltage of 10 kV. The temperatures of feed and stripping phases are measured by K-type thermocouples. All the experiments were carried out at room temperature (21 °C). Two manometers (MEX3D820B15, Bourdon) measure the pressure at tube and shell sides yielding values of overpressure close to 0 atm.

The stripping tank is placed on an electronic precision scale (PRACTUM1102-1S, Sartorius) with a readability of 0.01 g to register its weight every 60 s since the beginning of each experiment. This allows to have an accuracy estimation of the mass flow through the membrane as a function of time, i.e. a continuous monitoring of the dealcoholization process. The different volumes, flow rates and temperature of both streams used in this study are detailed in Table 3.2.

Table 3.2 Operating conditions at room temperature (21 ^{o}C) and V_f = 375 mL.

Condition	Q_f [mL·s^{-1}]	Q_s [mL·s^{-1}]	V_s [mL]	$V_f \cdot V_s^{-1}$ [-]
1	65	39	75	5
2	65	39	375	1
3	65	39	187.5	2
4	21	39	187.5	2
5	40	39	187.5	2
6	74	39	187.5	2

Q_f fed flow rate, Q_s stripping flow rate, V_f feed volume, V_s stripping volume**.**

During the experiments, 1 mL samples of the two streams leaving the module were taken at constant time intervals to analyze their ethanol concentration. 20 µL of methanol (HPLC grade, Scharlau) was added to each sample as internal standard. 0.5 µL of this mixture was injected on a gas chromatograph 7820A (Agilent Technologies) equipped with a PORAPAK Q80/100 column, 2 m x 1.8 in x 2 mm and FID detector. The injector worked in splitless mode with a ratio 1:100 at 250 °C. Helium was used as carrier gas at a constant flow of 1 mL·min^{-1} and the temperature in the oven was fixed at 200 °C. After each experiment, the aroma compounds in the partial dealcoholized wines were analyzed following a procedure previously developed and validated [150].

From the ethanol concentration of samples and stripping weight, mass flows at fixed time intervals were calculated following this equation:

$$J_{Exp}(t) = \frac{\Delta W}{A_e \Delta t} \quad (3.1)$$

Where ΔW is the variation of mass in the stripping or ethanol amount in the feed stream for an interval of time, Δt. Fixed time intervals were used for the previous calculations due to the fact that working in a recycle mode process decreases the driving force across the membrane as a function of time, what in turn reduces the ethanol flux through the membrane.

After each experiment, the membrane module was cleaned as follows. Milli-Q water was fed through the tube and shell sides for 20 min. Subsequently, a 0.5 v/v% NaOH solution preheated at 40 °C was recirculated at 65 mL·min^{-1} for 15 min through both membrane sides. Then the system was rinsed again with Milli-Q water using the same flow without recycling for 15 min. Finally, the membrane module was dried in two steps:

first vacuum drying was applied at room temperature during 2 h using a PFEIFFER vacuum pump (MVP-040-2). After that, nitrogen was forced to flow through the membrane during 30 min at 100 cm^3(STP)·min^{-1} to ensure that the membrane pores were completely dried.

3.3 Theory

As previously stated, during OD ethanol is transferred from the wine towards the stripping stream (water) through a hydrophobic hollow fiber membrane contactor. Due to the hydrophobicity of the membrane, the aqueous streams at both membrane sides are not in contact through the pores, thus a liquid-vapor interface is formed in each pore edge. This vapor-liquid equilibrium distribution between the feed phase-air and striping phase-air can be considered by means of the respective Henry's constant, H^i. In fact, recent studies suggest that the Henry's constant values correlate with the loss of volatile organic compounds (VOCs) from the wine through the membrane [103,104,151]. Therefore, the flux of each volatile component across the membrane in osmotic distillation, J^i (g·m-2·s^{-1}), can be expressed as:

$$J^i = K_G^i \left(\frac{\rho_f H_f^i}{M^i} C_f^i - \frac{\rho_s H_s^i}{M^i} C_s^i \right) \quad (3.2)$$

where K_G^i (g·m^{-2}·s^{-1}·Pa^{-1}) is the global mass transport coefficient and C_f^i and C_s^i are the concentrations of components in the feed and stripping sides, respectively.

K_G^i is inversely proportional to the global resistance to the mass transfer; and R_G^i is given by the sum of the three mass transfer resistances involved in the process (Eq. (3.3)): mass transfer resistance in the feed boundary layer, R_f^i, mass transfer resistance through the air gap in the membrane pores, R_m^i, and mass transfer resistance in stripping boundary layer, R_s^i [147,148].

$$R_G^i = R_f^i + R_m^i + R_s^i \rightarrow \frac{1}{A_e K_G^i} = \frac{H^i}{A_{in} M^i K_f^i} + \frac{1}{A_{lm} K_m^i} + \frac{H^i}{A_{ex} M^i K_s^i} \quad (3.3)$$

As a minor simplification, same values of Henry constant were considered in the feed and stripping sides when applying the previous equation. The mass transfer coefficients in the stripping, K_s, and feed, K_f, boundary layers can be calculated for each component from the Sherwood number, with the following expression:

$$Sh^i = \frac{K^i d_h}{D^i} \quad (3.4)$$

where D_i is the molecular diffusion coefficient in the liquid phase ($m^2 \cdot s^{-1}$), and d_h is the hydraulic diameter (m), which can be described by Eq. (3.5) as a function of the inner diameter of the module, d_a, the outer diameter of the central delivery tube, d_{co}, the external diameter of the hollow fibers, d_{ex}, and the number of hollow fibers, n.

$$d_h = \frac{4\ cross\text{-}sectional\ area\ of\ flow}{total\ fiber\ external\ circumference} = \frac{d_a^2 - d_{co}^2 - nd_{ex}^2}{d_a + nd_{ex}} \quad (3.5)$$

Here, the structure of the module did not show a central collector tube. Therefore, d_{co}value is 0 in the equation presented above. Sherwood number can be predicted by using correlations of the general form of Eq. (3.6):

$$Sh^i = Af(\phi)\left(\frac{d_h}{L}\right)^{\alpha} Re^{\beta} Sc^{\gamma} \quad (3.6)$$

where A, α, β and γ are constants from the correlation of experimental data as a function of ϕ, which is the packing density of the module. *Re* and *Sc* are Reynolds and Schmidt numbers, respectively (see below).

Regarding the stripping stream boundary layer, Lévêque correlation is widely used in the literature to predict the tube or stripping side mass transfer [109]. However, its limit of validity in terms of Graetz number, Gz, is not well defined. In the present chapter, Eq. (3.7) was chosen to predict Sh^i since a value of $Gz = 3.24$ was obtained and this equation is recommended when Gz is less than 6 [152].

$$Sh_s = O.5ReSc\left(\frac{d_h}{L}\right) \quad (3.7)$$

The mass transfer coefficient in the feed boundary layer on the shell side was calculated using the correlation of Shen et al. [153], Eq. (3.8), since the constraints of the correlation correspond to the current experimental conditions ($0.1 < Re < 250$; $0.32 < \emptyset < 0.45$).

$$Sh_f = 0.055Re_f^{0.72}\, Sc^{0.33} \quad (3.8)$$

Mass transfer resistance of the membrane can be obtained from the so-called dusty gas model [97]. This model considers that the ethanol diffusion mechanism into the membrane pore is led by the Knudsen diffusion (molecule-pore wall collisions) and molecular effective diffusion (molecule-molecule collisions). Hence, the membrane transport coefficient in the membrane pores is expressed as (Eq. (3.9)):

$$K_m^i = \frac{M^i \varepsilon}{R_g T \delta \tau} \left[\frac{1}{D_k^i} + \frac{1}{D_{m-air}^i} \right]^{-1} \quad (3.9)$$

Where ε and τ are the membrane porosity and tortuosity respectively, M^i is the molar weight of component *i*, *T* is the absolute temperature in K at which the experiment is carried out, R_g is the ideal gas constant, and D_{m-air}^i is the molecular effective diffusion estimated with the Fuller, Schettler and Giddings relation [154], as follows:

$$D_{m-air}^i = \frac{10^{-3} T^{1.75} \left(\frac{1}{M^i} + \frac{1}{M^{air}} \right)^{\frac{1}{2}}}{P \left[\left(\sum v^i \right)^{\frac{1}{3}} + \left(\sum v^{air} \right)^{\frac{1}{3}} \right]^2} \quad (3.10)$$

where v^i and v^{air} are the diffusion volumes ($cm^3 \cdot mol^{-1}$) for components i and air, respectively. Finally, Knudsen effective diffusion, D_k^i, is typically calculated with the following equation:

$$D_k^i = \frac{d_p}{3} \left(\frac{8 R_g T}{\pi M^i} \right)^{1/2} \quad (3.11)$$

where d_p is the pore diameter of the hollow fibers. It is noticeable that this diffusion was found negligible in the case of aroma compounds [104,155]. Therefore, the molecular effective diffusion leads its behavior through the membrane, and the mass transfer coefficient of the membrane is expressed as follows:

$$K_m^i = \frac{M^i \varepsilon D_{m-air}^i}{R_g T \delta \tau} \quad (3.12)$$

The influence of the interaction of each wine component with the membrane in terms of solubility, which is expected to contribute in some extent to the prediction of the components behavior during OD, is described here by the application of Hansen solubility parameters, *HSP*. These parameters integrate the dispersion force, δ_d, polar interaction (dipole-dipole), δ_p, and specific interaction such as hydrogen bonding, δ_h [98,156]. To predict the solubility of each component (1) on the membrane (2) the following expression can be used:

$$HSP = \left[(\delta_{d2} - \delta_{d1})^2 + \left(\delta_{p2} - \delta_{p1} \right)^2 + (\delta_{h2} - \delta_{h1})^2 \right]^{1/2} \quad (3.13)$$

where values of δ_{di}, δ_{pi} and δ_{hi} of each component and membrane polymer were obtained from previous literature [100] (Table S3.1). In fact, we propose the modification of previous Eq. (3.3) by introducing the *HSP*, within the global mass transfer resistance expression as follows:

$$R_G^i = R_f^i + R_m^i + R_s^i \rightarrow \frac{1}{A_e K_G^i} = \frac{H^i}{A_{in} M^i K_f^i} + \frac{1}{A_{lm}\left[\frac{HSP^i}{HSP^w}\right]^{\varphi} K_m^i} + \frac{H^i}{A_{ex} M^i K_s^i} \quad (3.14)$$

Here, each individual *HSP* is standardized with respect to membrane-water *HSP*. It is worth mentioning that the influence of this wine component-membrane interaction would be different for every component or family of components. Therefore, φ parameter, whose value would depend on each chemical family present in the wine (alcohols, esters and acids), is included in the expression. This modified model was applied to several alcohols, including ethanol, whose global mass transfer coefficients were properly defined and calculated accordingly (Table S3.2 and Table S3.3). Its further application to the rest of the volatile components is under study.

The calculations of the model were implemented through an Excel sheet from Microsoft Office Professional Plus 2016 applying the following procedure. Given the experimental system described above, the driving force across the membrane decreases as a function of time. This means that concentrations and fluxes of each component change with time. Knowing K_G^i by means of the theoretical model and the initial component *i* concentration in feed, the initial J^i (t = 0) is calculated using Eq. (2). This permeation flux allows us to obtain the mass of component *i* transferred and the new volumes of the feed and stripping phases, applying the boundary conditions corresponding to the membrane module and the volumes and flow rates used, after an infinitesimal time. Then, new concentrations in both phases can be obtained to recalculate the permeation flux of the component *i* for the next infinitesimal time. The calculation finishes when the dealcoholization time observed in the experimental section is reached.

3.4 Results and Discussion

3.4.1 Hollow fiber module characterization

Fig. 3.2 depicts the SEM images of one of the hollow fibers conforming the membrane module where it is possible to see its internal and external (290 ± 2 μm) diameter together with the membrane thickness (41 ± 2 μm). Besides, Fig. 3.2A and B show the cross-section and external surface of the hollow fiber, respectively. Membrane thickness and inner and outer diameters are in agreement with those provided by the module marketer. In addition, the inset in Fig. 3.2A shows the membrane cross-section at a higher magnification, where a relatively homogeneous morphology is observed.

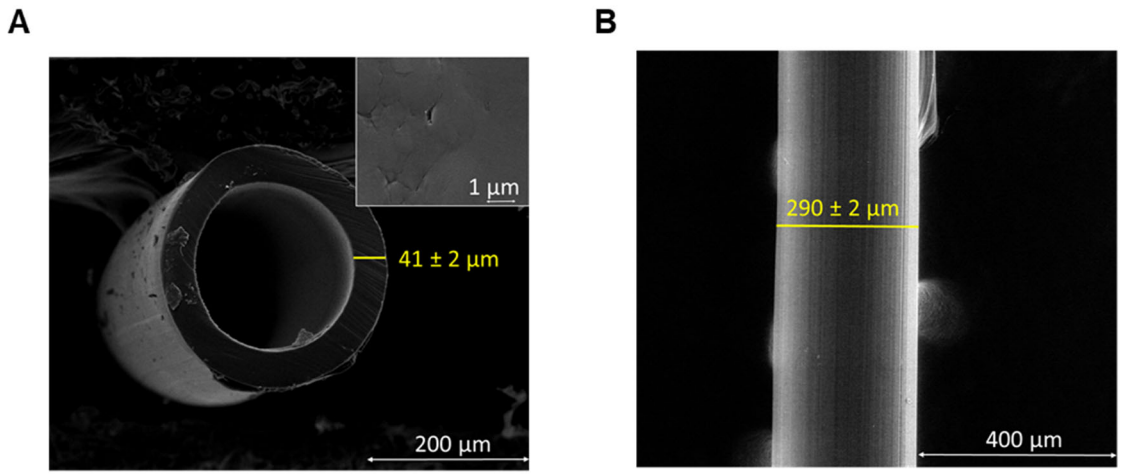

Fig. 3.2 Hollow fiber membrane cross-section (A) and external surface (B) SEM images of MM- 1 x 5.5 x- 50 Liqui-Cel™ hollow fiber. The inset of (A) shows a detail of the membrane cross section.

3.4.2 Osmotic distillation of water-ethanol

To study the performance of the OD setup, several preliminary experiments were carried out feeding water-ethanol solutions for dealcoholization. To accurately estimate the ethanol flow through the membrane from the stripping weight monitoring, each condition was replicated three times (Supplementary Tables S4 and S5). Indeed, the chromatographic analysis of ethanol at intervals of ca. 10 min that supported these studies demonstrated that the gain of weight in the striping reservoir corresponded to ethanol (Fig. S3.1 and Fig. S3.2 for the different working conditions in Table S3.4 and Table S3.5) within experimental error.

In addition, the good correlation of the ethanol behavior during the OD process with hydroalcoholic solutions with that observed with wine in previous reports [103,149] was confirmed here, allowing to use these results in further OD experiments with wine as feed (

Table S3.6).

3.4.3 Influence of feed/stripping ratio

Once the OD operation was validated with water-ethanol solutions, red wine was submitted to partial dealcoholization using the same experimental set up. With the goal of a decrease in the alcoholic degree of 3 v/v% (i.e. from the initial 14.5 v/v% to 11.5 v/v%), the volume ratio of both feed/stripping streams ($V_f \cdot V_s^{-1}$) was revealed as a critical variable in the operation of the OD carried out in this chapter. For a constant volume of feed phase, V_f, of 375 mL, volumes of stripping phase, V_s, between 75 and

375 mL were used. Fig. 3.3(A-C) show the variation of the ethanol content in the feed and stripping streams with time for different $V_f \cdot V_s^{-1}$ ratios. For an accurate comparison, Fig. 3.3(D) plots together the three curves of alcohol content in the feed. As the stripping volume increased, a higher loss of alcohol towards the stripping water was obtained under the same operation time. The alcohol content -$V_f \cdot V_s^{-1}$- time interaction suggests that it is possible to plan the achievement of a certain degree of alcohol in a relatively short period of time, what would minimize the wine exposure to conditions that may alter its properties. Besides the operation was done at near 20 ^{o}C.

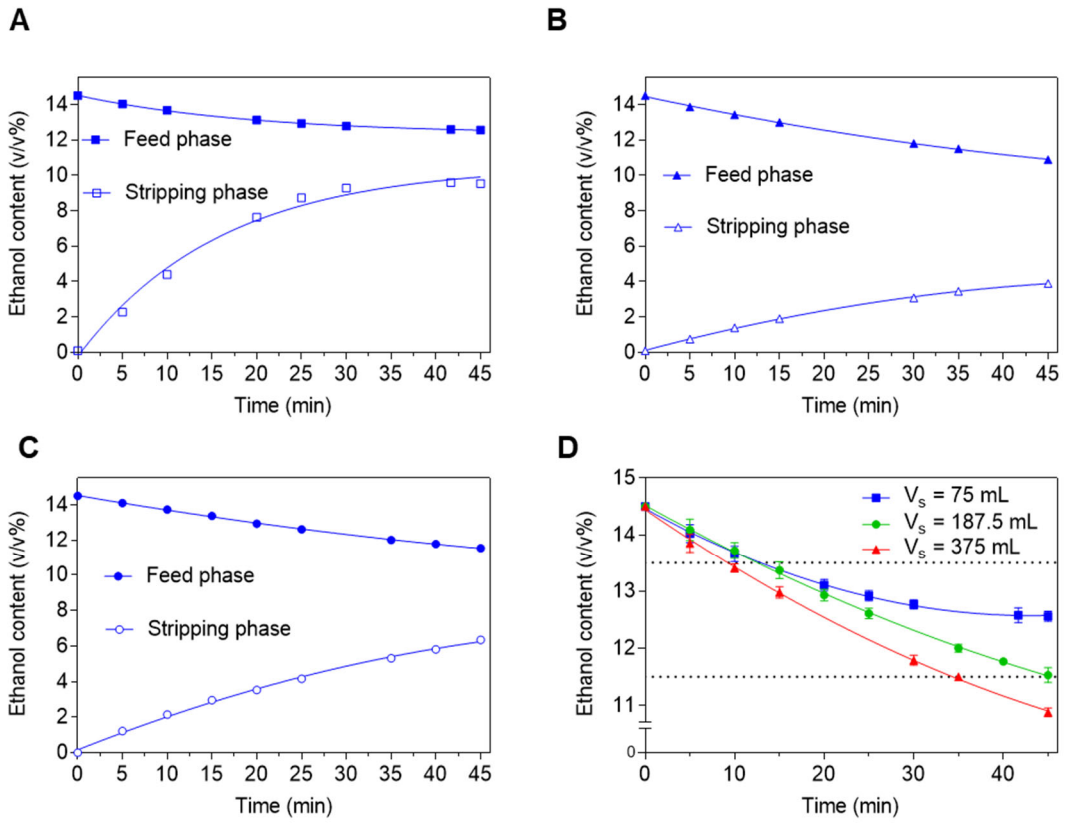

Fig. 3.3 Ethanol content as a function of time corresponding to a wine feed with 14.5 v/v% of ethanol. (A) $V_f \cdot V_s^{-1}$ = 5; (B) $V_f \cdot V_s^{-1}$ = 2; (C) $V_f \cdot V_s^{-1}$ = 1; (D) Simultaneous comparison of ethanol content in the feed phase at different volume conditions. V_f = 375 mL; temperature= 21 °C; Q_f = 65 mL.min-1; Q_s = 39 mL.min^{-1}. Represented data are the mean values with the corresponding standard deviations from a triplicated analytical measurement. The curves are only guides to the eye. Solid and open symbols correspond to feed and stripping sides, respectively.

It is noticeable that at $V_f \cdot V_s^{-1}$ = 5 (condition 1 in Table 2), the ethanol reduction was similar to those of the other ratios up to 20 min, and after that moment this operation condition limited the dealcoholization. This was due to the fact that the rapid decrease in the concentration gradient between feed and stripping streams, reaching almost

steady state (J_{Exp}^{EtOH}= 0) and preventing from achieving the degree of dealcoholization proposed (-3 v/v%). Moreover, no important difference in the evolution of the ethanol content as a function of time was observed with the other two $V_f \cdot V_s^{-1}$ values (conditions 2 and 3 in Table 3.2). The concentration gradient reached by working with these volume ratios allows the proposed degree of dealcoholization to be achieved with minimal differences in the operation time required (Fig. 3.3D). Thus, the optimal condition was set up at $V_f \cdot V_s^{-1}$ = 2 to use a lower amount of stripping phase for an approximately loss of 3 alcoholic degrees. In addition, the stripping phase after the osmotic distillation is considered as a waste, or at least a stream needed of further treatment, representing an economic loss. Therefore, further improvement of this process could be to obtain bioethanol from this waste with greater added value. In fact, in the latter case, it is possible to achieve a valorization of the stripping phase via distillation or pervaporation to obtain an alcohol-rich stream. In such case, the optimal condition ($V_f \cdot V_s^{-1}$ = 2), giving rise to a higher permeate ethanol concentration than $V_f \cdot V_s^{-1}$ = 1, would be more favorable from the energy point of view.

3.4.4 Influence of feed flow

Figure 4 shows the variation of the ethanol content for the experiments carried out with $V_f \cdot V_s^{-1}$ = 2. The stripping flow was set up at 39 mL·min^{-1}, while the feed flow was varied between 21 and 74 mL·min^{-1}. The effect of Q_s was not estudied in deph due to the lower influence on the ethanol transfer observed from water-ethanol experiments, in agreement with previous reported literature [149,157]. As Fig. 3.4 shows, an increment of the feed flow rate led to a faster decrease in the ethanol content of wine, what allowed to achieve the proposed goal (-3 v/v%) in 45 min at a Q_f of 74 mL·min^{-1}. In addition, working with a feed flow above 74 mL·min^{-1} did not have the expected increment of ethanol transport through the membrane. In consequence, it is not recommended to work with the current membrane area overpassing this flow.

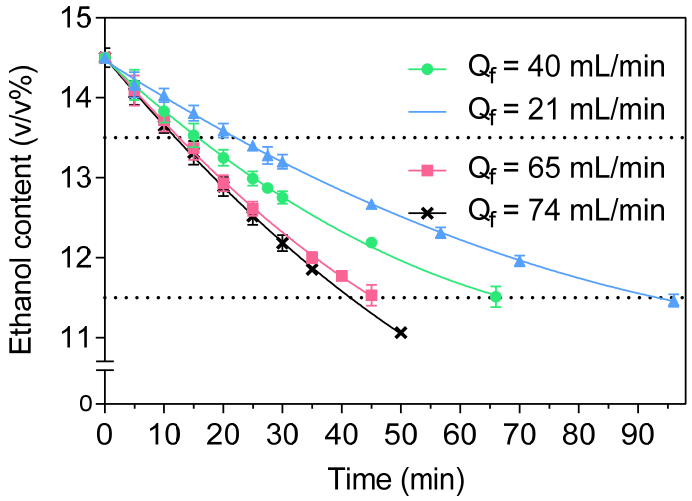

Fig. 3.4 Ethanol content as a function of time for a wine feed with 14.5 v/v% of ethanol and V_f/V_s = 2 and different feed flows; temperature= 21 ˚C. Represented data are the mean values with the corresponding standard deviations from a triplicated analytical measurement. The dotted lines represent the proposed dealcoholization degree (-3 v/v%) and (-1 v/v%) and the curves are only guides to the eye.

3.4.5 Validation of theoretical model

Using the proposed mathematical model, the theoretical mass transfer coefficients (K_s^i, K_f^i, K_m^i and R_G^i) were calculated for ethanol (shown in Table 3.3). The error corresponding to the ethanol concentration was estimated as follows:

$$Error\ (\%) = \frac{C_{Exp,t}^{EtOH} - C_{Theo,t}^{EtOH}}{C_{Exp,t}^{EtOH}} \tag{3.15}$$

where $C_{Exp,t}^{EtOH}$ and $C_{Theo,t}^{EtOH}$ are the ethanol experimental and theoretical concentrations, respectively, at a given process time (see Table 3.3).

Table 3.3 Theoretical mass transfer coefficients at different operation conditions.

Condition	$K_s \cdot 10^6$ [m·s^{-1}]	$K_f \cdot 10^6$ [m·s^{-1}]	$K_m \cdot 10^6$ [g·m^{-2}·s^{-1}·Pa^{-1}]	$K_G \cdot 10^6$ [g·m^{-2}·s^{-1}·Pa^{-1}]	Error [%]
1	9.57	2.91	210	31.8	1.8[a]
2	9.57	2.91	210	31.8	3.8[a]
3	9.57	2.91	210	31.8	4.5[a]
4	9.57	1.24	210	27.9	11.0[b]
5	9.57	2.02	210	30.4	8.3[c]
6	9.57	3.20	210	32.1	3.4[d]

[a] 45 min; [b] 96 min; [c] 66 min, [d] 50 min

From the membrane resistance, K_m calculation gave a value of $2.1 \cdot 10^{-4}$ g·m^{-2}·s^{-1}·Pa^{-1} which agrees with that obtained by Diban et al. [103,104], $1.6 \cdot 10^{-4}$ g·m^{-}2·s^{-1}·Pa^{-1}. As explained above, Hansen solubility parameters were applied to modify R_m to account for the influence of each component-membrane interaction (Eq. (3.14)). To validate the model, our study was focused on the alcoholic components (thus, excluding esters and acids), optimizing φ coefficient to minimize the sum of the standard errors between the theoretical and experimental concentration values of ethanol and other five different high alcohol compounds. In particular, alcohols whose presence is majority in the wine, and differing on the length of the aliphatic chain and/or the functional group (i.e. isoamyl alcohol, isobutanol, 1-hexanol, 2-phenylethanol and benzyl alcohol) were studied. The goodness of the theoretical approach was determined based on the sum of errors, which was calculated as follows:

$$Error\ (\%) = \sum \left(\frac{C_{Exp}^{i} - C_{Theo}^{i}}{C_{Exp}^{i}} \right)^2 \quad (3.16)$$

An error of 4.3 % was obtained using a φ value of 2.29, while the error was 30 % from the non-modified R_m. Then, R_m modified values correlated better with the loss of all alcohols tested than non-modified R_m values, showing a lower difference between theoretical and experimental values in case of high alcohol losses (Fig. 3.5).

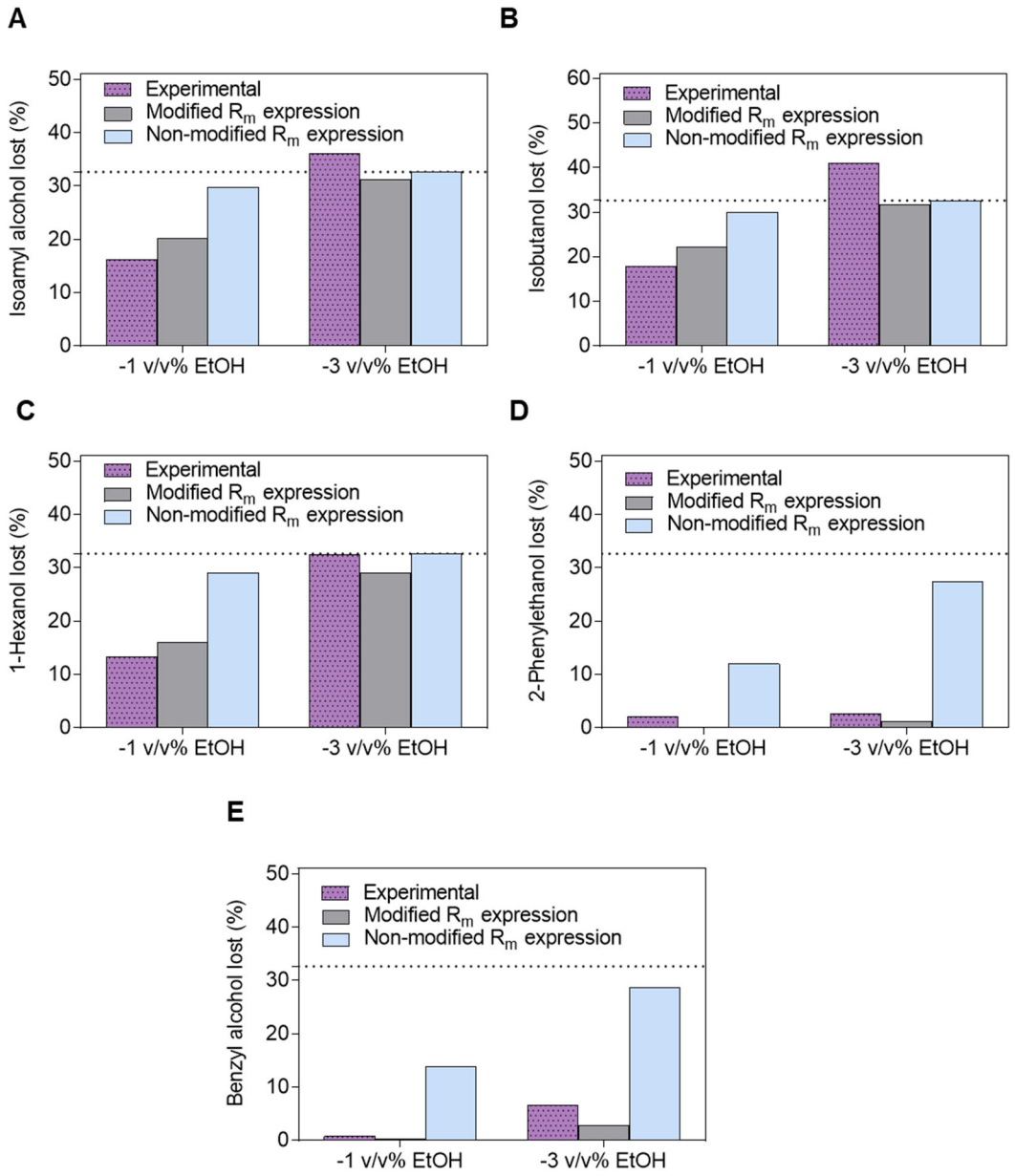

Fig. 3.5 Experimental and predicted losses of high alcohols from modified and non-modified Rm expression: (A) isoamyl alcohol, (B) isobutanol, (C) 1-hexanol, (D) 2-phenylethanol and (E) benzyl alcohol. The dotted line represents the steady state loss fixed by the ratio $V_f \cdot V_s^{-1} = 2$ (i.e. calculated from the mass balance when feed and stripping ethanol concentrations were equal); temperature= 21 °C.

The losses of aliphatic alcohols (isoamyl alcohol, isobutanol and 1-hexanol) after a partial dealcoholization of 3 v/v% were close to the steady state ($J^{EtOH} = 0$), being adequately predicted by both models. However, at a lower degree of dealcoholization (1 v/v%), both models differ in their predictions. Thus, after reducing one degree of ethanol, the flux calculated using the non-modified R_m values was overestimated in all the aliphatic alcohols tested, while using the current model this overestimation was corrected. On the other hand, aromatic alcohols (2-phenylethanol and benzyl alcohol)

showed an experimental behavior significantly different from that of the aliphatic alcohols tested due to their minor volatility and higher molar mass. This means that their fluxes depend mainly on R_m, what increases the difference between both theoretical predictions. Thus, for the two dealcoholization steps, the flux calculated using the non-modified R_m values was overestimated, while using the current (modified) model this overestimation was partially corrected. As can be seen in Fig. 3.5D and Fig. 3.5E, the model predictions for aromatic alcohols were not as good as for aliphatic alcohols, possibly related to the influence of aromatic ring on the –OH group.

Once the model to calculate the theoretical R_m values was optimized, the global mass transfer resistance was obtained to predict the ethanol transfer during dealcoholization process at different operating conditions. Fig. 3.6 depicts the theoretical estimation of each local resistance applied to calculate the global mass transfer resistance for ethanol. Fig. 3.6A and Fig. 3.6B show the results at different Q_f and Q_s conditions, respectively.

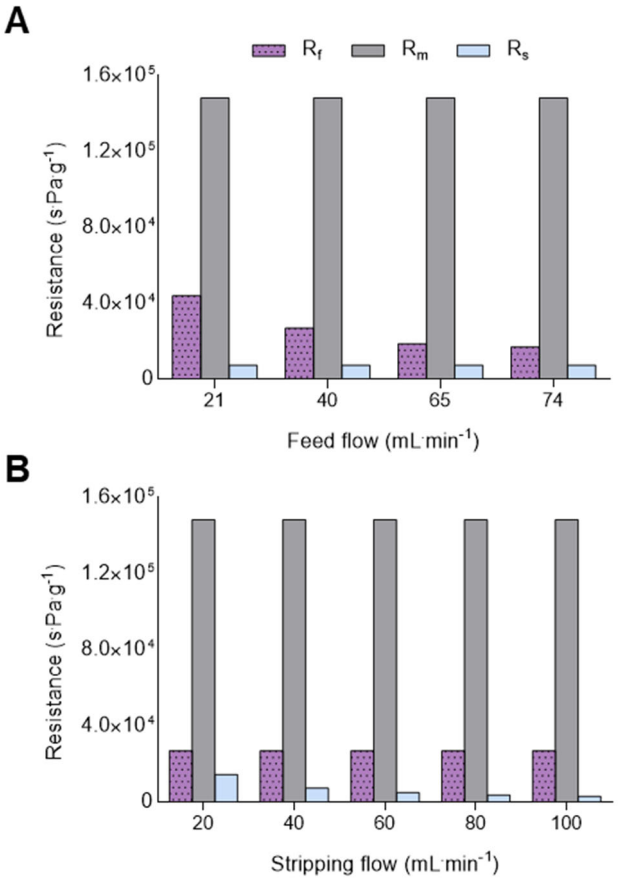

Fig. 3.6 Simulated contribution of each local resistance to the R_G for ethanol: (A) as a function of feed flow (Q_f) (conditions used in experiments 2, 4, 5 and 6, see Table 3.2); (B) results obtained varying the stripping flow (Q_s) in the 20 - 100 mL·min^{-1} range.

Fig. 3.6 demonstrates that high flows improve the hydrodynamic conditions minimizing the feed and stripping boundary layer resistances, locating the main resistance in the membrane. In addition, the influence of R_f becomes lower as the flow increases, giving rise to a global transfer resistance that is not dependent on the flow (Fig. 3.6A). Hence, from a certain flow, the resistance associated to the feed boundary layer reaches a minimum, maintaining the global transfer resistance independent from feed flow. Moreover, R_s shows the minor contribution comparing to the others (Fig. 3.6A and B) as mentioned above. These results are in agreement with our empirical observations (Fig. 3.4), and a similar tendency was found in previous experimental reports [104,157].

Graphical representations of the evolution of theoretical and experimental ethanol fluxes are shown in Fig. 3.7 and Fig. 3.8 to corroborate the suitability of the mathematical model. As can be seen, similar theoretical trends and values to the experimental ones can be inferred from these figures, in line with the reduced ethanol concentration error reported in Table 3.3. Besides, the experimental fluxes easily achieved from the weight gained by the stripping phase are similar to those obtained from the chromatographic analyses, meaning the mass transfer corresponds almost exclusively to ethanol. The largest deviation between the simulated curves and the experimental values as a function of $V_f \cdot V_s^{-1}$ ratio can be appreciated in condition 1 (Fig. 3.7A, Table 3.2) where the ethanol permeation flux almost reached steady state as Fig. 3.3A suggested.

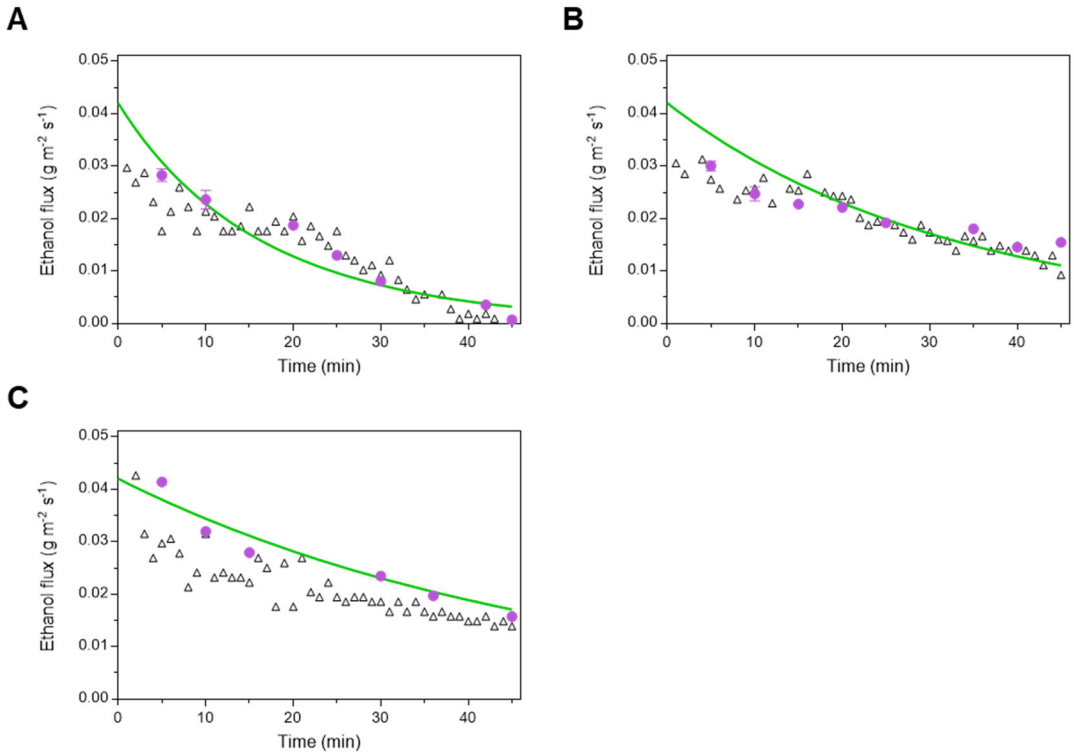

Fig. 3.7 Mass fluxes as a function of time for 375 mL of wine with 14.5 v/v% of ethanol at different volume ratios between feed and stripping phases (V_f/V_s): (A) 5, (B) 2, (C) 1. Temperature = 21 ºC. Q_f = 65 mL·min^{-1}, Q_s = 39 mL·min^{-1}. Green continuous lines represent the ethanol flux predicated by the model. Circles coincide with experimental ethanol mean values with the corresponding standard deviations (very small to be shown) from a triplicated chromatographic analytical measurement. Triangles represent the experimental total flux; determined by means of the stripping weight.

The influence of the $V_f \cdot V_s^{-1}$ ratio on the variation of the ethanol content was also adequately predicted by the mathematical model as Fig. 3.8 depicts, although it is noticeable that at low feed flow rates (Fig. 3.8A), the predicted results slightly deviate from the experimental values. This may be due to the influence of the concentration polarization on the ethanol flux, which has not been taken into account in the theoretical model.

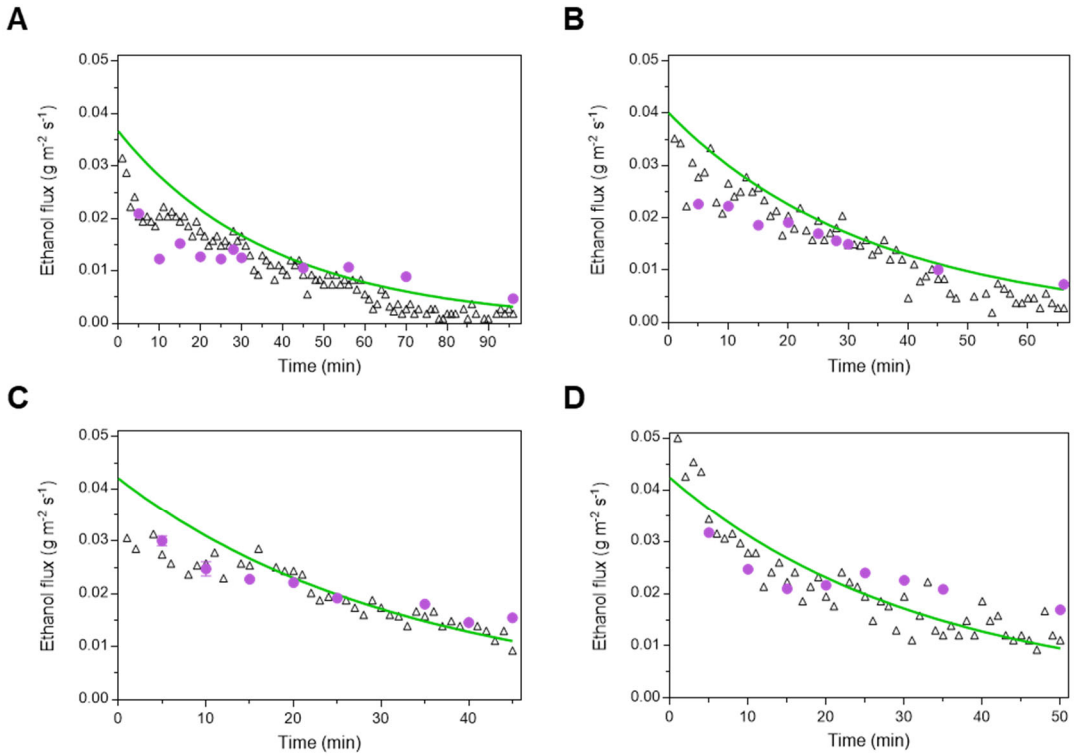

Fig. 3.8 Ethanol flux as a function of time for a wine with 14.5 v/v% of ethanol at stripping flow of 39 mL·min^{-1} and different feed flows (Q_f): (A) 21 mL·min^{-1}, (B) 39 mL·min^{-1}, (C) 65 mL·min^{-1}, (D) 74 mL·min^{-1}. (V_f = 375 mL, V_s = 187.5 mL, Temperature = 21 ºC). Green continuous lines represent the ethanol flux predicated by the model. Circles coincide with experimental ethanol mean values with the corresponding standard deviations (very small to be shown) from a triplicated chromatographic analytical measurement. Triangles represent the experimental total flux; determined by means of the stripping weight.

Finally, Fig. 3.9 compiles a set of 11 experiments carried out under the same experimental conditions and using the same polypropylene hollow fiber membrane module (in fact, the module was applied in more than 20 experiments) to dealcoholize both water-ethanol solutions and the Tempranillo wine. No important changes in ethanol permeation fluxes are appreciated with an average value of permeation flux of 0.025 ± 0.005 g·m^{-2}·s^{-1}. This suggests that the permeation flux was unaffected by the type feed (either hydro alcoholic solutions or red wines) but also by a possible fouling generated during every experiment [158], having in mind that the hollow fiber membrane modules were submitted to an exhaustive cleaning protocol (water-NaOH solution-water treatments followed by drying evacuation and N_2 (g) flushing) after every use, as described in the experimental section. In summary, this allows to discard membrane fouling along the cumulative operation of the hollow fiber membrane module.

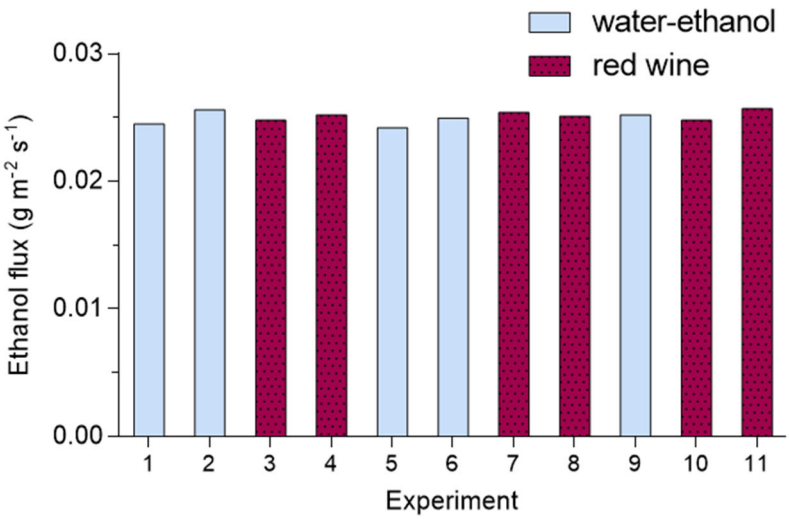

Fig. 3.9 Ethanol flux at 25 min obtained for 11 dealcoholization experiments carried out using the same hollow fiber membrane module under the same operation conditions of V_f = 250 mL; V_s = 125 mL; Q_f = 74 mL·min^{-1}; Q_s = 39 mL·min^{-1}.

3.5 Conclusions

A partial dealcoholization of wine was successfully carried out by osmotic distillation (OD) using a polypropylene hollow fiber membrane module with a membrane area of 0.18 m^2. The feasibility of the approach was first established using water-ethanol solutions, whose results showed a good correlation with those obtained with Tempranillo red wine. This variety was used to study the influence of different experimental conditions on the ethanol mass transfer observed during dealcoholization. The best results were obtained at feed/stripping volume ratio = 2 and feed flow = 74 mL min^{-1}.

Furthermore, a mathematical model was proposed to predict the OD performance, obtaining an error as small as 4.3 % in the prediction of alcohol loses. In this model, the membrane resistance expression, based on the so-called dusty gas model, was modified including a component-membrane specific interaction that allowed to describe the components behavior when permeating through the membrane as a function of their volatilities (Henry's constants) and their interactions with the membrane material in terms of Hansen solubility parameters (*HSP*).

The behavior of ethanol and other five high alcohols whose presence is majority in the wine was studied to develop the proposed membrane resistance expression. In addition, it was shown that the calculated membrane resistance (modified by the inclusion of Hansen solubility parameters, *HSP*) allowed an adequate prediction for alcohols with low Henry's constant (i.e. the aliphatic alcohols studied here), while it was

slightly overestimated for alcohols with high Henry's constant such as 2-phenylethanol and benzyl alcohol. It is worth noticing that the *HSP* based modification gave rise to relatively small errors when experimental and theoretical ethanol concentrations were compared in a relatively wide range of operating conditions, and also when experimental and theoretical high alcohols concentrations were compared at the best working conditions in terms of feed flow, feed/stripping volume ratio and dealcoholization degree.

Finally, the stable operation of the polypropylene hollow fiber membrane module was demonstrated through its use in more than 20 dealcoholization experiments with both water-ethanol solutions and red wine.

3.6 Supplementary information

Table S3.1 Hansen solubility parameters for water and alcohols studied.

Component	δ_d [MPa$^{0.5}$]	δ_p [MPa$^{0.5}$]	δ_h [MPa$^{0.5}$]	*HSP* [MPa$^{0.5}$]
Polypropylene	18	0	1	0.0
Water	15.5	16	42.3	44.4
Ethanol	15.8	8.8	19.4	20.5
Isoamyl alcohol	15.8	5.2	13.3	13.5
Isobutanol	15.1	5.7	15.9	16.2
1-Hexanol	15.9	5.8	12.5	13.1
2-Phenylethanol	19	5.8	12.8	13.2
Benzyl alcohol	18.4	6.3	13.7	14.18

Table S3.2 Parameters for experimental conditions 1 to 6.

Experimental condition	Component	Re_s [-]	Sh_s [-]	$K_s \cdot 10^6$ [m·s^{-1}]	Re_f [-]	Sh_f [-]	$K_f \cdot 10^6$ [m·s^{-1}]	$D_{m\text{-}air} \cdot 10^6$ [m^2·s^{-1}]
1	Ethanol	1.64	1.62	9.57	1.95	0.81	2.91	11.5
2	Ethanol	1.64	1.62	9.57	1.95	0.81	2.91	11.5
3	Ethanol	1.64	1.62	9.57	1.95	0.81	2.91	11.5
4	Ethanol	1.64	1.62	9.57	0.59	0.34	1.24	11.5
5	Ethanol	1.64	1.62	9.57	1.18	0.56	2.02	11.5
6	Ethanol	1.64	1.62	9.57	2.22	0.83	3.20	11.5

V^{EtOH} (cm^3): 50.32; V^{air} (cm^3) = 20.1; D^{EtOH} (m^2·s^{-1}): 1.29·10^{-9}; EtOH molar volume, V_m^{EtOH}, (cm^3·mol^{-1}): 58.32;

Continued...

Experimental condition	Component	$D_k \cdot 10^6$ [$m^2 \cdot s^{-1}$]	$K_m \cdot 10^6$ [$g \cdot m^{-2} \cdot s^{-1} \cdot Pa^{-1}$]	$\left[\frac{HSP^i}{HSP^w}\right]^{\varphi}$ [-]	$K_G \cdot 10^6$ [$g \cdot m^{-2} \cdot s^{-1} \cdot Pa^{-1}$]
1	Ethanol	3.7	210	0.027	31.8
2	Ethanol	3.7	210	0.027	31.8
3	Ethanol	3.7	210	0.027	31.8
4	Ethanol	3.7	210	0.027	27.9
5	Ethanol	3.7	210	0.027	30.4
6	Ethanol	3.7	210	0.027	32.1

Table S3.3 Parameters for the alcohols studied in experimental condition 6.

E.C.	Component	Sh_s [-]	Sh_f [-]	$K_f \cdot 10^6$ [$m \cdot s^{-1}$]	$D_{m\text{-}air} \cdot 10^6$ [$m^2 \cdot s^{-1}$]	$K_m \cdot 10^6$ [$g \cdot m^{-2} \cdot s^{-1} \cdot Pa^{-1}$]	$K_G \cdot 10^6$ [$g \cdot m^{-2} \cdot s^{-1} \cdot Pa^{-1}$]
6	Isoamyl alcohol	2.38	1	2.5	7.8	706	50
6	Isobutanol	2.13	0.97	2.7	8.7	661	66
6	1-Hexanol	2.65	1	2.3	7.2	748	55
6	2-Phenylethanol	2.50	1	2.4	6.9	864	87
6	Benzyl alcohol	2.29	0.99	2.5	7.5	830	98

Re_s: 1.64; Re_f: 2.22; V^{air} ($cm^3 \cdot mol^{-1}$): 20.1. H^i = Henry constant.

Continued…

E.C.	Component	$\left[\frac{HSP^i}{HSP^w}\right]^{\varphi}$ [-]	H^i [$m^3 \cdot Pa \cdot mol^{-1}$]	$D^i \cdot 10^{10}$ [$m^2 \cdot s^{-1}$]	V^i [cm^3]	V_m^i [$cm^3 \cdot mol^{-1}$]
6	Isoamyl alcohol	0.010	1.35	8.86	111.7	110.1
6	Isobutanol	0.016	1	9.86	92.2	91.3
6	1-Hexanol	0.009	1	8.20	132.2	125.6
6	2-Phenylethanol	0.009	0.05	8.41	137.1	120.1
6	Benzyl alcohol	0.012	0.06	9.17	116.6	104.0

Table S3.4 Experiments with ethanol – water at different V_s values with RSD being relative standard deviation.

Time [min]	$[EtOH]_{f,0}$ [v/v%]	V_f [mL]	V_s [mL]	$[EtOH]_{f,t}$ [v/v%]	$[EtOH]_{s,t}$ [v/v%]	RSD [%]
30	13	500	100	11.6	9.3	2.1
30	13	500	250	10.9	3.8	1.9
30	13	500	500	10.8	2.3	2.3

Q_f = 65 mL·min^{-1}; Q_s =39 mL·min^{-1}; temperature= 21 ^{o}C;

Fig. S3.1 Circles coincide with experimental ethanol mean values from the chromatographic analysis. Continuous line with dots represent the experimental ethanol values determined by means of the stripping weight. (A) V_s = 100 mL; (B) V_s = 250 mL; (C) V_s = 500 mL.

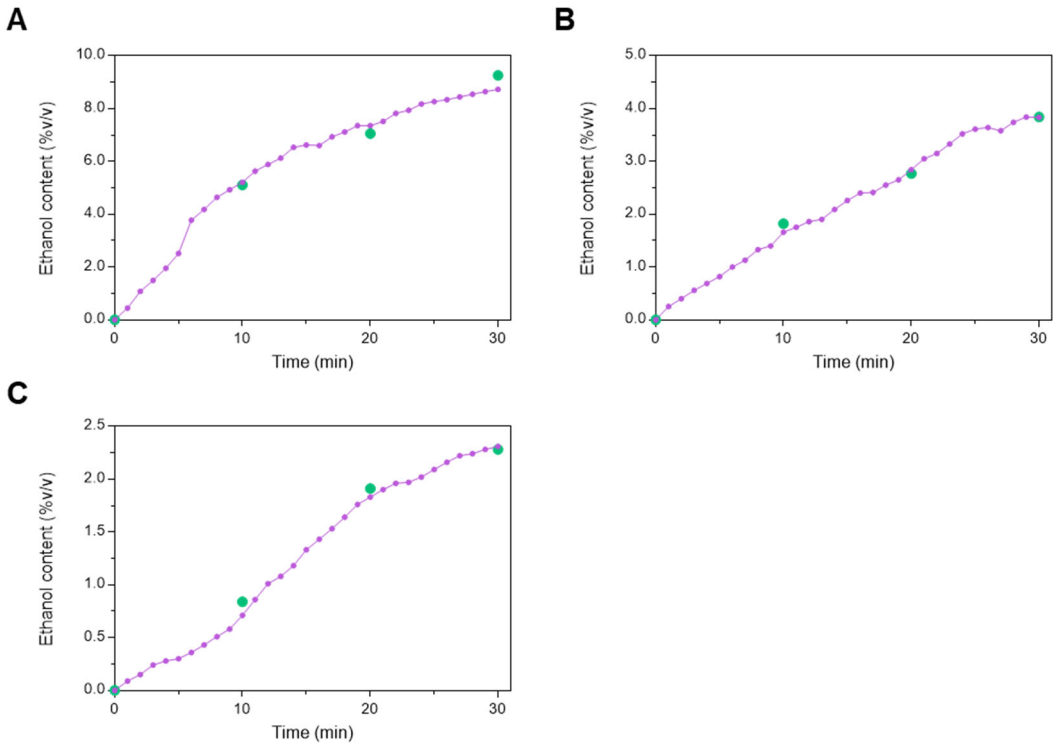

Table S3.5 Experiments with ethanol – water at different Q_f values with RSD being relative standard deviation.

Time [min]	$[EtOH]_{f,0}$ [v/v%]	Q_f [mL·min^{-1}]	Q_s [mL·min^{-1}]	$[EtOH]_{f,t}$ [v/v%]	$[EtOH]_{s,t}$ [v/v%]	RSD [%]
30	13	19	41	11.7	3.1	4.0
30	13	40	41	11.3	3.6	1.7
30	13	65	41	10.9	3.8	1.9
30	13	111	41	10.8	4.1	1.3

V_f = 500 mL; V_s =250 mL; temperature= 21 ^{o}C;

Fig. S3.2 Circles coincide with experimental ethanol mean values from the chromatographic analysis. Continuous line with dots represent the experimental ethanol values determined by means of the stripping weight. (A) Q_f = 19 mL·min^{-1}; (B) Q_f = 40 mL·min^{-1}; (C) Q_f = 65 mL·min^{-1}; (D) Q_f = 111 mL·min^{-1}.

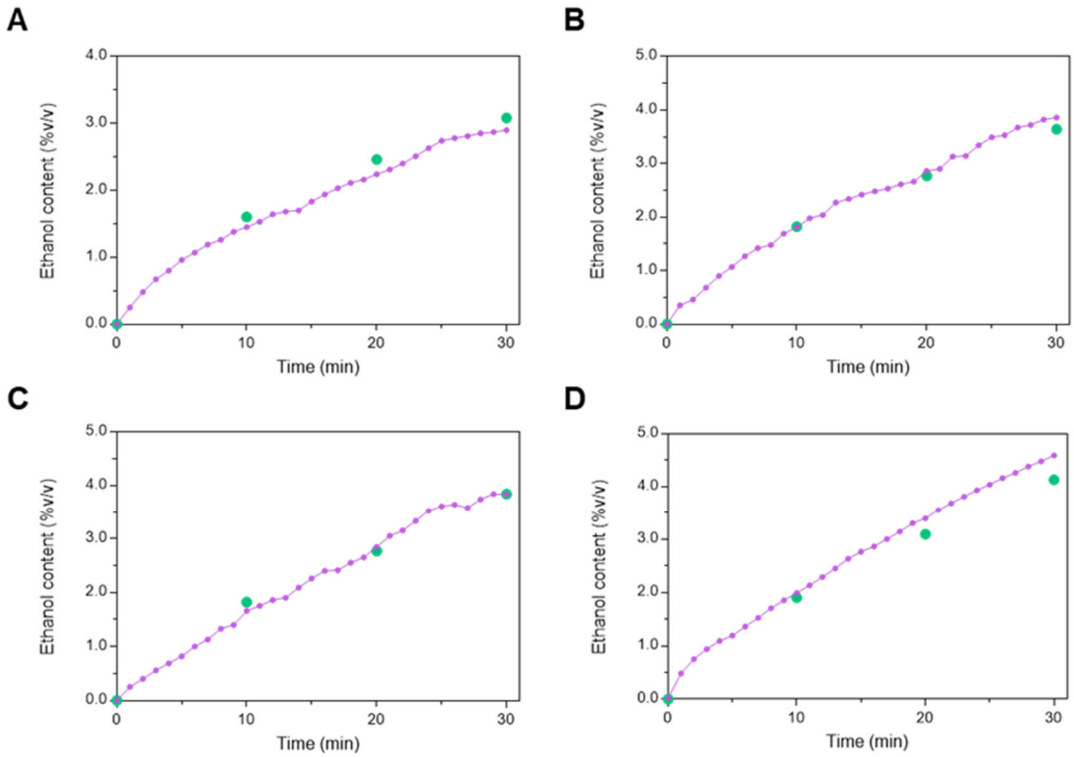

Table S3.6 Comparison between dealcoholization of ethanol – water solutions and wine with RSD being relative standard deviation.

Time [min]	$[EtOH]_{f,0}$ [v/v%]	Q_f [mL·min^{-1}]	$[EtOH]_{f,t}$ Wine [v/v%]	$[EtOH]_{f,t}$ EtOH-water [v/v%]	RSD [%]
96	14.5	19	11.5	11.3	0.8
50	14.5	74	11.1	11.4	1.8

V_f = 375 mL; V_s =187.5 mL; Qs = 41 mL·min^{-1}; temperature= 21 °C

CHAPTER 4

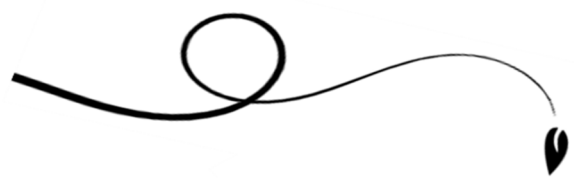

PVDF HYDROPHOBIC HOLLOW FIBER MEMBRANE FOR PARTIAL DEALCOHOLIZATION OF RED WINE BY OSMOTIC DISTILLATION AS A STRATEGY TO MINIMIZE THE LOSS OF AROMAS

From Esteras-Saz, J; De la Iglesia, Ó; Marechal, W; Lorrain, O; Peña, C; Escudero, A; Téllez, C; Coronas, J. PVDF hydrophobic hollow fiber membrane modules for partial dealcoholization of red wine by osmotic distillation as a strategy to minimize the loss of aromas, In preparation.

4 PVDF hollow fiber membrane modules for partial dealcoholization of red wine by osmotic distillation as a strategy to minimize the loss of aromas

4.1 Introduction

The consumption of low- or non-alcoholic beverages instead of alcoholic ones is a worldwide trend, being a common view particularly in Europe and North America, and wines are not outside this trend [159–164]. Regarding the social tendency towards a healthy lifestyle, with customers desiring fresh product choices and alternatives in order to reduce alcohol consumption, wine market is committed to offer wines with lower ethanol content that maintain satisfactory organoleptic profiles [20,41,142].

Besides, sugar accumulation is a feature of the ripening process in grape berries that confers the optimal flavour to a wine. Recent global increase of temperatures has an evident effect on the grape cultivation, resulting in the production of grapes with higher sugar levels [16], mainly glucose, which comprises 50 % of total fermentable sugars in the grape must [68]. Hence, wines at full phenolic maturation have an undesirably high ethanol content [20,135]. For instance, red wines from the Mediterranean region are already exceeding 14 v/v% [138], while Australian winemakers have seen an increment of the alcoholic strength in their wines from 12.4 to 14.4 v/v% [139]. Furthermore, these higher ethanol concentrations increase the bitterness and hotness taste and reduce acidity, masking some key aromas such as those related to monoterpenes, higher alcohols, and esters, and thus decreasing wine quality [22].

Another key issue is that ethanol is subject to import duties and taxes in some countries, and ethanol in wine is not an exception [146]. Taking into account all the aforementioned reasons, one of the most crucial challenges currently faced by the wine community is the creation of wines with lower alcohol content (i.e. 2–3° below the current ones) preserving as much as possible their organoleptic and sensorial properties together with their ludic character. Over the last 15 to 20 years, winemakers and researchers have studied different strategies for reducing the alcohol content of wines as a response to the high sugar concentration at their phenolic maturity and in order to either satisfy consumers demand for low-alcohol grape derived products or avoid the mentioned taxes ([67,143,144,165].

The techniques for reducing the alcohol in wine can be applied along the three different stages of its production (namely, pre-fermentation, fermentation and post-

fermentation), while the most popular are those focused on the third one, removing ethanol from finished, well developed wines by separation with or without a membrane (typical thermal distillation). In fact, techniques like spinning cone column (SCC) [47,166] or reverse osmosis (RO) [105,167,168] are already established in the wine industry. Nonetheless, RO requires water to effectively dealcoholize wine, which in turn represents a significant disadvantage due to the fact that it is frequently prohibited in many vintners nations [67,169]. In addition, the pressure required makes the process more cost-effective (even consuming less energy than distillation process). Moreover, SCC performance needs mild temperatures (around 28-38 °C) and low vacuum pressure, increasing both the cost of equipment and that associated with its operation [96]. Owed to its important benefits in energy demand, membrane osmotic distillation (OD), also known as evaporative pertraction (EP), is currently a technology to reduce ethanol content in alcoholic beverages gaining popularity and several studies have reported promising results regarding its performance for the mentioned purpose [95,103,104,107,146,157,170–173]. Energy efficiency of a process is closely related to the working conditions, and OD is able to operate adequately at low, nearly room temperatures (10 °C to 20 °C), indeed avoiding the thermal damage to wine components [107] and, since no pressure is required, reducing the pumping energy consumption.

OD is an isothermal membrane distillation where a hydrophobic porous membrane acts as a contactor between two phases, wine and extracting agent (usually water). Both phases are fed along to the opposite sides of the membrane (outer and inner sides of the hollow fibers, respectively), typically in a counter-flow configuration. The hydrophobic character of the membrane avoids the water transport between both streams, ethanol (which is in vapor phase inside the membrane pores [109,174]) being the main component in the permeate after water [170]. As a consequence, the driving force should be the gradient of concentration of ethanol and the other volatile compounds between the wine feed and the water stripping phase [157], expecting that components with less concentration (aromas) are retained better in the feed (wine).

Despite using the same polypropylene (PP) membrane in most cases (mostly commercial Liqui-Cel^{TM} from 3M), a fairly wide range of results for aromas can be found in the literature, showing larger aroma losses than expected [107,151]. This suggests that not only the driving force (i.e. the gradient of concentration between both streams) led the transfer of the components through the membrane. Recently, volatility has been revealed as a major factor determining the loss of volatile compounds during OD and, generally, those components with minor Henry constant show a higher loss than ethanol in spite of the higher driving force of the latter [146]. Moreover, it has been reported that the inclusion of Hansen solubility parameters (HSP) [99] to address the role of the

membrane in the separation mechanism during OD allowed an adequate prediction for the behavior of volatile alcohols during OD [170].

This research aims at gaining insight into the performance of membrane OD as a dealcoholization technique and into the behavior of volatile compounds of wine during its dealcoholization. In this regard, possible effects of compound volatility and concentration over the aroma losses through the contactor as well as the effect of temperature were studied. Tempranillo red wine was chosen to carry out the experiments based on previous studies that reported it as a promising variety to stand a dealcoholization process [104,170]. Lisanti et al. [106] obtained an average loss of 42 % for ethyl acetate, isoamyl acetate and ethyl hexanoate dealcoholizing Aglianico red wine, while losses around 30-40 % were obtained for the same components (70 % in case of ethyl octanoate) feeding Merlot red wine by Diban et al. [103]. However, other two different wines (Tempranillo and Garnacha) were later partially dealcoholized by Diban et al. [104] monitoring two key components: isoamyl acetate and ethyl hexanoate, obtaining better results for Tempranillo wine (around 20 % loss for both components instead of 32 % shown by Garnacha). Having said this, three different Tempranillo red wines that differed in their aroma composition were treated by OD in order to assess if the capability of membrane OD to obtain a final wine with a satisfactory aroma profile can be generalized to different red wines. Importantly, the effect of the membrane was analyzed by comparing the performance of the most used membrane in literature, the PP Liqui-Cel^{TM} membrane, with other PP membrane with higher pore size [175] (supplied by ZENA) and a superhydrophobic polyvinylidene fluoride (PVDF) membrane (developed by Polymem). PVDF constitutes a membrane material with recent promising results when applied to several separation technologies such as same membrane osmotic distillation [157,176,177], focusing only on a few aroma components and without comparison with other membrane materials, and nanofiltration [178].

4.2 Materials and methods

4.2.1 Wines submitted to OD

The three Tempranillo red wines dealcoholized in this chapter were kindly provided by Bodegas Matarromera (Valbuena de Duero, Valladolid, Spain). The initial composition of each wine, grouped into the main chemical families, is presented in Table 4.1, while Table S4.1 shows their detailed composition, distinguishing each major volatile compound.

Table 4.1 Concentration of main compounds in the different treated wines by membrane OD.

Wine	Ethanol [v/v%]	Esters ($mg \cdot L^{-1}$)		Acids [$mg \cdot L^{-1}$]	Alcohols ($mg \cdot L^{-1}$)		Methionol [$mg \cdot L^{-1}$]
		SC[a]	FA[b]		Aliphatic	Aromatic	
1	14.8	96	157	786	456	62	2.7
2	14.7	167	219	1299	374	50	2.8
3	14.1	56	65	404	250	32	1.4

[a] Derived from straight chain fatty acids. [b] Derived from fermentation acids.

4.2.2 OD membrane modules

Three modules have been used to carry out the OD experiments: Liqui-Cel™ (MM-1x5.5) membrane module, PP_1, from 3M (equipped with hollow fibers of hydrophobic porous polypropylene (PP)); hydrophobic higher pore size PP based hollow fibers, PP_2, from ZENA; and superhydrophobic PVDF hollow fibers, PVDF, developed by Polymem (Toulouse, France). The PVDF membranes present a "lotus effect" due to the control of their external roughness achieved during their fabrication. Main characteristics of the different hollow fiber membrane modules are detailed in Table 4.2 (and shown in Fig. S4.1).

Table 4.2 Characteristics of hollow fibers membrane modules.

Membrane module parameter	PP_1 (3M)	PP_2 (Zena)	PVDF (Polymem)
Effective membrane area (m^2)	0.18	0.14	0.036
Number of fibers	2300	1385	64
Nominal pore size (μm)	0.03	0.1	Not available
Porosity (-)	0.4	0.5[a]	Not available
Tortuosity (-) [b]	2.5	1.9	Not available
Water contact angle (°)	102[c]	104[d]	>125[e]
Effective fiber length (cm)	14	11	28
Membrane thickness (μm)	40	35	140
Inner fiber diameter (μm)	220	240	350
Outer fiber diameter (μm)	300	310	630

[a] [179]; [b] $\tau = 1/\varepsilon$; [c] [180]; [d] [181]; [e] supplied by the manufacturer.

4.2.3 OD membrane characterization

SEM characterization of PP_1 (3M membrane) was previously carried out by the authors, showing the cross section and external surface of a hollow fiber [170], being in agreement with those provided by the module marketer (Table 4.2). On the other hand, the higher pore size membrane named PP_2 (ZENA membrane) is shown on the manufacturer's webpage (www.zena-membranes.cz; last connection in January 2023)

Finally, Fig. 4.1 depicts the SEM images of one PVDF hollow fiber. The cross-section of the membrane (Fig. 4.1A) shows the asymmetric structure of the hollow fiber, with higher size pores at the inner side while the outer shows a spongy-like distribution. Besides, the hollow fibers have a thickness of 139 ± 10 µm. The estimated thickness of the outer surface modified for superhydrophobicity (see Fig. 4.1A inset) is around 20 µm (a SEM cross section with higher magnification can be seen in Fig. S4.2). In addition, Fig. 4.1B shows the membrane top view at a higher magnification, where the outer surface roughness can be observed.

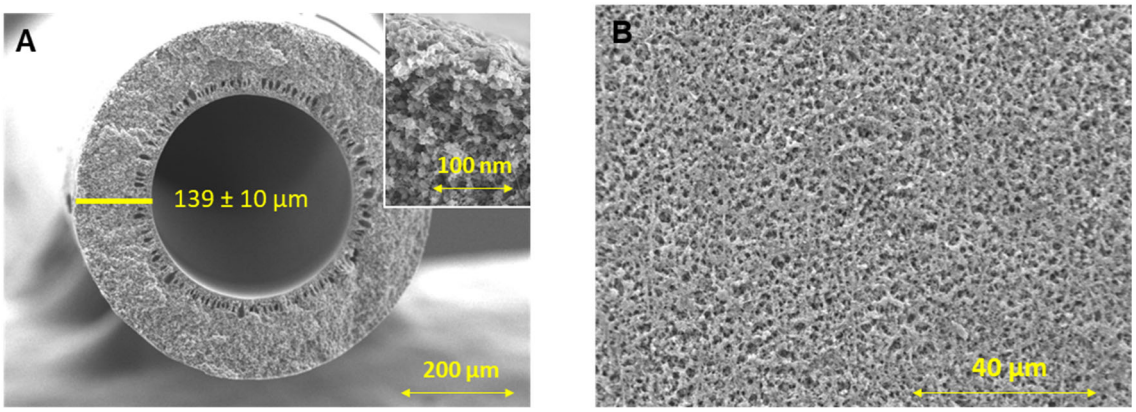

Fig. 4.1 SEM images of PVDF hollow fiber membrane: cross section (A) and top view (B). The inset in A shows a detail of the outer membrane cross section.

4.2.4 Experimental setup

OD experiments were carried out by duplicate in a lab scale plant equipped with the above-mentioned membrane modules, as well as with peristaltic pumps (Dinko, model 1.9735.15) and tube and shell side pressure (1 bar) and temperature indicators. The system temperature was controlled at 11 or 15 ^{o}C thanks to a chiller bath circulator (Julabo, CORIO-201F). Prior to each experiment, nitrogen (g) was forced to flow through the experimental system during 2 h at 100 $cm^3(STP)\cdot min^{-1}$ to achieve an inert atmosphere inside the dealcoholization set up.

To conduct an experiment, 250 mL of the wine was fed to the shell side of the membrane module at a rate of 74 mL·min^{-1}, while 125 mL of stripping stream (pure water) was fed at a rate of 40 mL·min^{-1} to the tube side. Retentate and permeate flows were continuously recirculated to the wine and the water tanks, respectively. All the experiments were finished when the dealcoholization degree proposed (-3 v/v%) was achieved. After each experiment, cycles with pressurized water and compressed air were applied to clean the OD system. Specifically, membrane modules were subjected to additional cleaning with 0.5 wt% NaOH water solution described elsewhere [170].

Table 4.3 summarizes the conditions corresponding to the partial dealcoholization trials carried out in this study. The effect of temperature was evaluated with runs 1 and 2. The influence of the aromas starting concentrations was studied in trials 2-4. The evaluation of the different membrane modules corresponds to trials 3, 5 and 6, carried out using the same wine-2 as feed.

Table 4.3 OD experiments carried out at distinct temperatures, membrane modules and wines.

Trials	Wine	Membrane	Temperature [^{o}C]	Time [min]	Flux [L·m^{-2}·h^{-1}]
1	1	PP_1	15	25	0.12
2	1	PP_1	11	27	0.11
3	2	PP_1	11	27	0.11
4	3	PP_1	11	27	0.11
5	2	PP_2	11	29	0.13
6	2	PVDF	11	90	0.17

4.2.5 Osmotic distillation performance

Performance of the membrane OD as a dealcoholization technique was assessed considering two main aspects: ethanol flux through the membranes (J, L·m^{-2}·h^{-1}) and aroma losses (%), as opposed to aromas retention in the partial dealcoholized wine, at the same dealcoholization degree (-3 v/v%). Aroma losses were obtained as follows:

$$Aroma\ loss = \frac{[aroma]_0 - [aroma]_i}{[aroma]_0} * 100 \quad (4.1)$$

Where $[aroma]_0$and $[aroma]_i$ are the aroma concentration in wine before and after be treated, respectively. Ethanol concentrations from both streams were analyzed by a FID equipped gas chromatograph 7820A (Agilent Technologies) with a

PORAPAK Q80/100 column, 2 m × 1.8 in × 2 mm, working in splitless mode with a 1:100 ratio at 250 °C. Helium, the carrier gas, was fed at a constant flow of 1 mL min $^{-1}$ while the temperature in the oven was fixed at 200 °C. The following equation was used to calculate ethanol flux through the membrane.

$$J_i(t) = \frac{\Delta W}{A_e \Delta t} \quad (4.2)$$

Where ΔW is the variation of the ethanol amount in any stream, calculated from GC analysis, for a given interval of time, Δt, and A_e is the effective membrane area. Wine aromas were analyzed by GC-FID after each experiment, following a procedure previously reported [150].

4.3 Results and discussion

4.3.1 Influence of temperature

The role of temperature on the membrane OD performance was evaluated in the partial dealcoholization (-3 v/v%) of wine-1. Two experiments were carried out under two different temperatures: the typical work temperature in wineries, 15 °C (also the most used in literature), and our proposed temperature, 11 °C. It is worth mentioning that working at temperatures lower than 11 °C is not recommended because it could led to the precipitation of some wine components such as tartaric acid [182].

The behavior of ethanol and other 23 aroma components was evaluated to find the optimum working temperature with the aim of minimizing the OD impact on the wine organoleptic profile. As shown in Table 4.3 (trials 1 and 2), at 11 °C the ethanol flux lowered from ca. 0.12 to 0.11 $L \cdot m^{-2} \cdot h^{-1}$. This effect over the ethanol flux is mainly due to the increase in viscosity, which should in turn increase the thickness of the feed boundary layer [183]., that together with the reduction of vapor pressure [184] (i.e. the driving force across the membrane) and diffusion coefficients led to an increase of the experimental time required to achieve the dealcoholization degree proposed (-3 v/v%) from 25 to 27 min, which entails an increment of only an 8 %. Hence, the negative impact of the decreasing temperature over the ethanol flux may be considered negligible. With respect to the effect of the temperature change on the aroma behavior, Fig. 4.2 depicts the losses of major compounds at both working temperatures as a function of their Henry (H) constants, as volatility related parameters (see Table S4.2).

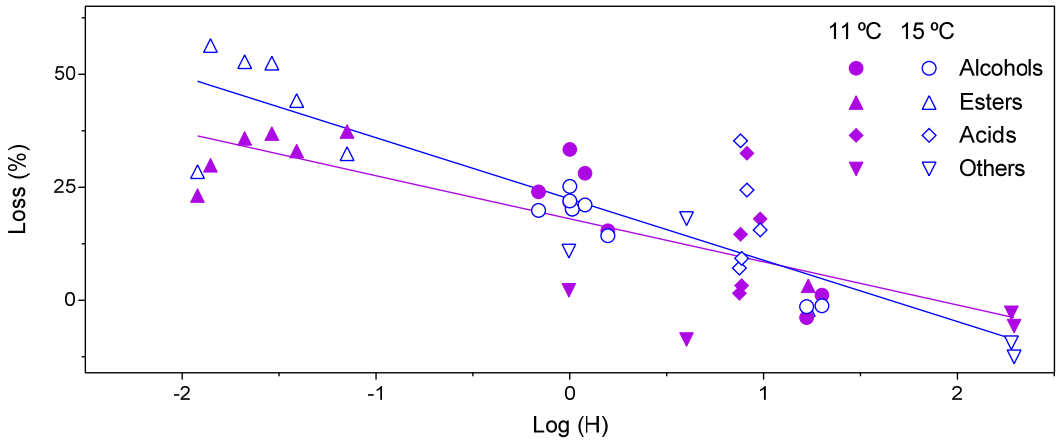

Fig. 4.2 Losses of volatile compounds as a function of Henry constant (log (H) with H in $mol \cdot m^{-3} \cdot Pa^{-1}$since for these compounds the decrease in vapor pressure with temperature is more marked, which decreases the driving force for their transport through the membrane.

Regarding the less volatile components (with a Log(H) value equal to or greater than zero), they showed a similar behavior independently of the working temperature. It is interesting to point out that working at 11 ºC allowed to improve the behavior of esters (in principle, more polar and soluble in water). Note that the hydrophobic membrane did not prevent from the esters transport as a function of their more polar character (as can be seen below). Therefore, a decrease of the temperature was probed to be a suitable strategy to reduce the loss of ester compounds without appreciably sacrificing the membrane flux. In consequence, the optimum temperature was set up at 11 ºC for the following dealcoholization trials. In addition, the mass balance of aroma compounds was more consistent (closer to 100 %) at 11 ºC for most aromas (Fig. S4.3). Indeed, in some cases the mass balance was still low, indicating the probable existence of a non-controlled loss phenomena (favored at the higher operation temperature). In this sense, Diban et al. [103] attributed some losses to the component sorption on the membrane. Finally, the mass balance discrepancies just observed can be related with the handling of the volumes obtained (feed and stripping phases) after the dealcoholization process, specially from the stripping phase due to the minor solubility of low polarity aromas in water; as expected, this effect was less pronounced at the lowest working temperature of 11 ºC.

4.3.2 Influence of wine composition

The effect of wine composition was evaluated dealcoholizing three different Tempranillo red wines (trials 2-4 in Table 4.3). It is worth mentioning that Tempranillo

was chosen because of its capability to withstand the dealcoholization process [103,104,106]. Fig. 4.3 shows the losses of 18 aromas along the dealcoholization process.

Considering all alcohols analyzed (Fig. 4.3A), with an average loss of 23 ± 1%, the three wines show a similar performance, independently of their initial concentrations in alcohols: wine-1: 518 $mg \cdot L^{-1}$, wine-2: 424 $mg \cdot L^{-1}$ and wine-3: 282 $mg \cdot L^{-1}$. In fact, wine-1 showed the lower overall loss of aliphatic alcohols (30%) despite being the wine with the highest percentage of them. The most important parameter driving the aroma loss is the solubility in water (visualized here in terms of Henry constant). Thus, isoamyl alcohol (H = 0.69 $mol \cdot m^{-3} \cdot Pa^{-1}$) is more soluble in water than isobutanol (H = 1 $mol \cdot m^{-3} \cdot Pa$) and hence is better retained in the wine (Fig. 4.3A). In fact, isobutanol was the alcohol with the worst retention in all wines. Besides, wine-2 (1.12 $mg \cdot L^{-1}$) showed less retention for isobutanol than wine-1 (1.18$\cdot mg \cdot L^{-1}$), something not explained in terms of H values but probably related to the behavior of the wine as a complex matrix with potential synergies between its components which differs from one wine to another. Similarly, cis-3-hexen-1-ol is the less volatile aliphatic alcohol and showed the highest retention in all wines.

It is clear that most of acids (Fig. 4.3B) were maintained more easily in wine than alcohols, with an average loss of 16 ± 11 %. This is in line with the corresponding H values (as can be seen in Fig. 4.2). Nevertheless, the overall loss of acids after OD (23 %) was lower than those shown by aliphatic alcohols (30 %). This can be explained by the vast contribution to the loss of acids of acetic acid (around 28 %) since it represents around 99 % of the total amount of acids in wine. In addition, acetic acid is the second most concentrated component in wine after ethanol. In any event, as for alcohols, no correlation between the initial concentration of any acid and its corresponding loss was evidenced.

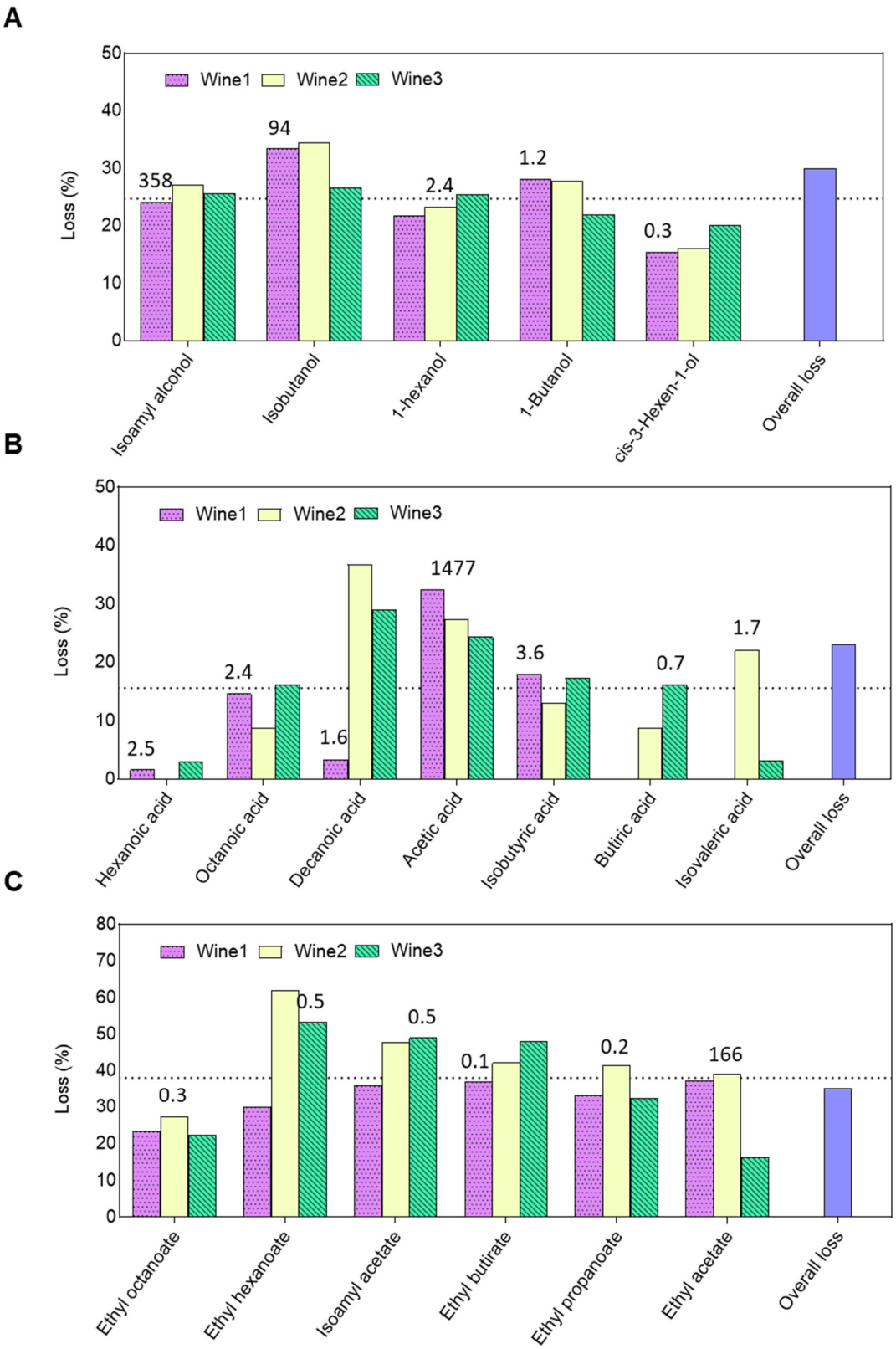

Fig. 4.3. Experimental losses of 18 aromas grouped into three different chemical families: (A) alcohols, (B) esters and (C) acids. Aromas appear from left to right in increasing order of H constant values. Initial concentration in ($mg \cdot mL^{-1}$) of each component is indicated above the bar of the wine with the highest concentration of it. Dot lines represents the average loss obtained for each chemical family.

Regarding the third main family of wine compounds, Figure 3C presents the loss of those esters derived from straight chain fatty acids (ethyl esters), whose concentrations were more prone to suffer a slightly decrease, while those derived from fermentation acids were not that affected by the OD (with respective average losses of 38 and 1 %, obtained from Table S4.1), as expected. As can be seen in Fig. 4.3, ethyl esters in the three wines show similar behavior regardless of the different initial wine composition, obtaining an average loss larger than in case of alcohols and acids, in agreement with their higher hydrophobicity (less polar character) and volatility previously mentioned. The behavior of all families is in agreement with previous studies with Tempranillo variety [104,170]. Note that the overall loss was similar to that of alcohols (35 %), led by the contribution of ethyl acetate in the total concentration of ethyl esters, which showed a minor loss value (28 %) than esters average.

Table 4.4 summarizes the final composition of each wine for the main chemical families. The results indicate that higher concentrations of compounds in the starting wine, which implies a greater initial driving force, do not appreciably affect the percentage of loss or retention in the various compounds analyzed. Accordingly, wines with higher aroma concentration seem to be more recommended for partial dealcoholization by membrane OD. Particularly, partial dealcoholized wine-2 being more concentrated in ethyl esters.

Table 4.4 Final composition of each wine for the main chemical families.

Wine	Mem.	Ethanol	Esters [mg·L^{-1}]		Acids	Alcohols [mg·L^{-1}]		Methionol
		[v/v%]	SC[a]	FA[b]	[mg·L^{-1}]	Aliphatic	Aromatic	[mg·L^{-1}]
1	PP_1	11.8	60	153	533	338	64	2.9
2	PP_1	11.2	102	236	1077	227	55	2.9
3	PP_1	11.2	46	60	307	186	33	1.5

[a] Derived from straight chain fatty acids. [b] Derived from fermentation acids.

Table 4.5 summarizes the behavior of 5 aromas representative of the organoleptic profile of a certain wine [120]. The partial dealcoholization of wine-2 by OD at 11 °C allowed to obtain a wine with 11 v/v% and an organoleptic profile similar to others obtained previously in the literature for a similar dealcoholization degree.

Table 4.5 Organoleptic profiles for several OD partially dealcoholized wines.

Type of wine [-]	Alcohol red. [º]	Volatile component					Ref.
		Isoamyl alcohol	Isoamyl acetate	Ethyl butirate	Ethyl hexanoate	Ethyl octanoate	
Tempranillo	-3	24	35	37	30	23	This work
Tempranillo	-3	22	48	42	62	27	
Tempranillo	-3	26	49	48	43	22	
Aglianico	-2	2	34	26[a]	43	48	[106]
Aglianico	-3	15	43	47[a]	55	49	[106]
Aglianico	-2	14	58	39[a]	39	34	[106]
Aglianico	-3	26	57	53[a]	45	36	[106]
Merlot	-2	14	35	-	33	68	[103]
Sangiovese	-5	58	64	-	77	94	[146]

[a] Losses correspond to ethyl 3-methylbutanoate.

In any event, these performances may not be sufficiently remarkable to maintain the organoleptic profile of the starting wine and are far from offering retention values of aromas close to those reported by Pham et al. [114,115] using a multi stage RO-OD. In fact, this two step-process showed a better retention of aromas in wine, even if its evident complexity and the expected increment in the total energy cost could be a significant impediment to its implantation at industrial scale.

4.3.3 Influence of membrane characteristics

In most cases, one-step dealcoholization by membrane OD was carried out with Liqui-Cel™ PP hollow fiber membrane modules, in fact, demonstrating the reliability, stability ad robustness of the 3M membranes. However, the availability of membranes that allow to overcome the mentioned loss of desirable aroma volatile compounds is still an open task to confirm the OD technique as a competitive one with the multi-stage approach in terms of global performance. Because of that, two different hollow fiber membrane modules, alternative to the 3M one, were studied. Thus, the partial dealcoholization of wine-2 (chosen as the most suitable wine to partial dealcoholization) was replicated at 11 °C with PP_2 (another membrane of PP with higher pore size, supplied by ZENA) and PVDF (the ”lotus” superhydrophobic PDVF membrane fabricated by Polymem).

The behavior of 14 aromas previously studied with module PP_1 at two different temperatures and three different Tempranillo wines was studied with wine-2 submitted to partial dealcoholization with modules PP_1, PP_2 and PVDF. It is worth mentioning that the selection of aromas was made in base of their concentrations, constant in wine-2 despite of the storage time. The influence of the PP membrane pore size was evaluated comparing the performance of PP1 (pore size = 30 nm) and PP2 (pore size = 100 nm), both membrane modules presenting very similar values in the rest of characteristics (Table 4.2). As can be seen in Table 4.3, the higher pore size of PP_2 membrane may be responsible for the slightly higher ethanol flux for PP_2 (0.13 $L{\cdot}m^{-2}{\cdot}h^{-1}$) than for PP_1 (0.11 $L{\cdot}m^{-2}{\cdot}h^{-1}$), what in turn would reduce the experimental time (in case of using the same membrane area) by ca. 20 %. Fig. 4.4 depicts the loss percentage of the 14 selected aromas as a function of the Henry constants of compounds. The losses were similar for PP_1 and PP_2, with overlapping of the general trend lines, even if module PP_2 exhibited a light enhancement in the retention of some alcohols (isobutanol and 1-butanol) and organic acids (isovaleric acid and isobutyric acid) as compared to PP_1. These results are in agreement with the hypothesis that the hydrophobic character of the membrane, as shown below, has a major contribution to its selectivity, instead of its structural properties; in both modules pore sizes, in the 30-100 nm range, are far above the molecular size of aroma compounds, ca. 1 nm.

In addition, the potential decrease of fouling with ZENA membrane module, due to its larger pore size, recently reported [111], could be an interesting issue when dealing with a more intense dealcoholization operation or with other applications related to feeds with suspended solids (e.g. beer treatment).

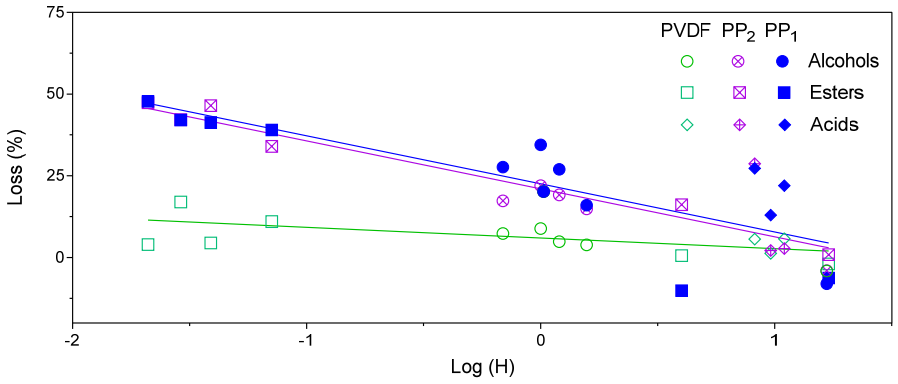

Fig. 4.4 Losses of volatile compounds as a function of Henry constant (log (H) with H in $mol{\cdot}m^{-3}{\cdot}Pa^{-1}$). Solid, open and crossed symbols correspond to losses obtained by OD carried out with PP_1, PP_2 and PVDF membrane modules, respectively. The lines as a guide to the eye.

Having seen that the two PP membrane modules performed similarly, the last comparison was done with the more hydrophobic PVDF (water contact angle higher than 125 º, far above that of 102-104 º for PP, see Table 4.2) membrane module. PVDF module showed a better performance than both PP modules in terms of ethanol flux (0.17 $L \cdot m^{-2} \cdot h^{-1}$), decreasing by 50% the experimental time needed to achieve the same degree of dealcoholization in wines (estimated after applying the same membrane area). This enhancement can be related with the non-wetting "lotus effect" effect reported for superhydrophobic membranes [185], allowing to the PVDF membrane module the exhibition of its hydrophobic capabilities (i.e. ethanol/water selectivity) [186]. As a result, Fig. 4.5 shows how the evolution of ethanol in wine as a function of normalized time (since not all the membrane modules have the same membrane area) is consistent with a more efficient dealcoholization achieved with the PVDF membrane module. Moreover, the ethanol decrease with PP membranes has a logarithmic tendency, supporting the higher aromas flux through the membrane at the beginning of the experiment, as previously reported [103]. However, the ethanol evolution is linear for PVDF in correspondence with a much better preservation of the wine aromas, even improving the results previously reported by the more energetically expensive multi-stage process [114,115]. As Fig. 4.4 shows, the PVDF module decreased the losses of compounds in case of the alcohol, ester and carboxylic acid families of aromas, and no significant differences between the partial dealcoholized wine and the starting wine in terms of the overall aroma concentration can be found (Table 4.6).

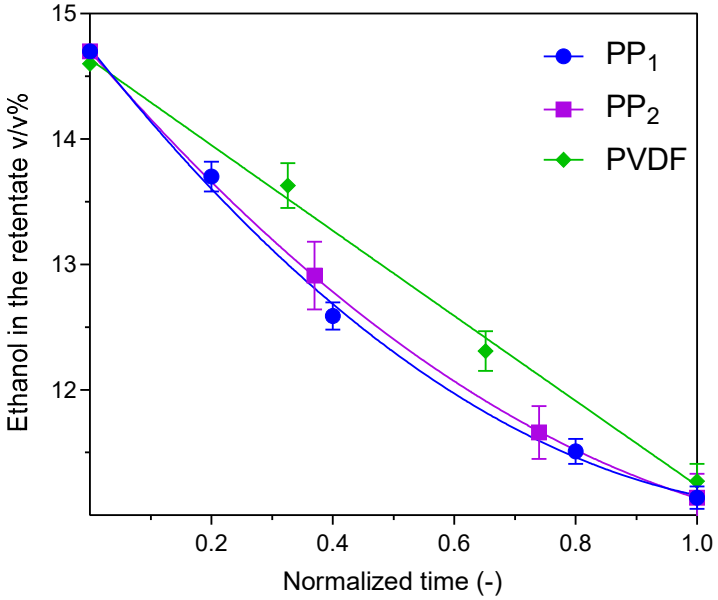

Fig. 4.5 Ethanol content as a function of normalized time corresponding to wine-2 feed using the three different modules.

The hydrophobicity of the PVDF membrane module (i.e. the "lotus effect") was enhanced by modifying the outer surface of the hollow fibers controlling their micro rugosity, therefore creating a superhydrophobic surface (WCA over to 125 °). As compared to the PP membrane modules, this active surface improved the retention of wine aromas. Although the whole membrane is made of PVDF, the inner porous PVDF sublayer only plays a support role, providing the needed mechanical strength for the hollow fiber membrane. In agreement with this result, Ma et al. [187] reported the relevant role of the membrane superhyrophobicity when removing organic compounds from water. The intrinsic hydrophobicity of the PVDF allied with the surface rugosity mentioned increases the apparent hydrophobicity according to the Wenzel equation [188], hence reducing the drag effect (by the main permeating compound, i.e. ethanol) under laminar conditions [189]. In addition, the non-wetting effect avoids the penetration of ethanol (in liquid phase) into the membrane pores [190], which would favor the transport of the minor components (aromas in the feed side), minimizing the average loss of ethyl esters from straight chain fatty acids (37 % with PP, no significant loss with PVDF), acetates (47 % with PP, 2 % with PVDF) aliphatic alcohols (22 % with PP, no significant loss with PVDF) and acids (12 % with PP, no significant loss with PVDF).

Table 4.6 Content of volatile compounds in the starting wine-2 (W_0) and the partial dealcoholized ones (W_{PD}) with the different membrane modules. Concentrations expressed in $mg \cdot L^{-1}$.

Compound	Wine-2 (PP_1)		Wine-2 (PP_2)		Wine-2 (PVDF)	
	W_0	W_{PD}	W_0	W_{PD}	W_0	W_{PD}
Aliphatic alcohols						
Isobutanol	73.9	47.6	70.2	54.7	60.8	62.0
1-Butanol	1.12	0.80	1.10	0.91	0.86	0.87
Isoamyl alcohol	297	216	293	244	222	227
cis-3-Hexen-1-ol	0.19	0.16	0.19	0.17	0.15	0.15
Total	*372*	*265*	*364*	*300*	*284*	*290*
Aromatic alcohols						
Benzyl alcohol	49.1	54.2	53.2	53.5	33.0	25.6
Total	49.1	54.2	53.2	53.5	33.0	25.6
Acetates						
Isoamyl acetate	0.44	0.23	0.43	0.23	0.45	0.44
Total	*0.44*	*0.23*	*0.43*	*0.23*	*0.45*	*0.44*
Ethyl esters from straight chain fatty acids						
Ethyl propanoate	0.15	0.09	0.17	0.09	0.14	0.13
Ethyl butirate	0.11	0.07	0.14	0.07	0.13	0.11
Ethyl acetate	166	101	182	120	171	173
Total	*166*	*101*	*182*	*120*	*171*	*173*
Ethyl esters from fermentation acids						
Ethyl lactate	204	217	220	219	177	189
Diethyl succinate	14.5	18.5	16.8	14.1	11.0	11.0
Total	*219*	*236*	*237*	*233*	*188*	*200*
Acids						
Acetic acid	1477	1069	1386	987	989	1038
Isobutyric acid	2.65	2.30	2.28	2.20	2.10	2.20
Isovaleric acid	1.68	1.31	1.53	1.49	1.42	1.51
Total	*1481*	*1073*	*1390*	*991*	*993*	*1042*

4.4 Conclusions

Osmotic distillation (OD) is a suitable tool for partial dealcoholization (-3 alcoholic degrees) of red wines, although so far its aromas retention ability has not been high enough to produce a partial dealcoholized wine with suitable profile of aromas, as similar as possible to that of the starting wine. In this work, experiments of partial dealcoholization of different Tempranillo wines were performed with different working temperatures and membrane modules. It was observed that the loss of aroma

compounds could be diminished by different ways, mainly decreasing the operation temperature and selecting the appropriate hydrophobic membrane material.

Three main families of wine components were studied (alcohols, carboxylic acids and esters) to analyze each strategy, finding always a good correlation between the volatility (expressed in terms of Henry constant, H) and the component average loss for every family. Aroma loss increased as follows: esters > alcohols > acids. According to the obtained results, reducing the working temperature from 15 to 11 °C allowed to slightly reduce the esters loss without noticeable loss of permeance. The different concentrations of aromas in the initial wine did not influence on the OD performance, and all the Tempranillo wines exhibited similar loss values of the three families of components above mentioned. Regarding the membrane modules studied, partial dealcoholization trials with the PP membranes with higher pore size ($d_p(PP_2)$ = 0.1 µm; $d_p(PP_1)$ = 0.03 µm) required a shorter experimental time compared to the stablished membranes. When changing the membrane material to PVDF (with "lotus effect" external surface treatment), not only the ethanol flux was higher (reducing in turn the treatment time) but the losses of aromas of all families (esters, alcohols and acids) were not significant. As an outstanding conclusion, the selection of the material of the membrane module can play a fundamental role, thus in the wines studied here, the use of modules with superhydrophobic membranes can favor obtaining partially dealcoholized wines with organoleptic properties similar to those of the starting wine.

4.5 Supplementary information

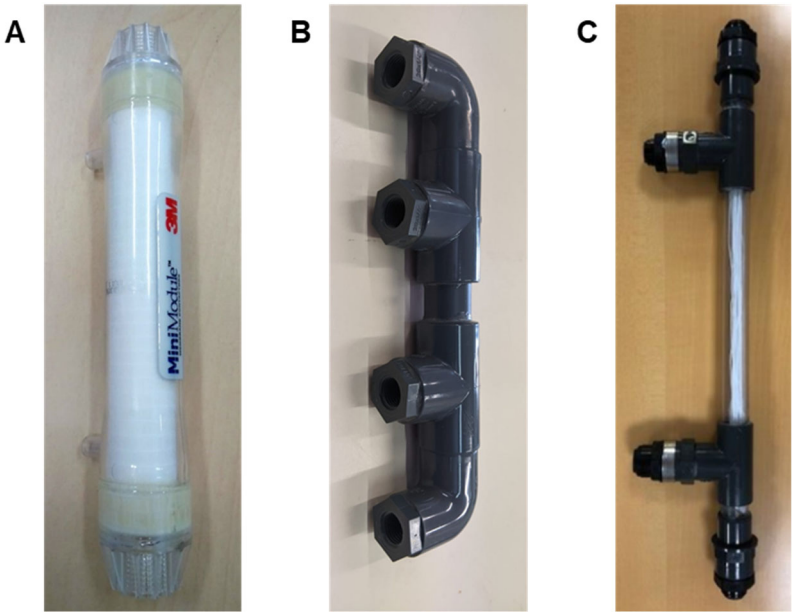

Fig. S4.1 Membrane modules used in OD. A) PP_1 (3M); B) PP_2 (ZENA); C) PVDF (Polymem).

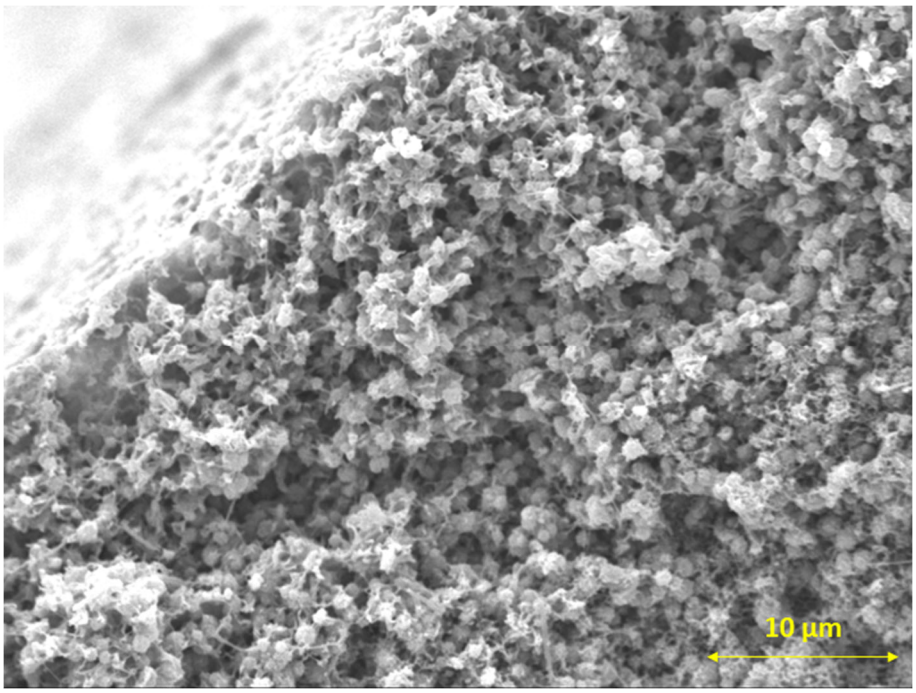

Fig. S4.2 Hollow fiber cross section SEM image of PVDF superhydrophobic membrane.

Table S4.1 Content of volatile compounds in fresh (W_0) and treated wines at 11 °C (W_{PD}) ($mg \cdot L^{-1}$). [a] Concentration expressed as $mL \cdot mL^{-1}$. Wine-1 was treated under two different temperatures (11 and 15 °C).

Compound	**Wine-1**			**Wine-2**		**Wine-3**	
	W_0	$W_{PD,\ 15}$	$W_{PD,\ 11}$	W_0	W_{PD}	W_0	W_{PD}
[a] Ethanol	14.8	11.8	11.8	14.7	11.2	14.1	11.2
Aliphatic alcohols							
Isobutanol	93.8	70.1	62.5	84.0	47.6	28.6	21.0
1-Butanol	1.18	0.93	0.85	1.12	0.80	0.82	0.64
Isoamyl alcohol	358	287	272	297	216	218	162
1-Hexanol	2.38	1.85	1.86	2.49	1.91	1.99	1.48
cis-3-Hexen-1-ol	0.26	0.22	0.22	0.19	0.16	0.07	0.06
Aromatic alcohols							
Benzyl alcohol	0.34	0.35	0.34	0.48	0.52	0.41	0.43
2-Phenylethanol	61.5	62.3	63.8	49.1	54.2	31.6	32.5
Acetates							
Isoamyl acetate	0.40	0.19	0.25	0.44	0.23	0.48	0.24
Ethyl esters from straight chain fatty acids							
Ethyl propanoate	0.16	0.09	0.10	0.15	0.09	0.09	0.06
Ethyl butirate	0.15	0.07	0.09	0.12	0.07	0.12	0.06
Ethyl hexanoate	0.46	0.20	0.32	0.35	0.13	0.32	0.15
Ethyl octanoate	0.21	0.19	0.16	0.29	0.21	0.20	0.15
Ethyl decanoate	0.00	0.00	0.00	0.00	-	0.16	0.17
Ethyl acetate	94.3	63.8	59.1	174.6	101	54.18	45.6
Ethyl esters from fermentation acids							
Ethyl lactate	141	144	136	204	217	58.2	52.7
Diethyl succinate	16.3	13.3	17.7	14.5	18.5	7.18	5.82
Acids							
Acetic acid	776	587	524	1477	1069	398	301
Butiric acid	0.00	-	-	0.74	0.64	0.50	0.44
Isobutyric acid	3.60	3.04	2.95	2.65	2.30	0.91	0.75
Isovaleric acid	0.00	-	-	1.68	1.31	1.13	1.15
Hexanoic acid	2.49	2.31	2.45	2.04	2.20	1.78	1.72
Octanoic acid	2.44	1.58	2.08	1.74	1.58	1.57	1.32
Decanoic acid	1.64	1.50	1.59	0.27	0.14	0.17	0.19
Others							
Acetoin	3.76	3.35	3.67	0.67	0.76	59.0	53.4
□-Butyrolactone	19.2	19.2	19.8	20.3	20.8	15.7	17.4
Methionol	2.70	3.04	2.86	2.82	2.91	1.36	1.46

Table S4.2 Heny's constant (H^i) values for the components quantified in wines [191].

Chemical family	Component	H^i ($m^3 \cdot Pa \cdot mol^{-1}$)
Aliphatic alcohols	Ethanol	1.9
	Isobutanol	1
	Isoamyl alcohol	0.69
	1-Butanol	1.2
	1-Hexanol	1
	cis-3-Hexen-1-ol	1.57
Aromatic alcohols	2-Phenylethanol	19.00
	Benzyl alcohol	18.00
Acetates	Isoamyl acetate	0.021
	Ethyl acetate	0.062
Ethyl esters from straight chain fatty acids	Ethyl propanoate	0.039
	Ethyl butyrate	0.029
	Ethyl hexanoate	0.014
	Ethyl octanoate	0.012
	Ethyl decanoate	0.017
Ethyl esters from fermentation acids	Ethyl lactate	17
	Diethyl succinate	4
Acids	Acetic acid	8.2
	Butyric acid	9.7
	Isobutyric acid	9.6
	Isovaleric acid	11
	Hexanoic acid	7.5
	Octanoic acid	7.6
	Decanoic acid	7.7
Others	Acetoin	0.99
	γ-Butyrolactone	190
	Methionol	196

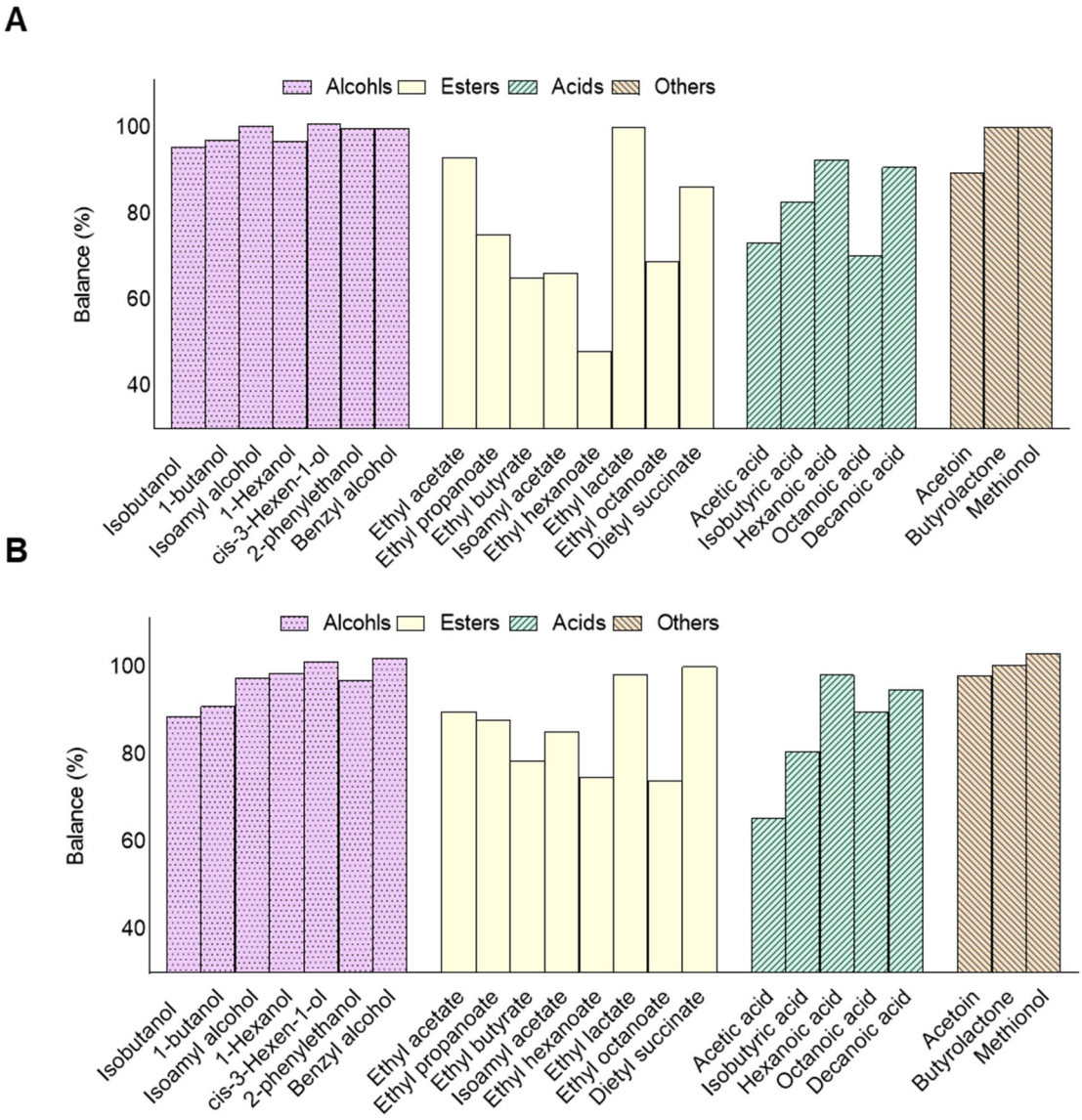

Fig. S4.3 Balance in mass from the wine-1 partial dealcoholization carried out at two temperatures: (A) 15 ^{o}C; (B) 11 ^{o}C (trials 1 and 2 in Table 3, respectively).

Table S4.3 Content of volatile compounds in streams from the adsorption test ($mg \cdot L^{-1}$). W_0 fresh, untreated wine; W_A wine obtained after the adsorption test with a PP membrane; E_A ethanol solution with aromas desorbed from PP. Mean values and standard deviations were obtained from four replicates.

Compound	W_0	W_A	E_A
Aliphatic alcohols			
Isobutanol	51.6	48.1 ± 3.80	0.00 ± 0.00
1-Butanol	1.16	1.10 ± 0.09	0.00 ± 0.00
Isoamyl alcohol	293	283 ± 6.80	0.16 ± 0.50
1-Hexanol	2.07	2.01 ± 0.03	0.00 ± 0.00
cis-3-Hexen-1-ol	0.06	0.06 ± 0.00	0.00 ± 0.00
Aromatic alcohols			
Benzyl alcohol	0.76	0.72 ± 0.03	0.00 ± 0.0
2-Phenylethanol	52.88	51.2 ± 0.93	0.08 ± 0.06
Acetates			
Isoamyl acetate	0.20	0.15 ± 0.02	0.00 ± 0.00
Ethyl esters from straight chain fatty acids			
Ethyl propanoate	0.11	0.10 ± 0.01	0.00 ± 0.00
Ethyl butirate	0.1	0.08 ± 0.00	0.00 ± 0.00
Ethyl hexanoate	0.25	0.22 ± 0.01	0.00 ± 0.00
Ethyl acetate	55.1	50.51 ± 2.01	1.69 ± 0.52
Ethyl esters from fermentation acids			
Ethyl lactate	96.3	0.00 ± 0.0	0.21 ± 0.16
Diethyl succinate	11.4	0.00 ± 0.0	0.00 ± 0.00
Acids			
Acetic acid	370	345 ± 23.8	0.00 ± 0.00
Butiric acid	0.29	0.29 ± 0.01	0.00 ± 0.00
Isobutyric acid	1.10	1.04 ± 0.06	0.00 ± 0.00
Hexanoic acid	1.91	1.83 ± 0.08	0.00 ± 0.00
Octanoic acid	1.99	1.82 ± 0.10	0.00 ± 0.00
Decanoic acid	0.99	0.93 ± 0.07	0.18 ± 0.12
Others			
Acetoin	1.54	1.76 ± 0.16	0.00 ± 0.00
γ-Butyrolactone	17.86	16.5 ± 1.23	0.00 ± 0.00
Methionol	2.30	2.16 ± 0.14	0.00 ± 0.00

CHAPTER 5

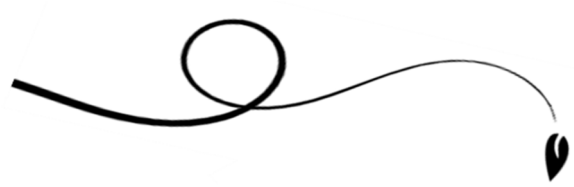

PERVAPORATION OF THE LOW ETHANOL CONTENT EXTRACTING STREAM GENERATED FROM THE DEALCOHOLIZATION OF RED WINE BY MEMBRANE OSMOTIC DISTILLATION

From Esteras-Saz, J; De la Iglesia, Ó; Peña, C; Escudero, A; Téllez, C; Coronas, J. Pervaporation of the low ethanol content extracting stream generated from the dealcoholization of red wine by membrane osmotic distillation. Submitted to J. Ind. Eng. Chem.

5 Pervaporation of the low ethanol content extracting stream generated from the dealcoholization of red wine by membrane osmotic distillation

5.1 Introduction

Global warming, leading to obtain grapes with an excessive sugar concentration, is altering the cycle of wine. This results in wines with an undesirably high concentration of ethanol, which increases the solubility of some volatile compounds in wine and reduces its quality [22,135,192]. Different strategies have been developed to produce balanced wines with low alcoholic strength, those that remove the ethanol content from the finished wines being the most used [94,143–145,193].

In addition to the simple addition of water to grape must, usually restricted or only recently authorized in most of the wine producing countries [118], one of the most promising techniques to dealcoholize wine is based on membrane osmotic distillation (OD). This is a membrane operation able to work at low pressures and temperatures, hence diminishing the required energy costs and the impact on the composition and sensory attributes of the processed wines.

In fact, OD has already been used to dealcoholize, partial or totally, beer and wine [103,104,106,107,146,149,151,170,172,194]. In OD, the feed and the extracting solution (usually water) are faced by a hydrophobic membrane (typically of polypropylene, PP). As a result, the component concentration gradients between both membrane sides act as the driving force for the separation. The hydrophobic membrane prevents the entry of the aqueous solution into the pores, while the use of water as stripper creates an ethanol vapor pressure difference between both membrane sides which increases the ethanol flux and reduces the water activity across the membrane and therefore its transport [195]. The rest of minor components, with much lower concentrations than ethanol, should preferentially remain in the feed.

OD is considered as a clean technology [118], due to the fact that the extracting solution generated is essentially water with a low ethanol content and minimum amounts of aromas from wine. Up to date, this extracting solution is not reused and becomes a waste due to the fact that its ethanol concentration is very low, often around 5 wt% or even less [170,196,197]. Consequently, the used water in relation to the processed wine is high (with a minimum ratio of 0.5 liter of water per liter of wine [12]), representing an important economic loss and hampering the OD development and its

implementation in wineries. Developing a separation stage for the extracting solution would allow the recycle of water, reducing the generation of wastewater close to zero and producing an alcohol-rich stream, which could in turn be regarded as second generation (2G) bioethanol (i.e. not produced from direct fermentation of sugars, see below for further details). All this would make the process of wine dealcoholization by OD more sustainable and favorable.

Bioethanol is the most popular biofuel since it can be mixed with petrol in different proportions or even used directly as fuel for transportation [198,199]. Furthermore, bioethanol can be produced by fermentation of cheap and abundant agricultural by-products rich in sugars or starch, like those related to rice, millet, sorghum or sugar-cane [200–204]. In fact, bioethanol production through this way, giving rise to first generation (1G) bioethanol, has been growing steadily since the 1920's [205,206]. Nevertheless, the use of food materials as feedstock has increased the cost-effectiveness of 1G bioethanol, restraining the growth of biofuels as an alternative to petrol [207]. Therefore, the current trend is the production of the so-called 2G bioethanol, which can be obtained from inexhaustible raw materials [208,209]. The search for cheap and abundant sources of raw material is an important issue to develop the production of 2G bioethanol [210,211] and OD waste could help meet its demand.

Moreover, the separation of ethanol as minor component by a typical distillation is ineffective. Thus, pervaporation (PV) appears as an interesting separation operation, which has already been used to dehydrate concentrated alcohol solutions and, to a minor extend, for the ethanol recovery from diluted hydroalcoholic solutions [75]. Under these conditions, PV constitutes a clear alternative to distillation [78,79]. In addition, PV is accepted as an energy-saving operation to separate close boiling point and azeotropic mixtures due to its high separation selectivity, reasonable flux, and low operational cost [76,77,212–215]. PV can be carried out either with hydrophilic or hydrophobic membranes. Hydrophilic membranes allow the dehydration of a given organic solvent or the separation of the most polar component of an organic mixture; on the contrary, hydrophobic ones provide the preferential permeation of the least polar component of a certain mixture [216,217].

When dealing with diluted alcohol solutions, an interesting approach is the sequential hydrophobic-hydrophilic PV. This process, recently validated through theoretical and economic studies [218,219], uses a hydrophobic membrane to remove alcohol from the diluted alcohol solutions to subsequently dehydrate the alcohol-rich permeate with a hydrophilic membrane. This is the case of the anhydrous ethanol production by a hydrophobic (PDMS)-hydrophilic (carboxymethyl cellulose) PV [220]

and when applying (PDMS)-hydrophilic (polyvinyl alcohol) PV to diluted isobutanol aqueous solutions [221].

In this chapter, a red wine was partially dealcoholized by membrane OD using pure water as extracting agent, following our previously developed OD methodology based on the application of PP membranes [170]. Next, the wastewater obtained (a dilute hydroalcoholic solution) was treated by hydrophobic-hydrophilic PV. As shown in Fig. 5.1, hydrophobic PV (HFB-PV), using PDMS or zeolite silicalite-1 membranes, was directly applied to the OD waste. Subsequently, the permeate from the HFB-PV was dehydrated by hydrophilic pervaporation (HPL-PV), using faujasite or mordenite zeolite membranes. As a consequence, bioethanol and water were obtained. This water (with very low ethanol content) was reused as stripping agent in a new OD operation of wine dealcoholization. This wine was compared in terms of aroma composition with that obtained by typical OD, using pure water as extracting agent. To the best of our knowledge the hydrophobic-hydrophilic PV process proposed here, has never been applied to process the wastewater from membrane OD treated wine, this being the main achievement of this chapter.

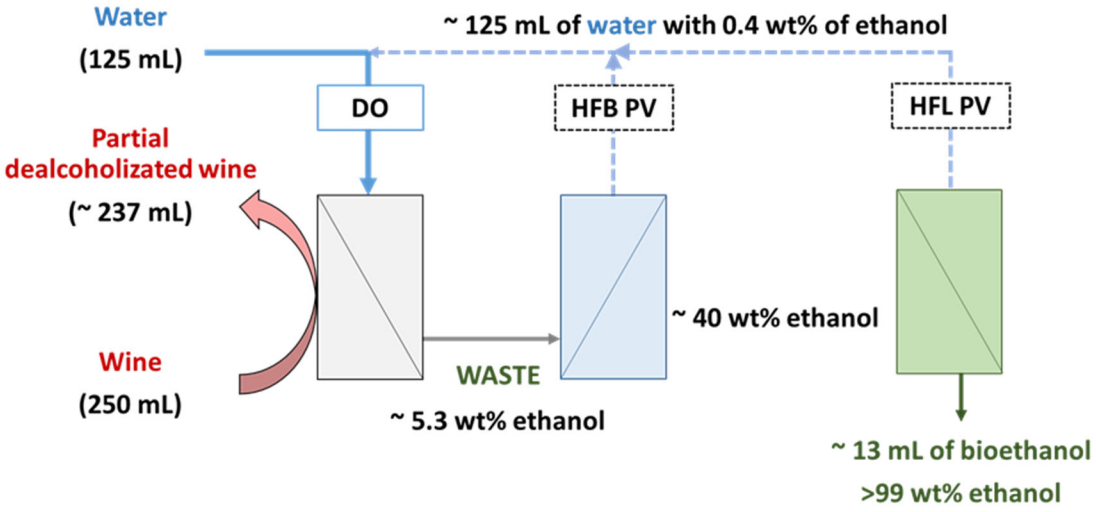

Fig. 5.1 General scheme of the osmotic distillation-pervaporation coupling.

The demonstration of the feasibility of this OD-PV combination will help the up-scaling of the technology. In fact, a life cycle analysis (LCA) of wine dealcoholization by OD demonstrated its low environmental impact [96], while hydrophilic PV is commercially available for ethanol (and other solvents) dehydration since many years ago [222] and recently PV has been presented as a promising method for the bioethanol separation in an industrial context [78]. Finally, it should be noted that the sustainability

of the OD-PV intensified process is guaranteed, since, beyond the use of membranes as a low cost tool, the proposed solution agrees with the rule of the three Rs (reduce, reuse and recycle) within the framework established by the 2030 Sustainable Development Agenda.

5.2 Materials and methods

5.2.1 Membranes

The OD membrane module is equipped with Liqui-Cel™ MM-1x5.5 hydrophobic porous polypropylene (PP) hollow fiber membranes from 3M. The main characteristics of the membrane module are: 2300 hollow fibers with inner and outer diameters of 220 and 300 μm, thickness of 40 μm and nominal pore size of 30 nm. The effective length is 14 cm yielding a 0.18 m^2 of membrane area.

Concerning PV, hydrophobic flat sheet membranes (15 cm^2 of membrane area) of PDMS were purchased to Deltamem AG (PDMS™ 4060), while tubular zeolite membranes (25 cm^2 of membrane area; 1.2 cm of outer diameter and 0.86 cm of inner diameter) of hydrophobic silicalite-1 (MFI type structure with pores of 0.51 x 0.55 nm and 0.53 x 0.56 nm) and hydrophilic mordenite (MOR type structure with pores of 0.26 x 0.57 nm and 0.65 x 0.7 nm) and faujasite (FAU type structure with pores of 0.74 nm) were prepared on mullite tubular supports following previous reports. Silicalite-1 membranes (SIL) with ca.10 μm thickness were obtained by rubbing seeding followed by secondary growth [223]. In detail, silicalite-1 nanoseeds of 100 nm were obtained with a 1 SiO_2:0.36 TPAOH: 20 H_2O gel at 130 °C for 48 h, TPAOH being tetrapropylammonium hydroxide. These nanoseeds were applied mechanically to the outer surface of tubular supports.

Then, silicalite-1 (SIL) membranes were prepared by secondary growth carried out with a 1 SiO_2: 0.20 TPAOH: 0.10 TPABr: 0.10 NH4F: 500 H_2O gel at 185 °C for 12 h, where TPABr is tetrapropylammonium bromide [223]. SIL membranes were calcined at 500 °C for 20 h to remove the organic structure directing agent (OSDA) used for their synthesis. Mordenite (MOR) and faujasite (FAU) membranes with ca. 1 μm thickness were prepared by crystallization but without OSDA, therefore they were not calcined [224,225]. In detail, MOR membranes were crystallized at 170 °C for 6 h with a 1 SiO_2: 0.08 Al_2O_3: 0.2 Na_2O: 0.1 NaF: 35 H_2O gel previous rubbing seeding with MOR commercial crystals (Wako) [224], while FAU membranes were also obtained after rubbing seeding with Si/Al= 2.5 NaY commercial crystals (Wako) and secondary

hydrothermal synthesis at 80 °C for 6 h with a 25SiO_2: 1 Al_2O_3: 72 Na_2O: 990 H_2O gel [225].

The physicochemical characterization of the zeolite membranes was not addressed in this chapter since this has been previously reported in the just given citations [54-56].

5.2.2 Multi-stage setup

Fig. 5.1 shows the schematic representation of the laboratory approach for coupling OD and PV membrane processes. A complete description of the membrane OD lab-scale plant can be found elsewhere [170]. Briefly, this includes the membrane module with feed (Q_f) and extracting (Q_s) flow systems, pressure and temperature controllers. A chiller bath Julabo^{TM} (Corio-201F) maintains the desired temperature on both membrane sides at 11 °C. In addition, two manometers (MEX3D820B15, Bourdon) measured the pressure at tube and shell sides yielding pressure different values close to 0 bar.

The red wine studied was Tempranillo, which corresponds to a black grape variety mainly grown in Spain, kindly provided by Bodegas Matarromera (Valbuena de Duero, Valladolid, Spain). OD tests were performed recirculating 250 mL of wine through the shell side of the membrane module at 74 mL·min^{-1}. Meanwhile, 125 mL of the extracting agent (deionized water) was fed at 40 mL·min^{-1} to the tube side of the membrane module. Deionized water allowed to minimize the water transport across the membrane and therefore its extraction from wine and its potential transport to it, estimated in less than 0.1 v/v% decrease in the ethanol content by dilution with water. Both streams were continuously applied in a counter current configuration working at 11 °C to minimize the losses of aromas, especially esters. Flows and volumes were established in a previous publication where the influence of different variables in the operation of the OD was investigated [170]. OD experiments were performed by duplicate. After each experiment, the OD module was cleaned at 40-60 °C with a 0.5 wt/v% NaOH solution following a procedure previously described [170].

The PV setup consists of two steps, carrying out a first hydrophobic separation process (HFB-PV) followed by a hydrophilic one (HFL-PV). The HFB-PV separated ethanol from the OD waste, obtaining a permeate enriched in ethanol. Subsequently, this permeate was subjected to a step of dehydration with a hydrophilic membrane, obtaining an ethanol-rich stream as retentate. This scheme allowed the reuse of the retentate of the HFB-PV and the permeate of the HFL-PV as extracting agent in a next OD process.

As shown in Fig. S3.1, two different membrane modules were used to place the PV membranes. Tubular membranes were coupled in a homemade stainless steel

permeation module sealed with viton o-rings, while flat sheet membranes were placed in a stainless steel permeation module from Sartorius™. The driving force for the separation is the difference in partial pressures between both membrane sides, which was achieved by a Pfeiffer vacuum pump (MVP-040-2) connected to the permeate side.

In both types of PV, a flow of 15 mL·min^{-1} was fed to the membrane module at atmospheric pressure, while the permeate vacuum pressure was controlled at 4 mbar by a needle valve and monitored with a pressure transducer connected to a digital display. The permeated vapor was condensed by means of two consecutive glass traps immersed in liquid nitrogen (-196 °C) dewar flasks and collected at fixed times, while the retentate stream was recycled back to the feed tank. Preliminary experiments, fed with water-ethanol synthetic solutions (5.3 wt% ethanol in HFB-PV and 40 wt% ethanol in HFL-PV), were performed to fix the optimum operation conditions and choose the best membranes in terms of PV flux and separation factor. Once the PV setup was validated with water-ethanol solutions, both PV steps were carried out feeding real solutions as above mentioned. Table 5.1 shows the experimental conditions applied in both PV tests. To obtain average values and standard deviations, each experiment under non steady state conditions was carried out twice (E1-E3, E6-E8), while in those under steady state three successive samples were taken at 3 h intervals (E4 and E5).

Table 5.1 Summary of PV experiments carried out with water-ethanol solutions. SIL, MOR1 and MOR2 and FAU are zeolites membranes of silicalite-1, mordenite and faujasite, respectively.

Exp	Membrane	Temperature	Feed	Feed ethanol
	-	[ºC]	[g]	[wt%]
E1	SIL	40	100	5.3
E2	SIL	60	100	5.3
E3	PDMS	60	100	5.3
E4	MOR1	55	1000	40
E5	MOR1	75	1000	40
E6	MOR1	75	100	40
E7	MOR2	75	100	40
E8	FAU	75	100	40

Membrane performance in PV was assessed based on the permeation flux (J, kg·m^{-2}·h^{-1}) and the separation factor (α). The total PV flux was obtained at fixed time intervals from the following equation:

$$J = \frac{\Delta W}{A_e \Delta t} \tag{5.1}$$

where ΔW(kg) is the variation of total mass in a given interval of time, Δt (h), and A is the effective membrane area (m^2). From ΔW and the corresponding concentrations of permeate samples, ethanol and water permeate fluxes were also obtained. The separation factor ($\alpha_{A/B}$) was calculated as follows:

$$\alpha_{A/B} = \frac{Y_A/Y_B}{X_A/X_B} \quad (5.2)$$

where X_A and $X_B$and Y_A and Y_B are the weight fractions of A (desired component) and B in the retentate and permeate sides, respectively. For experiments carried out under steady state conditions (E4 and E5), $\alpha_{A/B}$ was calculated as an average of three runs with the same membrane once the steady state was reached. For non-steady state ones (E1-E3; E6-E8), $\alpha_{A/B}$ was obtained from each collected permeate along the experiment. Moreover, permeances (P_i) were calculated normalizing each individual flux by the driving force as follows:

$$P_i = \frac{j_i}{p_{i,R} - p_{i,P}} \quad (5.3)$$

$p_{i,R}$ and $p_{i,P}$ being the vapor pressures of component *i* in the retentate and permeate sides, respectively.

After each experiment, mass compositions of retentate and permeate were determined to calculate the recovery efficiency to ethanol. Finally, both OD and PV polymeric membranes were cleaned with pure ethanol at 60 °C for 8 h followed by drying overnight at 60 °C. As the silicalite-1 membrane suffered from fouling due to the presence of some organic compounds in the PV feeding, a calcination step was undergone in a furnace at 480 °C for 12 h with a heating rate of 0.5 $°C \cdot min^{-1}$. In both processes 1 mL volumes of the different streams (OD and PV) were taken at constant time intervals to analyze their ethanol and major volatile compounds concentration, following the same procedure reported in 3.2.1.

5.3 Results and discussion

5.3.1 Partial dealcoholization of red wine by membrane OD

Feed for the further PV setup was obtained from partial dealcoholization of red wine (initial composition in **¡Error! No se encuentra el origen de la referencia.**) by OD, using deionized water as extracting agent. Under the previously mentioned experimental conditions, a 3 v/v% (2.5 wt%) ethanol decrease in wine was achieved after 25 min. This means that 250 mL of wine feed (V_f) and 125 mL of water (V_s) were pumped to both sides of the membrane module. In these conditions, 125 mL of a stripping phase with a

5.3 wt% ethanol was produced in each OD run (corresponding to an ethanol osmotic pressure of 0.26 atm), while in the feed side the ethanol concentration was reduced from 14.0 to 11.2 v/v% (corresponding to a change in the ethanol osmotic pressure from 0.56 to 0.45 atm).

The difference in osmotic pressure of the main solute of wine (ethanol) between both membrane sides generates the needed driving force for the dealcoholization. In successive OD dealcoholization experiments, water recovered from the pervaporation modules (125 mL, 0.4 wt% ethanol) was used instead of fresh, deionized water.

A total of 25 compounds were identified and quantified by gas chromatography in the starting wine and in the two dealcoholized wines (W_A and W_B, one with fresh deionized water and other with the recycled PV water, respectively). As expected, both wines W_A and W_B systematically have less content of aromas than fresh wine. Hence, loss of some volatile compounds is unavoidable due to the existence of favorable concentration gradients for these components between both membrane sides, which act as driving force for the transfer of volatile compounds across the membrane. Moreover, other factors such as volatility of each component, interaction with the wine matrix and affinity to the membrane material also have an impact on the loss of volatile compounds [103,104,106,149,151,170]. These compounds can be grouped in the following chemical families: alcohols, esters, acids, ketones, lactones and sulfur compounds. The behavior of each volatile compound (Fig. 5.2A) and of each chemical family (Fig. 5.2B) during OD adequately correlated with the corresponding Henry's constant (H^i) value (in water; values obtained from previous literature, see Table S3.1 [191]) using both stripping agents. The expected trend is the higher the H^i value of a given component *i*, the higher its water solubility and the lower its loss. This behavior has already been observed in recent studies, being consistent with the loss of components towards the stripping phase together with the ethanol [103,104,149,151,170].

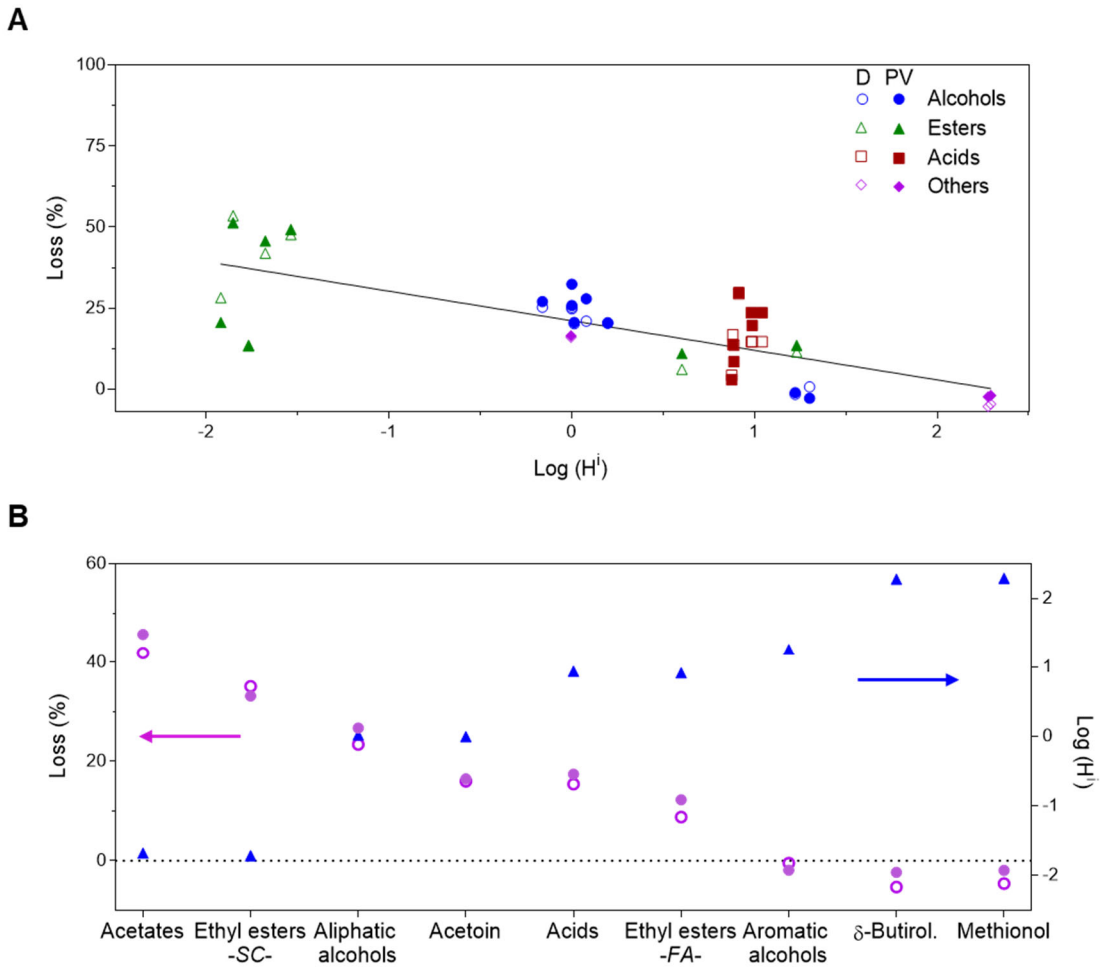

Fig. 5.2 . A) Losses of volatile compounds as a function of Henry's constant (log H^i with H^i in $mol \cdot m^{-3} \cdot Pa$). B) Average losses and log H^i values of volatile compounds grouped by chemical families. In A and B, solid and open symbols correspond to OD with fresh (D) and recycled water (PV), respectively. *SC* and *FA* in B refer to ethyl esters from straight chain fatty and ethyl esters from fermentation acids, respectively.

As Fig. 5.2A depicts, all the aliphatic alcohols exhibit a similar behavior with an average loss of 26 %, close to the ethanol loss (ca. 20 %) in agreement with their close Henry's constant values (with an average value of 1.2 $mol \cdot m^{-3} \cdot Pa$). However, aromatic alcohols remained in wine after achieving the same degree of dealcoholization. The different behavior between both alcohol types (aliphatic and aromatic) was in agreement with the H^i for aromatic alcohols (18 $mol \cdot m^{-3} \cdot Pa$), supported by the π-π staking interactions and that of the –OH groups with the rest of the wine components [226].

Concerning esters, the concentrations of those derived from straight chain fatty acids (ethyl esters -*SC*-) suffer a slightly higher average decrease (ca. 33 %) than aliphatic alcohols. This agrees with their lowest overall average value of Henry's constant (0.022 $mol \cdot m^{-3} \cdot Pa$) (Fig. 5.2B). In addition, those derived from fermentation acids (ethyl

esters -*FA*-; ethyl lactate and diethyl succinate) were the esters with the lowest loss (14 % and 11 %, respectively), in line with their higher Henry's constant values (17 and 4.0 mol·m^{-3}·Pa, respectively). Moreover, isoamyl acetate, an acetate, shows the highest concentration decrease (46 %) in agreement with its small Henry`s constant (0.021 mol·m^{-3}·Pa). In any event, these losses are lower than those previously reported by other authors [106,107,151] also using the same membrane technique. This can be due to the low temperature applied here (11 °C) for the membrane OD.

Acids show a lower loss (17 % in average) than alcohols and esters (Fig. 5.2B). This agrees with their higher Henry's constant values (8.7 mol·m^{-}3·Pa), although the most volatile carboxylic acid, acetic acid, shows a ca. 30 % loss, close to the values corresponding to aliphatic alcohols.

Acetoin, methionol and δ-butyrolactone were also studied. Acetoin, shows a relatively small loss, in agreement with its Henry's constant value as can be seen in Fig. 5.2B. The concentrations of methionol, a sulphur compound, and δ-butyrolactone, a lactone, were not significantly affected by the dealcoholization process, as expected from their high Henry's constant values shown (100 and 190 mol·m^{-3}·Pa, respectively).

In summary, the aroma losses reported here and the profile of each chemical family were basically in agreement with the literature, suggesting that experimental conditions used in this chapter, advantageous due the low temperature applied, are appropriate to accomplish the dealcoholization by OD [106,146,168].

Finally, the OD polypropylene membrane module used in here was discontinuously operated along ca. 3 years accumulating 26 h of red wine dealcoholization, 7 h of water-ethanol dealcoholization, ca. 15 h of 0.5 wt.% NaOH cleaning at 40-60 °C and almost 8 days under vacuum (4 mbar). Despite this, the module showed reproducible dealcoholization results, proving its stability.

5.3.2 Hydrophobic PV of water-ethanol solutions

To study the performance of the PV setup (see Fig. 5.1) and establish the best membrane for each step, several preliminary experiments were carried out feeding different water-ethanol solutions for their dealcoholization (with hydrophobic membrane) or dehydration (with hydrophilic membrane). In case of experiments done under non-steady state (E1-E3; E6-E8), the composition changed notably during the experiments and, as a result, PV flux and separation factor varied during the experiment. In these conditions, PV flux and separation factor were obtained from each collected permeate along the experiments. In any event, the runs carried out correspond to batch

experiments accounting for relatively small amounts of wine and the different PV solutions to treat. However, it is expected that the results gathered from them help establish the conditions for a suitable continuous industrial process.

The first PV step for the treatment of the OD extracting stream is its dealcoholization by HFB-PV. A synthetic ethanol-water mixture with the same composition as the OD extracting stream (ethanol content 5.3 wt%) was submitted to PV with hydrophobic membranes. Membranes used for this purpose were made of hydrophobic PDMS (membrane PDMS) and zeolite silicalite-1 (membrane SIL). Experiments were stopped when a reference content of alcohol in retentate around of 0.4 wt% was reached, as a compromise between decreasing the ethanol content in the extracting phase and the fact that an excessive experiment time may dilute the permeate stream, hindering the next PV stage (since an ethanol content close to 40 wt% is required for HFL-PV).

In order to select the most favorable experimental conditions for HFB-PV, several experiments were carried out to determine the optimum temperature and membrane type. Table 5.2 and Fig. 5.3 show the results corresponding to these experiments. In addition, the average values of total permeate weight collected of each experiment are summarized in Table S5.2. As shown in Fig. 5.3A, all HFB-PV experiments were carried out under non-steady state conditions, the driving force for ethanol permeation decreasing and leading to a reduction in the ethanol permeation flux with experiment time. As a result, ethanol concentration in the retentate side diminished along the experiments (see Fig. 5.3B).

Table 5.2 Pervaporation with hydrophobic membranes (HFB-PV) at 40 and 60 °C. Ethanol in the feed was 5.3 ± 0.1 wt%. Ethanol concentrations of retentate and permeate and total fluxes at the end of each experiment.

Membrane	Run	Temperature [^{o}C]	Ethanol content [wt%]		$\alpha_{ethanol/water}$ [-]	Total flux [kg·m^{-2}·h^{-1}]
			Retentate	Permeate		
SIL	E1	40	0.46 ± 0.0	23 ± 3	18.0 ± 4.8	0.32 ± 0.0
SIL	E2	60	0.40 ± 0.1	36 ± 1	37.4 ± 4.5	0.69 ± 0.1
PDMS	E3	60	0.94 ± 0.0	12 ± 0	6.0 ± 0.3	1.7 ± 0.0

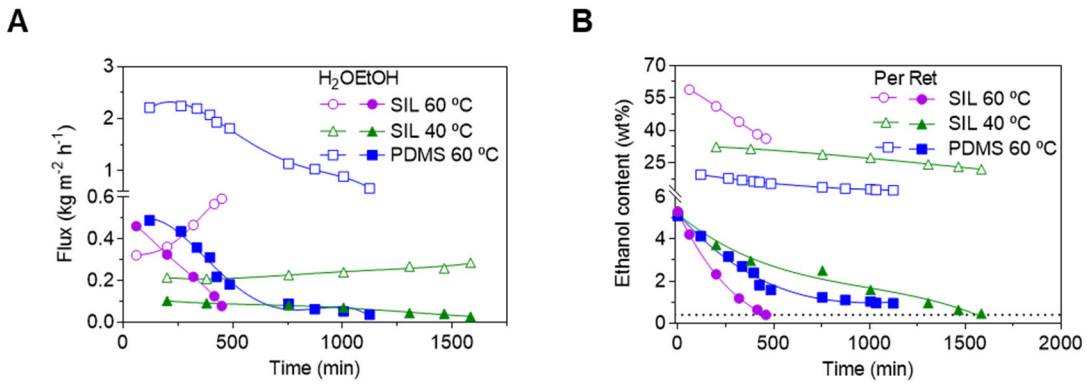

Fig. 5.3 HFB PV of 100 g of a water-ethanol solution with 5.3 ± 0.1 wt% of ethanol. A) Ethanol (closed symbols) and water (open symbols) fluxes as a function of time. B) Ethanol content as a function of time in retentate (closed symbols) and permeate (open symbols); the dashed straight line corresponds to the 0.4 wt% ethanol concentration. The continuous lines are guides to the eye.

As can be seen in Fig. 5.3B, the degree of ethanol removal (considering the above-mentioned ~0.4 wt% limit) was successfully achieved at both temperatures of 40 and 60 °C working with membrane SIL. However, a lower total flux was shown by membrane SIL at 40 °C (Table 5.2), meaning a longer time to reach the target ethanol content in retentate of 0.4 wt%. Besides, the temperature did not seem to influence on the total PV flux tendency, remaining it approximately constant along the experiment at both temperatures (Fig. S5.2). Thus, working at 60 °C allowed to obtain a higher PV flux for ethanol than for water (0.46 and 0.32 $kg{\cdot}m^{-}2{\cdot}h^{-1}$, respectively) at the beginning of the HFB-PV experiments. This led to the recovery of a higher amount of retentate (87 % at 60 °C; 76 % at 40 °C) with an ethanol concentration around 0.4 wt%. This low ethanol concentration in the retentate stream will contribute to generate the stripping agent for reuse in OD. Under these conditions and as shown in Fig. 5.2B, a permeate with a higher ethanol content was obtained at 60 °C (36 wt%) than at 40 °C (23 wt%), the first being closer to the ethanol concentration fixed as an adequate feed (40 wt%) for the next HFL-PV step. In consequence, the optimum temperature to carry out HFB-PV was set at 60 °C.

As can be seen in Fig. 5.3A, membrane PDMS exhibits the highest total flux value (Table 5.2), decreasing sharply with time until reaching values close to those of membrane SIL at the same temperature (60 °C). However, this higher total flux obtained with PDMS in comparison with that of SIL did not cause the expected reduction in ethanol content in the retentate, due to the lower ratio between ethanol and water fluxes shown. This is in agreement with a higher separation factor of membrane SIL with respect to membrane PDMS as shown in Table 5.2. In fact, the PDMS ethanol PV flux diminished over time until reach a very small value (0.04 $kg{\cdot}m^{-2}{\cdot}h^{-1}$ after 1000 min), while

the water flux remained at a considerable high level (0.65 $kg \cdot m^{-2} \cdot h^{-1}$ after 1000 min). This prevented from achieving the degree of dealcoholization proposed, obtaining an alcohol concentration of 0.94 wt% in the retentate and generating an insufficient ethanol concentration in the permeate of 12 wt% (Table 5.2). In summary, membrane SIL is considered as the best to carry out the hydrophobic separation and decrease the alcohol concentration in the retentate below 0.4 wt%, the optimum temperature being set at 60 °C to obtain an alcohol rich permeate in a short time (Fig. 5.3B). In these conditions, an ethanol/water separation factor of up to 37.4 (as compared to 6.0 with PDMS) with an ethanol flux of 0.69 $kg \cdot m^{-2} \cdot h^{-1}$ were obtained (Table 5.2). In any event, the PV flux and separation factor values are in agreement with those achieved with similar hydrophobic membranes applied generally to higher concentration feeds [227].

Another interesting information can be gathered from the PDMS membranes. As a preliminary work, membrane PDMS was used to evaluate the PV performance from different feeds, from a synthetic ethanol-water solution (13 wt% ethanol concentration) to red wine full of aromas (13 wt% ethanol concentration). A summary of these results is shown in Fig. S5.3. No significant differences in ethanol/water separation factors were observed as a function of feed concentration, while a decrease of PV flux was observed from 0.9 $kg \cdot m^{-2} \cdot h^{-1}$ (ethanol-water solution) to 0.6 $kg \cdot m^{-2} \cdot h^{-1}$ (red wine) in agreement with some dissolution of the wine aromas on the PDMS membrane slowing the PV flux. In any event, the concentration in volatile compounds in the OD waste is much lower than that in wine, as will be shown below.

5.3.3 Hydrophilic PV of water-ethanol solutions

A synthetic hydroalcoholic solution with 40 wt% ethanol (fixed as an adequate concentration to carry out the dehydration process) was used as feed for the second HFL-PV step with the aim of increasing the ethanol concentration and obtain a water-like permeate that can be used as stripping agent in further OD. Membranes used for this purpose were made of hydrophilic zeolites mordenite (membranes MOR1 and MOR2) and faujasite (membrane FAU). These types of zeolite membranes prepared on tubular mullite supports have shown very good performance when dehydrating organic compounds or separating the most polar compound in a given organic mixture [228].

Table 5.3 Pervaporation with hydrophilic membranes (HFL-PV) under steady state conditions at two different temperatures. Ethanol in the feed was 40 ± 0.1 wt%.

Membrane	Run	Temperature [ºC]	Ethanol content [wt%]		$\alpha_{water/ethanol}$ [-]	Total flux [kg·m^{-2}·h^{-1}]
			Retentate	Permeate		
MOR1	E4	55	40 ± 0.5	3.7 ± 0.3	17.4 ± 1.5	0.69 ± 0.0
MOR1	E5	75	40 ± 0.7	2.1 ± 0.3	39.1 ± 3.6	1.2 ± 0.0

Given the important effect of temperature observed on the hydrophobic separation, this parameter was first studied to enhance the HFL-PV. Membrane MOR1, whose results are summarized in Table 5.3, was tested at 55 and 75 °C, at steady state conditions (i.e. ethanol concentration at feed or retentate side approximately constant at 40 wt%). As temperature increased so did the total PV flux and the separation factor, which is in agreement with a previous work using hydrophilic zeolites where the water flux was thermally activated in this temperature range [229]. This allowed to fix 75 °C as the optimal temperature to carry out the HFL-PV.

Once fixed the optimum temperature to carry out the HFL-PV, Table 5.4 shows the comparison between mordenite and faujasite membranes operating under non-steady state conditions to emulate the further dehydration of the permeate from HFB-PV. In addition, Fig. 5.4 depicts the evolution of the HFL-PV fluxes and the water retentate and permeate concentrations as a function of time for each membrane, under non-steady state. Sooner (membrane FAU because of its high water PV flux, see Fig. 5.4A) or later (membranes MOR1 and MOR2) the retentate reached in all cases an ethanol concentration over 99 wt%, as shown in Fig. 5.4B related to the low water concentration achieved at certain operation time. In this sense, membrane FAU allowed a faster decrease in the water concentration, according to its higher total PV flux (3.4 kg·m^{-2}·h^{-1}) than those of the two mordenite membranes (ca. 1.1-1.2 kg·m^{-2}·h^{-1}), reaching the bioethanol target concentration of 99% 3 times faster. However, the high total flux shown by FAU did not allow to reuse the permeate generated as stripping phase in the OD, due to the high ethanol concentration remained (18.7 wt%), unsuitable for the stripping phase. This is in agreement with the low water/ethanol separation factor of 21.2 for FAU as compared to the much higher values for MOR of up to 7225, see runs E8 and E7 in Table S5.2.

The previous results can be explained by the evolution of water and ethanol fluxes that permeate through membrane FAU along time. As observed in Fig. 5.4A, the water flux started at a higher value (4.6 kg·m^{-2}·h^{-1}) than that of the ethanol flux (0.26 kg·m^{-2}·h^{-1}), generating a permeate with a 5.7 wt% ethanol concentration. Nevertheless, it rapidly

became lower than the ethanol flux, meaning that only 65 % of total ethanol in the feed was recovered as bioethanol. Besides, although no important differences in permeance of mordenite membranes were observed (Table 5.4), membrane MOR1 required more time to reach the same dehydration degree. This result can be explained by the similar water flux of both membranes but with a less ethanol flux of MOR2 (Fig. 5.4B). Therefore, permeates obtained with MOR2 working at 75 ^{o}C are more suitable to be reused as stripping phase in OD.

Table 5.4 Pervaporation with hydrophilic membranes (HFL-PV) under non-steady state conditions at 75 ^{o}C. Ethanol in the feed was 40 ± 0.1 wt%. Ethanol concentrations of retentate and permeate and total PV flux obtained at the end of each experiment.

Membrane	Run	Ethanol content [wt%]		$\alpha_{water/ethanol}$	Total flux
		Retentate	Permeate	[-]	[kg·m^{-2}·h^{-1}]
MOR1	E6	>99	3.1 ± 0.4	736 ± 296	1.1 ± 0.2
MOR2	E7	>99	< 0.2	7225 ± 2009	1.2 ± 0.2
FAU	E8	>99	19 ± 4	21.2 ± 7.5	3.4 ± 0.4

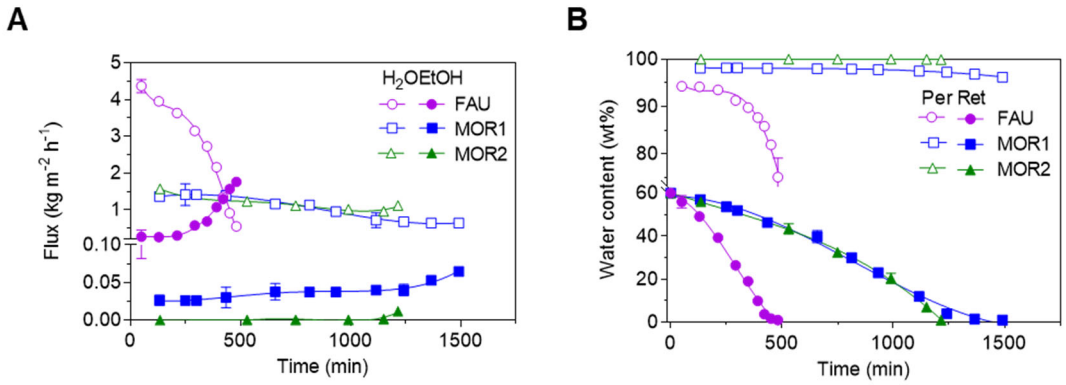

Fig. 5.4 HFL-PV results feeding 100 g of a water-ethanol solution with 40 ± 0.1 wt% of ethanol. A) Ethanol (closed symbols) and water (open symbols) fluxes as a function of time. B) Water content as a function of time in retentate (closed symbols) and permeate (open symbols). The continuous lines are guides to the eye.

Finally, as shown in Fig. S5.3, regarding the experiments in Table 5.2 and Table 5.4, water and ethanol pervaporation permeances were calculated according to Eq. 4.3. Even though the discussion along the work has been done in terms of fluxes, it is true that these values are not only function of the intrinsic properties of the membranes used (in this case very different since both hydrophobic and hydrophilic membranes have been applied), but also depend on the operating conditions (feed concentration and

temperature and vapor pressure driving force) [230]. The presentation of permeances may facilitate the comparison of the current work results with those obtained under different pervaporation conditions but with the same mixtures studied here.

5.3.4 PV of extracting solutions

As compared to SIL membranes with a much higher Si/Al ratio [222], MOR and FAU membranes are characterized by a low Si/Al ratio [223,224]. This low Si/Al ratio allows the introduction of compensation cations in the zeolite framework turning it hydrophilic. It is generally admitted that non-zeolite pores and structural defects in zeolite membranes have a stronger effect on hydrophobic membranes than on hydrophilic ones because of the presence of silanol groups on the zeolite surface which favors the PV of polar compounds [217]. This explains the much higher separation factors achieved with MOR membranes than with SIL membranes, both being the best performing hydrophobic and hydrophilic membranes to be used for the PV of OD extracting solutions in this section.

The hydrophobic-hydrophilic PV, equipped with the membranes chosen in the present study (SIL as a hydrophobic membrane and MOR2 as a hydrophilic one), was tested using OD waste as feed as shown in Table 5.5. In what concerns the ethanol recovery, carrying out the global PV process under the optimum conditions, HFB-PV allowed to recover 92 % of the ethanol removed from red wine by membrane OD. This ethanol (36 wt%) was fed to the subsequent HFL-PV where in turn 98 % of ethanol was retained as dehydrated ethanol (bioethanol) with MOR2. This bioethanol is more than 99 wt% in ethanol, having overcome the azeotropic composition. It is interesting to note that the alcohol concentration in the permeate of the hydrophobic PV is high enough as to avoid the need of a thermal process of ethanol concentration in between [231]. In summary,

In summary, from a reduction of 3 v/v% in the alcoholic degree of wine, the combined hydrophobic-hydrophilic PV setup allowed to recover 88 % of the ethanol removed from wine as bioethanol (percentage calculated by total mass balance). In addition, no significant major differences in the membrane SIL performance were found when facing water ethanol solution or OD wastewater with traces of organic compounds (See Table 5.6). This suggests that ethanol recovery from OD waste is probably easier than from fermentation broths [232]. MOR2 showed a comparable performance with both feeds too, confirming the high stability reported for this type of zeolite membrane [224,233].

Table 5.5 PV performance with best hydrophobic (silicalite-1, SIL, ethanol/water separation factor) and hydrophilic (mordenite, MOR2, water/ethanol separation factor) membranes. W/E means water-ethanol solutions.

	Feed	Ethanol content [wt%]	Time	Ethanol recovery	$\alpha_{-/-}$	Total flux
		Retentate (final)	[min]	[%]	[-]	[kg·m^{-2}·h^{-1}]
HFB-PV	W/E 100 g, 5.3 wt%	0.4	460	93	37.4 ± 4	0.69 ± 0.1
	OD waste 125 g, 5.2 wt%	0.4	550	92	36 ± 4	0.72 ± 0.0
HFL-PV	W/E 100 g, 40 wt%	>99	1215	99	7225 ± 2009	1.2 ± 0.2
	Permeate from HFB-PV 17 g, 36 wt%	>99	300	98	6918 ± 728	1.2 ± 0.2

Despite having selected membrane SIL as the optimum membrane based on the results obtained from HFB-PV experiments with water-ethanol solutions, both hydrophobic membranes PDMS and SIL were fed with OD wastewater. This was mainly due to the fact that a fouling phenomenon was observed in previous experiments with solutions enriched (aroma concentrate, as compared to the OD wastewater, see Table 5.6) in some selected aroma organic compounds using membrane SIL. However, this effect was not observed with the low PV performance membrane PDMS (not shown).

Table 5.6 Aroma compositions of red wine, aroma concentrate (balanced with 50%/50% ethanol/water) and OD wastewater as determined by chromatography.

Aroma	Wine [mg·L^{-1}]	Aroma concentrate [mg·L^{-1}]	OD wastewater [mg·L^{-1}]
Isoamyl acetate	0.44 ± 0.07	3.5 ± 0.17	0.15 ± 0.03
Ethyl acetate	56 ± 3	5.7 ± 0.2	14.1 ± 0.6
Ethyl lactate	61 ± 4	3.7 ± 0.3	4.8 ± 0.5
Isoamyl alcohol	222 ± 5	154 ± 7	103 ± 1.3
-Phenylethanol	32.0 ± 0.6	10 ± 0.2	0.79 ± 0.29
Acetic acid	429 ± 40	0.43 ± 0.07	0.68 ± 0.07
Hexanoic acid	1.8 ± 0.0	3.3 ± 0.08	0.11 ± 0.00
δ-Butyrolactone	17.0 ± 0.6	4.0 ± 0.4	0.36 ± 0.00

The study of the stability of the membrane PV operation when dealing with realistic mixtures is of great importance. Abounding on the silicalite-1 membrane performance,

Fig. 5.5 and Table S5.4 show the history of membrane SIL submitted to 174 h of accumulated experiments under different conditions. Experiments 1, 2, 16 and 17 were carried out at 40 °C with a PV flux of ca. 0.3 $kg \cdot m^{-2} \cdot h^{-1}$, runs 3-8, 14, 15 and 18-21 were at 60 ºC with higher PV flux in the 0.6-0.7 $kg \cdot m^{-2} \cdot h^{-1}$ range regardless of using water-ethanol solutions or OD wastewater (with traces of aromas, as shown in Table 5.6). Nevertheless, experiments 9 and 10 with an aroma concentrate feed (at much higher concentrations than those observed in the OD wastewater) accelerated the fouling of the hydrophobic zeolite membrane provoking a huge diminishing of its PV flux. This was not recovered during next runs 11-13 with water-ethanol and required of a calcination stage at 480 °C for 12 h to retrieve the initial performance of the membrane (from rum 14).

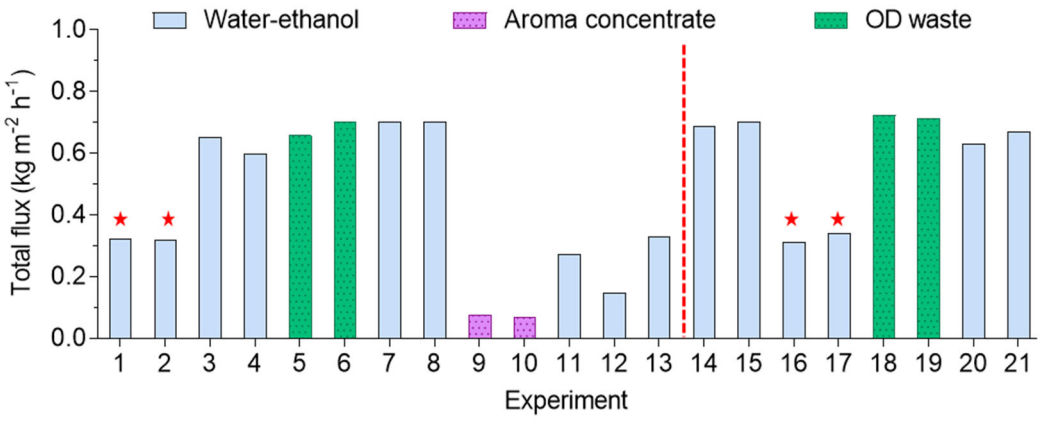

Fig. 5.5 Total PV flux for 21 experiments carried out with membrane SIL at 60 ºC, except in those marked with a star, carried out at 40 ºC. Total accumulated time: 174 h. The vertical red line indicates the calcination of the membrane at 480 ºC.

To complete the discussion about the PV membrane stability, Table 5.7 summarizes the histories of the four PV membrane types applied in this chapter. In case of PDMS, a different membrane sample was used for each different feed, while membranes SIL and MOR (in this case with two samples) were intensively exposed to different PV conditions regarding temperature and feed concentration, as seen above for membrane SIL, demonstrating their high stability and robustness. Hydrophilic membrane FAU was studied only with water-ethanol solutions due to its worse performance in terms of separation factor as compared to membranes MOR.

Table 5.7 Experiments carried out with each membrane under several experimental conditions. W/E means water-ethanol solutions with an ethanol concentration of 1-5 wt%, aroma/W/E has the concentration shown in Table 6.

Membrane	Samples	Range of temperature [ºC]	Time under stream [h]	Feed	Activation Treatment
PDMS	4	30-60	89	W/E; wine; OD waste; aroma/W/E	-
SIL	1	40-60	174	W/E; OD waste; aroma/W/E	480 ºC, 12 h
MOR	2	55-75	100	W/E; OD waste treated	-
FAU	1	75	16	W/E	-

As shown in Table S5.5, these results agree with previous work in which the ethanol-water mixture was separated by hydrophobic PV with a PDMS membrane (working at similar levels of PV flux and separation factor in case of membrane PDMS but much lower than those achieved with the silicalite-1 membrane) generating a permeate with 80 wt% ethanol [220]. This permeate was submitted to secondary PV with carboxymethyl cellulose (CMC) membrane giving rise to 99 wt% water. Similar strategy was used with PDMS/PVA (polyvinyl alcohol) hydrophobic/hydrophilic membranes to obtain 99 wt% isobutanol from a 2 wt% aqueous isobutanol solution [221]. Even if the hydrophilic PV with the PVA membrane yielded a very low water/alcohol separation factor, that reported with the CMC membrane was comparable to those achieved in this study with the MOR membranes but with considerably lower PV flux: below 0.15-0.2 $kg \cdot m^{-2} \cdot h^{-1}$ at 25-30 °C with both CMC and PVA membranes. This highlights the advantages of the zeolite membranes, which are more stable, in the case of silicalite-1 able to withstand a thermal reactivation treatment at 480 °C and also to perform with higher alcohol/water separation factors than the PDMS membranes, and much more permeable in the case of the hydrophilic membranes.

5.3.5 Partial dealcoholization of red wine with recycled water from membrane OD

Once both PV steps were optimized and validated with the water-rich volume generated in the membrane OD performed with fresh water, membrane OD was carried out with recycled water. This recycled water was constituted by combining the retentate

of the hydrophobic PV with the permeated of the hydrophilic PV. This recycled water was used as extracting solution in a new membrane OD experiment, allowing a reduction in the water consumption associate to OD by 99 %, from 0.5 to less than 0.005 liter of water per liter of wine (see Fig. 5.1), and giving rise to analogous partially dealcoholized wine than when using fresh deionized water in terms of contents of aroma compounds (see Fig. 5.2), than when using fresh deionized water. Indeed, together with the production of bioethanol, this is the main achievement of this study, thus demonstrating the saving of water during the whole operation of partial dealcoholization of wine without affecting its aroma profile as compared to the OD using fresh water.

In fact, in most cases the losses of aromas are comparable, within the experimental error, reusing the PV water (see W_B in Fig. S5.1) and applying fresh water (W_A). This allows to confirm that the reuse of water for the OD operation is an acceptable option from the separation point of view. It is worth mentioning that acids did show a slightly higher retention in wine when PV water was used as stripping stream. This can be due to the fact that PV water could include traces of some components, especially those that show a higher polarity, decreasing their driving force for the OD process.

These results demonstrate the feasibility of the approach carried out in this chapter where the OD wastewater is converted in bioethanol and the remaining water is reused for new OD. This agrees with previous LCA carried out on several common partial dealcoholization techniques, including membrane OD applied to wine, demonstrating that the high consumption of natural resources can be reversed by valorizing the wastewater [96], as done here by PV. Moreover, OD has other inherent advantages, since it can be done at a relatively low temperature (11 °C) as compared, for instance, to the widely used spinning cone column treatment (working at 30 °C) [193], consequently affecting less the properties of wine.

5.4 Conclusions

Membrane osmotic distillation (OD) technology was applied to carry out a partial dealcoholization of red wine using a polypropylene hollow fiber membrane module. For a more sustainable process, OD was combined with hydrophobic-hydrophilic pervaporation (PV) carried out on the OD wastewater (only 5.3 wt% ethanol) allowing both the production of bioethanol and the recycle of water for the OD operation. In addition, the following conclusions can be gathered from this study:

Preliminary (PV) experiments with ethanol-water solutions demonstrated the suitability of hydrophobic silicalite-1 (over polymeric PDMS) and hydrophilic mordenite (over faujasite) zeolite membranes to carry out the respective hydrophobic and hydrophilic PV.

Constituting an illustrative example of process intensification, the combination of OD with a sequential hydrophobic-hydrophilic PV process, mainly based, respectively, on zeolite membranes of silicalite-1 (working at 60 °C) and mordenite (at 75 °C) adds value to the water-rich waste product from OD, transformed into recycled water with ca. 0.4 wt% ethanol, constituted by combination of the retentate of the hydrophobic pervaporation with the permeate of the hydrophilic pervaporation, and bioethanol (ca. 99 wt.% ethanol), i.e. the retentate of the hydrophilic pervaporation.

The recycled water was used as extracting solution in a new membrane OD operation, giving rise to analogous partially dealcoholized wine, in terms of contents of aroma compounds, than that achieved when using fresh deionized water. This strategy reduced the water consumption to practically zero in the whole process, which is of paramount importance to validate the industrial potential of membrane OD to dealcoholize wine.

Finally, 88 % of the ethanol removed from wine could be recycled into sustainable bioethanol, alternative to fossil fuels, confirming that the global process frames within the rule of the three Rs of reuse, recycle and reduce.

5.5 Supplementary information

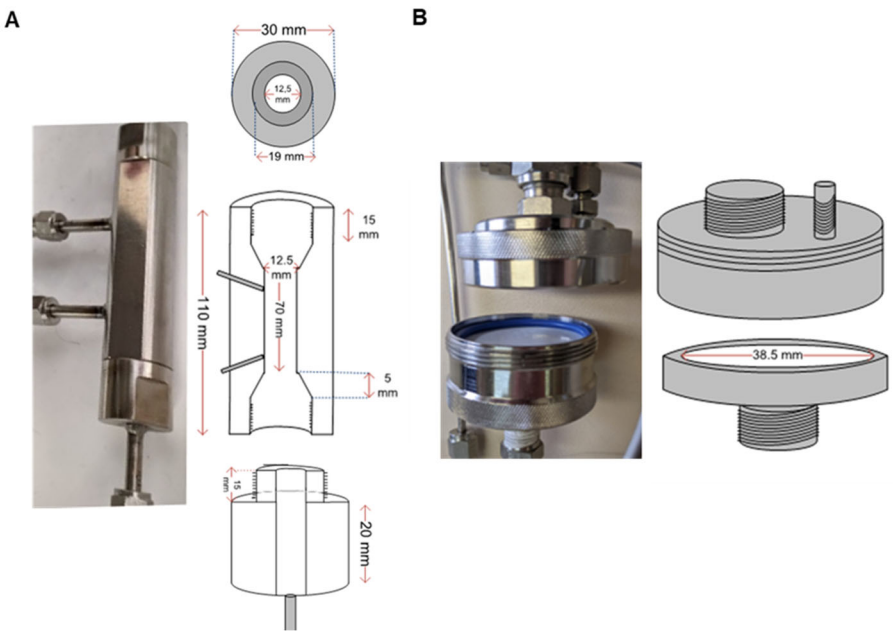

Fig. S5.1 Membrane modules used in PV, including main dimensions, for: A) tubular zeolite membranes. B) PDMS flat sheet membranes.

Table S5.1 Content of volatile compounds in wines ($mg \cdot L^{-1}$). W0 fresh, untreated wine; W_A wine obtained with deionized water as stripper agent; W_B wine obtained with PV treated water as stripper agent. Mean values ± standard deviations were obtained from two replicates. a Concentration expressed as $mL \cdot mL^{-1}$.

Compound	W_0	W_A	$(W_0-W_A)/W_0$ [%]	W_B	$(W_0-W_B)/W_0$ [%]
[a] Ethanol	14.0 ± 0.2	11.2 ± 0.06	20.6	11.2 ± 0.08	20.2
Aliphatic alcohols					
Isobutanol	31.1 ± 3.0	21.0 ± 0.7	32.4	23.3 ± 2.0	25.2
1-Butanol	0.88 ± 0.08	0.64 ± 0.02	27.9	0.70 ± 0.05	21.0
Isoamyl alcohol	222 ± 5	162 ± 1	27.0	166 ± 1	25.3
1-Hexanol	2.00 ± 0.02	1.48 ± 0.00	25.8	1.50 ± 0.02	24.8
cis-3-Hexen-1-ol	0.07 ± 0.00	0.06 ± 0.00	20.3	0.05 ± 0.00	20.5
Aromatic alcohols					
Benzyl alcohol	0.42 ± 0.02	0.43 ± 0.01	-1.1	0.43 ± 0.02	-1.6
2-Phenylethanol	31.7 ± 0.6	32.5 ± 0.8	-2.8	31.5 ± 2.3	0.7
Acetates					
Isoamyl acetate	0.44 ± 0.07	0.24 ± 0.00	45.7	0.26 ± 0.00	41.9
Ethyl esters from straight chain fatty acids					
Ethyl propanoate	0.09 ± 0.01	0.06 ± 0.01	36.23	0.06 ± 0.01	38.1
Ethyl butirate	0.11 ± 0.03	0.06 ± 0.01	49.3	0.06 ± 0.00	47.7
Ethyl hexanoate	0.31 ± 0.05	0.15 ± 0.01	51.4	0.14 ± 0.00	53.3
Ethyl octanoate	0.19 ± 0.05	0.15 ± 0.00	20.6	0.14 ± 0.04	28.2
Ethyl decanoate	0.20 ± 0.05	0.17 ± 0.02	13.5	0.17 ± 0.04	13.4
Ethyl esters from fermentation acids					
Ethyl lactate	60.9 ± 3.8	52.7 ± 0.8	13.5	53.9 ± 0.4	11.5
Diethyl succinate	6.60 ± 1.1	5.8 ± 0.3	11.80	6.1 ± 0.1	6.9
Acids					
Acetic acid	429 ± 40	301 ± 12	29.8	303 ± 9	29.4
Butiric acid	0.55 ± 0.05	0.44 ± 0.02	19.7	0.47 ± 0.00	14.6
Isobutyric acid	0.99 ± 0.09	0.75 ± 0.01	23.6	0.84 ± 0.01	14.6
Isovaleric acid	1.2 ± 0.1	1.1 ± 0.02	6.3	1.1 ± 0.02	13.4
Hexanoic acid	1.78 ± 0.04	1.72 ± 0.05	2.9	1.70 ± 0.08	4.3
Octanoic acid	1.5 ± 0.1	1.3 ± 0.1	13.8	1.3 ± 0.2	16.8
Decanoic acid	0.16 ± 0.04	0.19 ± 0.06	8.5	0.14 ± 0.07	13.6
Others					
Acetoin	64 ± 6	53.44 ± 6.18	16.46	53.72 ± 3.98	16.0
δ-Butyrolactone	17 ± 2	17.43 ± 0.07	-2.33	17.93 ± 0.44	-5.3
Methionol	1.43 ± 0.1	1.5 ± 0.0	-1.95	1.5 ± 0.0	-4.6

Table S5.2 Average values of ethanol/water separation factor obtained of each collected permeate and retentate samples feeding water-ethanol solutions.

Membrane	Run	Temperature [°C]	Permeate weight [g]	$\alpha_{-/-}$ [-]	Total flux [kg·m^{2}·h^{-1}]
SIL	E1	40	22 ± 1.3	18.0 ± 4.8	0.32 ± 0.0
SIL	E2	60	13 ± 0.2	37.4 ± 4.5	0.69 ± 0.1
PDMS	E3	60	37 ± 0.2	6.0 ± 0.3	1.7 ± 0.0
MOR1	[a] E4	55	-	17.4 ± 1.5	0.69 ± 0.0
MOR1	[a] E5	75	-	39.1 ± 3.6	1.2 ± 0.0
MOR1	E6	75	63	736 ± 296	1.1 ± 0.2
MOR2	E7	75	60	7225 ± 2009	1.2 ± 0.2
FAU	E8	75	73	21.2 ± 7.5	3.4 ± 0.4

[a] Experiments carried out under steady state conditions.

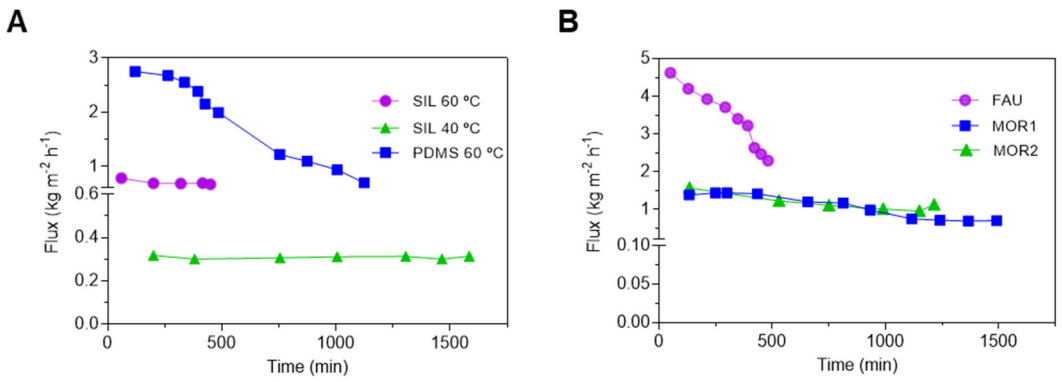

Fig. S5.2 Total flux as a function of time in both PV process. A) Total flux trough hydrophobic membranes; HFB PV results feeding with a 100 g of a water-ethanol solution with 5.3 ± 0.1 wt% of ethanol. B) Total flux trough hydrophilic membranes; HFL PV results feeding with a 100 g of a water-ethanol solution with 40.0 ± 0.1 wt% of ethanol.

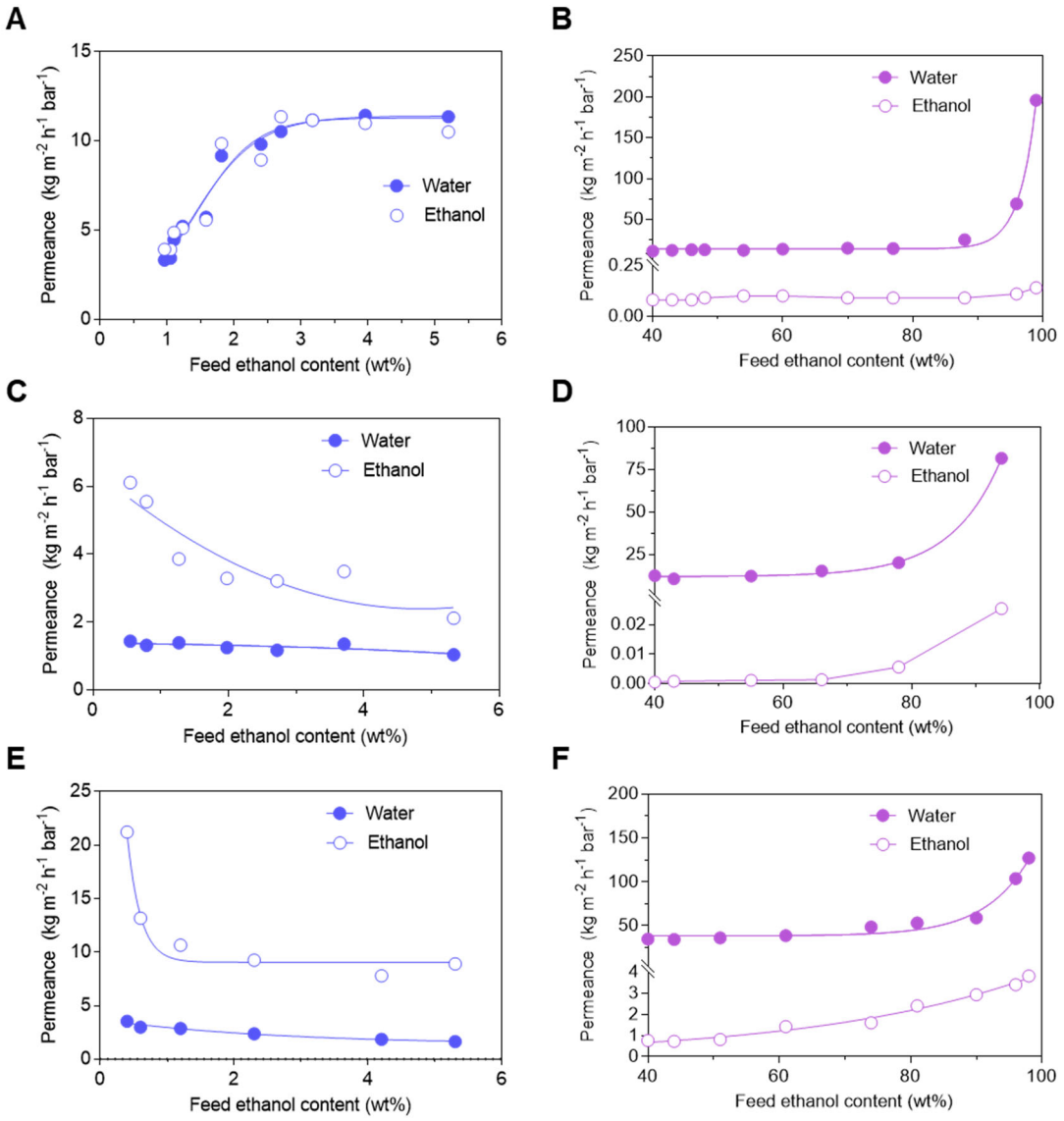

Fig. S5.3 Pervaporation permeances as a function of ethanol concentration in the feed corresponding to the runs in Tables 2 and 4: A) membrane PDMS at 60 ºC, C) membrane SIL at 40 ºC, membrane SIL at 60 ºC, B) membrane MOR1 at 75 ºC, D) membrane MOR2 at 75 ºC and F) membrane FAU at 75 ºC.

Table S5.3 Average values of ethanol/water separation factor and total flux obtained with PDMS membranes at 30 ^{o}C with two different feeds.

Feed	Ethanol content [wt%]		$\alpha_{ethanol/water}$	Total flux [kg·m^{-2}·h^{-1}]
	Retentate	Permeate		
Water-ethanol solution	13 ± 0	53 ± 1	7 ± 1	0.9 ± 0.3
Red wine	13 ± 1	46 ± 1	6 ± 0	0.6 ± 0.0

Table S5.4 Average values of ethanol/water separation factor and total flux obtained with SIL membranes under different experimental conditions.

Feed	T [°C]	Ethanol content [wt%]		$\alpha_{ethanol/water}$	Total flux [$kg \cdot m^{-2} \cdot h^{-1}$]
		Retentate	Permeate		
Water-ethanol (0.91 wt%)	40	0.4 ± 0	9.4 ± 1	18 ± 0	0.32 ± 0.0
Water-ethanol (0.91 wt%)	60	<0.1 ± 0	7.3 ± 1	25 ± 0.4	0.62 ± 0.2
OD waste (0.92 wt%)	60	<0.1 ± 0	7.6 ± 0	24 ± 1	0.67 ± 0.0
Water-ethanol (5.3 wt%)	60	0.4 ± 0	35.6	36. ± 0.4	0.7
[1]Aroma concentrate	60	54 ± 0	91.5 ± 3	9 ± 0.3	0.07± 0.0
*Water-ethanol (5.3 wt%)	60	0.4 ±0.1	35.5 ± 1	37 ± 4	0.69 ± 0.1
*Water-ethanol (5.3 wt%)	60	0.4 ±0.1	35.5 ± 1	37 ± 4	0.69 ± 0.1
Water-ethanol (5.3 wt%)	40	0.46 ± 0	23± 3	18 ± 4.8	0.32± 0.0
OD waste (5.2 wt%)	60	0.4 ±0.2	36.0 ± 2	35 ± 4	0.72 ± 0.0

Table S5.5 Comparison of hydrophobic-hydrophilic PV application.

Application	Hydrophobic membrane	Hydrophilic membrane	Alcohol concentration achieved	Water concentration achieved	Ref.
OD waste treatment	Silicalite-1	Mordenite	>99 wt%	>99.6 wt%	This chapter
Ethanol production	PDMS	CMC	>80 wt%	98-99 wt%	[220]
Isobutanol purification	PDMS	PVA	99.7 wt%	Not available	[221]

CHAPTER 6

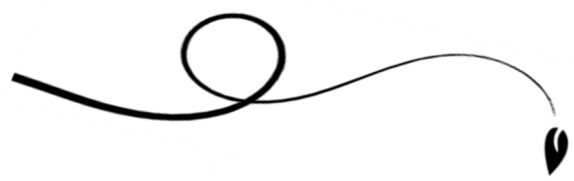

LIGHT BEER PRODUCTION BY MEMBRANE OSMOTIC DISTILLATION

From Esteras-Saz, J; De la Iglesia, A; Téllez, C; Coronas, J. Light beer production by membrane osmotic distillation. In preparation.

6 Light beer production by membrane osmotic distillation

6.1 Introduction

Beer is one of the most important alcoholic beverages in the world with an annual production of almost 2000 million hectoliters per year [122], being also the most consumed alcoholic beverage in Western society (America and Europe) [234]. Currently, beer industry is betting on a series of innovative products such as gluten-free beer, alcohol-free beer or low-sugar beers, in response to current social trend for a healthier life. Among them, non-alcoholic beer has recently grown in interest due to the fact that it allows beer consumption by people like pregnant women or people having certain pathologies (e.g. celiac disease), belonging to different cultures or professing different religions. Indeed, non-alcoholic beer could be the key to Islamic market, where alcohol consumption is prohibited by law. Non-alcoholic beer seeks to maintain the intrinsic healthy and organoleptic properties of beer, without the adverse effects of ethanol; however, the "normal beer" sensory characteristics are not fully being obtained in dealcoholized beers, since they are negatively affected by dealcoholization process. For instance, the reduction of ethanol due to enzymatic activity generates a very sweet taste in beer, as well as those processes that require an increment in temperature that lead to less intense products with a reminiscent caramel flavor [126,127].

The use of membranes for beer dealcoholization (mainly nanofiltration and reverse osmosis) has increased along the last years, due to their ability to adequately diminish the ethanol content in alcoholic beverages operating at room temperature, thus avoiding a thermal damage in the organoleptic and nutritional characteristics of the final product [84,128–130]. Moreover, membrane processes, such as osmotic distillation, show the ability to work also at low pressure reducing the energy consumption as compared to most of membrane and non-membrane based technologies. Nowadays, membrane osmotic distillation (OD) has drawn growing attention as a dealcoholization technique given its ability to work at low pressures and temperatures (further reducing the required energy consumption), having been already used in wine and beer dealcoholization [106,149,151,170,172,194].

In OD, the feed (beer in this case) is separated by the membrane from a solution with low content in the component of interest (ethanol) and a partial pressure gradient between both membrane sides acts as the driving force. Two streams are generated: dealcoholized beer and the extracting stream, which is basically water with a low ethanol content. Unfortunately, beers dealcoholized by membrane technologies,

including OD where the mentioned driving force affects the rest of components different from ethanol to a greater or lesser extent, are still far from meeting the preferences of consumers, who find them poor in body and aroma [127].

Furthermore, the role played by the volume ratio between feed and extracting streams in the performance of membrane OD is evident when a loss limit of aroma components is established. In fact, while total dealcoholization of wine by OD reported a relative loss of volatile compounds of up to 98 % [107,151], lower degrees of dealcoholization (until -5 points of v/v%) made possible to obtain wines with sensory characteristics closer to those of the fed wine [103,106]. A similar behavior was expected for a beer subjected to partial dealcoholization by OD. In fact, De Francesco et al. [194] reported that beer aroma and taste are less related to those components that undergo the highest losses, namely higher alcohols and esters, than in wine. Hence, the knowledge of parameters such as ethanol content, pH, antioxidant activity, total carbohydrates, bitterness and color, typically controlled in the brewing industry, are usually enough to evaluate the evolution of the beer attributes upon its dealcoholization. In view of the above, OD seems to be an effective tool to carry out beer partial dealcoholization with a higher preservation of volatile components due to the soft operation conditions applied.

In this work, membrane OD is proposed for partial dealcoholization of beer in order to achieve a product with 50 % of the ethanol content of a normal beer, intending to minimize the impact on the beer sensory properties. This type of beer with half the ethanol concentration is very consumed in the US market under the name of “light beer”. In fact, in 2010, “light beer” consumption accounted for more than 50% of the total beer sales in the United States [131]. Not requiring a total dealcoholization, “light beer” makes possible to achieve a trade-off between the decrease of the alcoholic degree and the loss of beer properties, being a healthier beverage with aroma and body profiles similar to those of a regular beer. Having said this, several experiments using Lager beer were carried out monitoring the typical quality parameters of the brewing industry in order to assess the membrane OD performance in terms of comparison of properties of the original and partially dealcoholized beers.

6.2 Materials and Methods

6.2.1 Materials

Beer submitted to dealcoholization in this work was kindly provided by La Zaragozana S.A. (Zaragoza, Spain): Ambar Especial, a Lager beer with an alcoholic content of 5.2 v/v% whose main quality parameters are in Table 6.1.

Table 6.1 Lager beer quality parameters measured in this work.

Beer quality parameter	Value
Ethanol concentration (v/v%)	5.3
pH (-)	4.2
Antioxidant activity (µM Ga)	301
Total carbohydrates (g·100 mL^{-1})	4.7
Bitterness (IBU)	24
Color (EBC)	12.3

Hydrophobic porous polypropylene membrane modules supplied by 3M with an effective membrane area of 0.18 m^2 (MM – 1x5.5 x-50 Liqui-Cel^{TM}) were used in this work. Structural and morphological characteristics of this membrane were previously obtained by scanning electron microscopy (SEM) [170]. The 3M membrane module was equipped with 2300 hollow fibers with a nominal pore size of 0.03 µm, an effective membrane length of 14 cm, and an internal and external fiber diameter of 220 and 300 µm, respectively.

6.2.2 Experimental setup

OD experiments were carried out by duplicate in a lab scale plant equipped with the above described PP membrane modules. In each dealcoholization trial, 200 mL of beer was fed to the shell side of the membrane module, while a certain volume of stripping (deionized water) was fed with an adjustable rate to the tube side in counter-current configuration to enhance the ethanol extraction [152]. Retentate and permeate flows were continuously recirculated to the beer and the water tanks thanks to two peristaltic pumps (Dinko, model 1.9735.15), respectively. Pressure (1 atm) and temperature (11 ^{o}C) in the system were monitored and controlled by pressure indicators and a chiller bath circulator (Julabo, CORIO-201F), respectively. An inert atmosphere inside the

dealcoholization module, vessels and pipes was achieved before each dealcoholization trial forcing nitrogen to flow through the experimental system during 2 h at 100 cm^3(STP)·min^{-1}. After each experiment, a cleaning protocol ensured that the OD plant and the membrane module were in suitable conditions. Briefly, several cycles with pressurized water and compressed air were applied to clean the OD system and the membrane modules were subjected to additional cleaning with 0.5 wt% NaOH water solution at 60 °C.

Table 6.2 shows the conditions corresponding to the partial dealcoholization trials carried out in this work. The effect of feed flow was evaluated in trials C1 and C2 while the influence of volume ratio between feed and stripping stream was studied in trials C2-C4. It is worth mentioning that beers were previously decarbonated by a slight aging under inert atmosphere during 4 h. Quality parameters from original and decarbonate beer measured shown comparable values (Fig. S6.1).

Table 6.2 Operating conditions at room temperature (11 °C) and V_f = 200 mL.

Condition	Q_f [mL·min^{-1}]	Q_s [mL·min^{-1}]	V_s [mL]
C1	20	39	400
C2	74	39	400
C3	74	39	200
C4	74	39	300

6.2.3 Chemical analysis

During the experiments, aliquots of both streams leaving the module were taken at constant time intervals in order to analyze their ethanol concentration and the other quality parameters. Regarding the ethanol analysis, 20 µL of methanol (HPLC grade, Scharlau) was added to 1 mL of sample as internal standard. This mixture (0.5 µL) was injected in a gas chromatograph 7820A (Agilent Technologies) equipped with a PORAPAK Q80/100 column, 2 m x 1.8 in x 2 mm and a FID detector. The injector worked at 250 °C in splitless mode with a 1:100 ratio. Helium was used as carrier gas at a constant flow of 1 mL·min^{-1} and the temperature in the oven was fixed at 200 °C. From ethanol concentration and stripping weight, membrane fluxes at fixed time intervals were calculated with the following equation:

$$J_{Exp}(t) = \frac{\Delta W}{A_e \Delta t} \quad (6.1)$$

where ΔW is the variation of ethanol mass for an interval of time, Δt, and A_e corresponds to the effective membrane area.

Parameter pH was measured with Thermo Scientific™ pH-meter Orion Star™ A2011. A UV–vis spectrophotometer (Jasco V-670) was used to obtain several parameters in order to characterize beer. These parameters are: color (EBC units, European Brewing Convention), bitterness (IBU, International Bitterness Units), total carbohydrates (g·100 mL^{-1}), antioxidant activity. Beer color was evaluated according to the standard method (EBC, 2008), measuring directly the sample absorbance at a wavelength of 430 nm. It is calculated with the following equation:

$$Color_{EBC} = 25 * Abs_{430} \quad (6.2)$$

EBC method 9.8 was followed to measure their bitterness extracting the bitter substances from beer, mainly iso-α-acids [235]. The following procedure was applied: 10 mL of beer, 1 mL of HCl 3 M (ACS reagent, Sigma Aldrich), 20 mL of isooctane (>99 %; Carlo Erba) and 50 µL 1-octanol ((>99 %; Sigma-Aldrich) were added into a 50 mL centrifuge tube. The mix was vortexed (Lbx instruments V05 series) at 60 % for 15 min. The resulting emulsion was centrifuged at 1900 rpm for 5 min at room temperature, generating two phases. The upper phase (organic solution) was collected and analyzed by UV spectrometry at 275 nm using 50 µL 1-octanol/20 mL isooctane solution as blank. Bitterness was calculated in IBU as follows:

$$Bitterness\ (IBU) = 50 * Abs_{275} \quad (6.3)$$

To measure the total carbohydrate concentration, the phenol-sulfuric acid method was applied [236]. Briefly, a certain amount of beer was diluted by a factor of 1:1000 and 2 mL of this was mixed with 1 mL of phenol (90 %; Sigma Aldrich) 0.5 M. After that, 5 mL of sulfuric acid (> 95%; Scharlau) was added to the previous resulting mixture. standard solution was prepared following the same procedure using a solution of dextrose (2 v/v%) instead of beer, while2 mL of distillated water was mix with the same phenol/sulfuric acid than sample and standard solutions. All solutions were vortexed for 10 min (until a homogenous color was seen) and analyzed by UV spectrometry at 490 nm. The total carbohydrate concentration in the sample was expressed in g·100 mL^{-1} applying the following equation:

$$Total\ carbohydrates = \frac{0.9*(Abs_{sample} - Abs_{blank})*2*100}{(Abs_{standard} - Abs_{blank})*100} \quad (6.\ 4)$$

Antioxidant activity in beer was evaluated following the DPPH method previously used by Tafulo et al. [237]. Shortly, a solution of DPPH, 2,2-diphenyl-1-picrylhydrazyl

(pure, Sigma Aldrich) (0.19 mM) was prepared in a sodium acetate hydroalcoholic solution (50 v/v% ethanol) 0.1 M. A certain amount of beer (200 µL) was diluted 15 times with the DPPH solution. After 10 min, the DPPH radical reaction was measured at 525 nm, expressed as Ga equivalent concentration (µM)

6.3 Results and discussion

To link the behavior of several quality parameters with the beer composition, the beer was diluted with deionized water producing several diluted beers. The spectrophotometric analysis used to obtain the values of the quality parameters of the diluted beers showing, as expected, a linear correlation with the dilution grade Fig. S6.1. Meanwhile, several studies have reported that, upon total dealcoholization by OD, some of these parameters. (pH, antioxidant activity, total carbohydrates, bitterness and color) maintained at acceptable values with a minor loss of volatile components loss close to 90 % [238,239]. This suggests that the concentration of these volatile compounds has not a major influence on the typical beer quality parameters evaluated here.

6.3.1 Influence of experimental conditions on ethanol

Once the analysis of quality parameters was validated with sample dilution, 200 mL of Lager beer was submitted to partial dealcoholization by OD under different experimental conditions (Table 6.2) until achieving a light beer with 2.5 v/v%. The critical role of the ratio $V_s \cdot V_f^{-1}$ (V_s and V_f being stripping and feed volumes, respectively) is well-known. This determines the maximum amount of each component that migrates from the beer to the stripping stream through the membrane. In fact, the dealcoholization degree and eventual loss of volatile components are strongly dependent on the volume ratio used. With the same objective of dealcoholization (a reduction of alcoholic degree until 2.5 v/v%, i.e. around 50 % regarding the total amount of ethanol), three trials were carried out with the same feed flow (74 mL·min^{-1}) and different $V_s \cdot V_f^{-1}$ ratios. C3: the minimum that allows the removal of the ethanol objective, $V_s \cdot V_f^{-1} = 1$; C2: same volume ratio/relative ethanol removal previously used, $V_s \cdot V_f^{-1} = 2$; and C4: an intermediate ratio, $V_s \cdot V_f^{-1} = 1.5$. As shown in Table 6.3, the higher the volume ratio the lower the experimental time required to produce the “light beer”, as a consequence of the higher ethanol flux achieved.

Table 6.3 Beer partial dealcoholization performance under different experimental conditions in terms of ethanol behavior. Operating conditions at room temperature (11 °C) and V_f = 200 mL.

Condition	Ethanol flux [L·m^{-2}·h^{-1}]	Ratio $V_s \cdot V_f^{-1}$ [-]	[EtOH]$_s$ [v/v%]	$t_{1/2}$ [min]
C1	0.039	2	1.4	50
C2	0.043	2	1.4	45
C3	0.031	1	2.6	45[a]
C4	0.031	1.5	2.0	60

Q_f, feed flow rate; Q_s, stripping flow rate; V_f, feed volume; V_s, stripping volume; $t_{1/2}$, time to reduce from 5.2 to 2.5 v/v%. [a] time to reduce up to 2.7 v/v%.

The effect of feed flow was also evaluated with the comparison of trials C1 and C2, using feed flows of 20 and 74 mL·min^{-1}, respectively. In agreement with the previous results, the ethanol flux increased from 0.039 to 0.043 L·m^2·h^{-1} and, in consequence, the time for 50% dealcoholization decreased from 50 to 45 min (Fig. 6.1). The ethanol fluxes obtained here are in line with those previously reported for beer dealcoholization: an ethanol flux of 0.04 L·m^2·h^{-1} was obtained by Liguori et al. [172] working with a $V_s \cdot V_f^{-1}$ ratio of 2 and a temperature of 10 °C, while 0.028 L·m^2·h^{-1} was achieved by De Francesco et al. with higher volume ratio and dealcoholization degree [238]. Nevertheless, in general, all these ethanol fluxes, including the ones obtained here, are minor than those obtained from the wine partial dealcoholized (0.10-0.12 L·m^2·h^{-1} [170]). The difference is probably due to the presence of traces of dissolved CO_2 in beer, which may clog the pores of the membrane hindering the passage of ethanol through it. Figure 1 shows the variation of ethanol content in the feed and stripping stream as a function of time under different experimental conditions (C1 - C4).

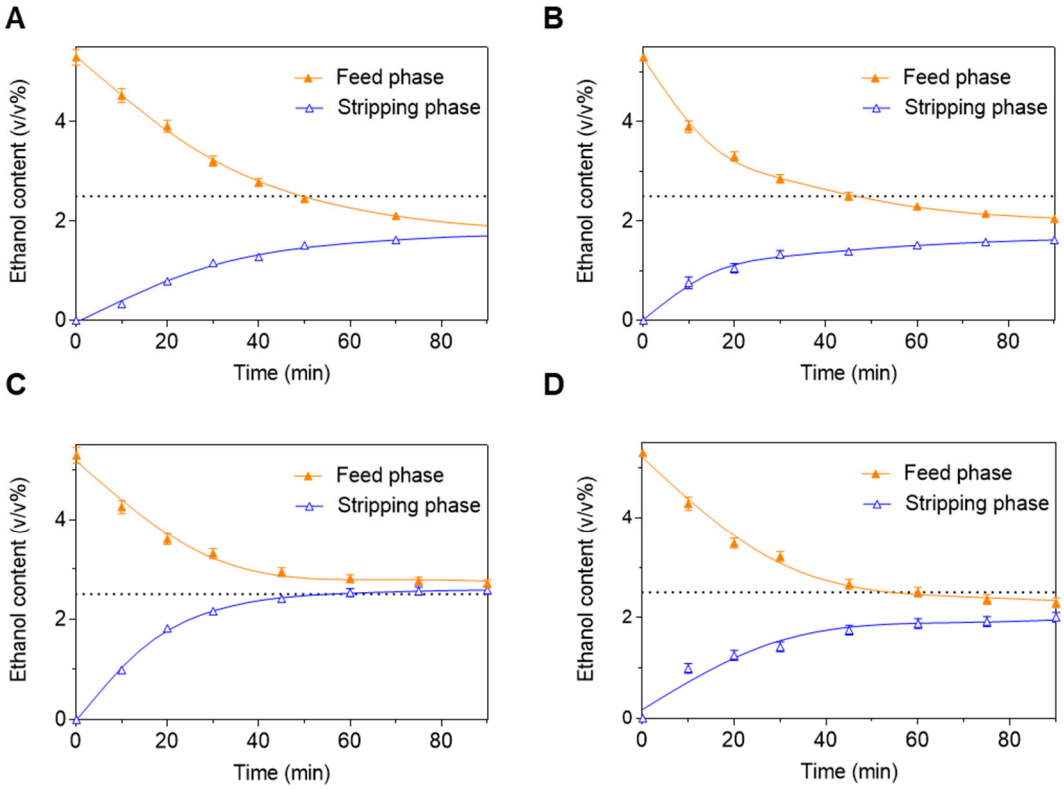

Fig. 6.1 Ethanol content as a function of time corresponding to a beer feed with 5.3 v/v% of ethanol. The experimental conditions for A-D) correspond to C1-C4 in Table 1. Represented data are the mean values with the corresponding standard deviations. The curves are only guides to the eye. Dashed horizontal lines indicate the target for the degree of dealcoholization 2.5 v/v%.

Under C3 operation conditions (see Table 6.1), the partial dealcoholized beer only achieved an alcoholic degree of 2.7 v/v% when reaching the steady state after about 45 min due to the limitation of the stripping volume with the lowest value tested of 200 mL (Fig. 6.1). In any event, this value is not far from the target of 2.5 v/v% but with a considerable saving of water as compared to the other conditions. A slightly dilution, an allowed practice in the brewing industry [240], of the beer obtained under these conditions could help achieve the objective of dealcoholization. Regarding C2 and C4, a a higher volume ratio allowed to obtain the light beer in a faster way (45 and 60 min, respectively). However, this time enhancement implied the use of higher amount of stripping stream (water needed in C4 was reduced by 33 %) consequently increasing the consumption of water and generation of waste. Moreover, the possible valorization of this waste via distillation or another separation technology like pervaporation (see chapter 5) would require a less energy demand as the wastewater would show a higher ethanol concentration (see Table 6.3). The optimum condition in terms of ethanol behavior corresponds to C4, achieving the dealcoholization degree target in a reasonable time with a less amount of water (stripping phase) consumption.

6.3.2 Influence of experimental conditions on quality parameters

To study the influence of the experimental conditions on the quality of the light beer obtained, five quality parameters and their dependence on the dealcoholization degree were evaluated. It is worth mentioning that the values obtained from C3 conditions were not included here due to the fact the alcohol removal target was not achieved. It is evident that the values of quality parameters should raise due to the removal of ethanol during OD, i.e. increasing in a 2.5 % after a reduction of 50 % in the alcohol degree (just due to a simple concentration effect). All the values obtained for these parameters in this chapter were compared to those previously reported in literature for total dealcoholization of beer by OD (see Table S6.1).

pH and antioxidant activity

The pH analysis of beer allows the estimation of the presence of acids playing in turn an important role in the beer resistance to microbial contamination [241]. These acids are organic ones such as acetic, pyruvic, lactic or succinic [242]. However, as Table 4 shows, there is no correlation between the pH, the dealcoholization degree (when comparing C0 with the rest of conditions) and the different dealcoholization conditions applied. The slight changes observed were independent on the mentioned conditions and can be related to the presence of traces of dissolved CO_2 in beer. The absence of correlation indicates a non-significant impact of OD on the acid composition, which is in agreement with previous reports [171,172,238]. Carboxylic acids are in general more polar than alcohols, what limits their transport through the hydrophobic PP membrane, therefore their composition remains unaltered. This hypothesis is in accordance with recent studies reporting that the acid composition in beer was not significantly altered by a OD dealcoholization, except for acetic acid [243]. Interestingly, this exception has also been found in the wine dealcoholization experiments shown in chapters 3, 4 and 5 and previously reported in literature, where the loss of acetic acid was explained by its high volatility as compared to those of other polar compounds[107,151].

Table 6.4 Quality parameters without correlation with the dealcoholization degree.

Condition	C0	C1	C2	C4
Alcoholic degree (v/v%)	5.2	2.5	2.7	2.5
pH value	4.19 ± 0.01	4.20 ± 0.01	4.19 ± 0.00	4.19 ± 0.01
Antioxidant activity (μM Ga)	301 ± 8	292 ± 15	296 ± 19	287 ± 5

Concerning beer antioxidant activity, this has been typically evaluated by the measurement of the scavenging capacity of a free radical like DPPH. DPPH assessment is based on the changes observed in the stable radical DPPH by the electron donating ability of the sample [244]. As can be seen with Table 6.3 and Table 6.4, the antioxidant activity decreases with the time required by each condition to reach the same dealcoholization degree, from 296 to 287 µM Ga for C1-C4 conditions, being 301 µM Ga in the starting beer). A strong relation between beer antioxidant activity and the presence of polyphenols generated from the Maillard reaction (e.g. the chemical reaction between reducing saccharides and amino acids) has been previously stablished [245,246]. In this sense, the change in the antioxidant activity of beer can be explained by the higher oxidation degree of polyphenols as a consequence of the handling of the beer samples and the exposure time to the dealcoholization conditions [247], even if the necessary precautions were taken into consideration during the treatment of beer (e.g. purging the system with N_2 to remove the air).

Total carbohydrates

As depicted in Fig. 6.2, the concentration of total carbohydrates shows, for all the experimental conditions studied) a non-linear increase as a function of the percentage of ethanol removal. The results suggest that for C4 conditions total carbohydrates could be close to the expected maximum values, not being recommended a higher dealcoholization degree for the rest of conditions (C1 and C2) where the losses of carbohydrates were slightly greater.

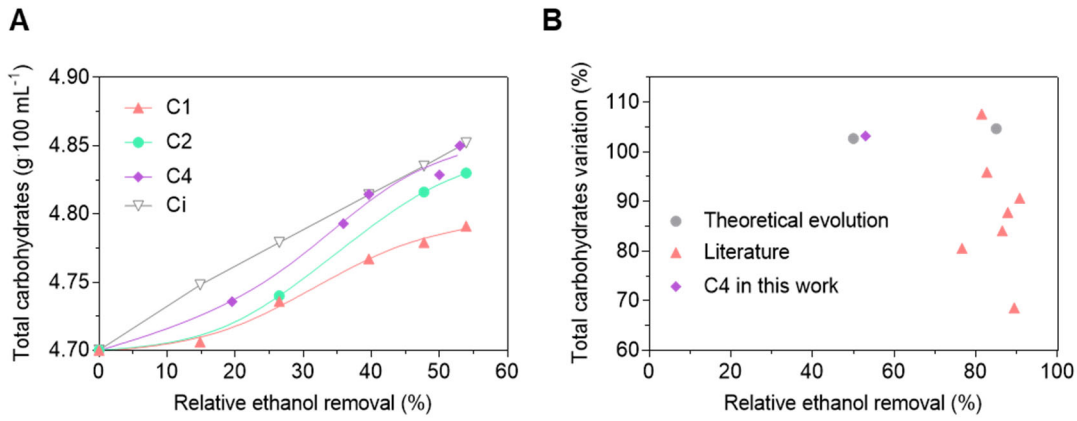

Fig. 6.2 Total carbohydrates in beer as a function of relative ethanol removal. A) Evolution of total carbohydrates from starting beer (4.70 mg·L^{-1}) under C1, C2 and C4 conditions. The "theoretical values" (Ci) correspond to the concentration increase due to the removal of ethanol. B) Relative total carbohydrates retention in dealcoholized beers obtained from different studies (Fig. S6.1). The lines are only guides to the eye.

Comparing the values of total carbohydrates obtained from each condition with each other and with the values (Ci) obtained from the concentration increase due to the removal of ethanol are included, the light beers obtained when applying C1 (4.79 g·100 mL^{-1}) and C2 (4.83 g·100 mL^{-1}) conditions present a less amount of carbohydrates, while those corresponding to C4 and Ci are equal (ca. 4.85 g·100 mL^{-1}), at the same ca. 50 % dealcoholization. Together with ethanol, carbohydrates are the main source of calorific energy in beer, thus being relevant in the nutritional value of the product. Even if the carbohydrate composition is complex, two main chemical families of carbohydrates can be found in beer: fermentable sugars (25 %), such as maltotriose or maltose, and dextrins (75 %), a non-fermentable sugar coming from the hydrolysis of starch [248][249]. The first ones are directly related with the sweetness of beer and contribute to the beer body on mouthfeel [249]. Meanwhile, dextrins have also a great contribution to the beer taste and body [250]. Therefore, the similar values of total carbohydrates displayed by C4 light and original beers suggest that the light beer obtained would present the body that consumers demand in a non-alcohol beer. In addition, the light beer obtained has a better total carbohydrate remain higher than those of most of the non-alcoholic beers reported in literature (Figure 2B). The difference observed may be associated with the instability of fermentable sugars remaining in beer as a result of the total ethanol removal (in the corresponding cases). For instance, maltotriose can react with amino compounds to form α-dicarbonyl compounds by a peeling-off mechanism [251]. This degradation could be diminished if a certain ethanol amount remained in the final beer.

Bitterness

As can be seen in Fig. 6.3A, the bitterness parameter was much more affected than total carbohydrates under all the experimental conditions studied. The worst result was obtained when running the OD with the lower feed flow (i.e., C1 condition at 20 mL·min^{-1} feed flow). This dealcoholization condition produced bitterness values far below those of the original beer (Ci value, corresponding to the concentration correction as said above) and of the other light beers obtained under C2 and C4 conditions. In fact, these two conditions produced light beers with bitterness values higher than that of the original one (24 IBU), although the bitterness tended to decrease as the dealcoholization degree approached the target in both cases.

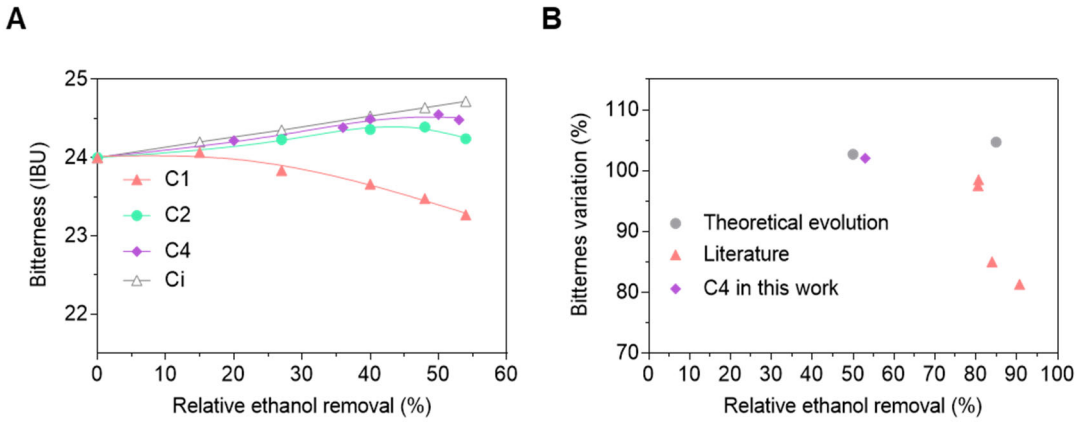

Fig. 6.3 Bitterness (IBU) in beer as a function of relative ethanol removal. A) Evolution of bitterness from feed beer (with 24 IBU) under C1, C2 and C4 conditions. The "theoretical values" (Ci) correspond to the concentration increase due to the removal of ethanol. B) Relative bitterness value retention in dealcoholized beers obtained from different studies (Fig. S6.1). The lines are only guides to the eye.

Polar compounds, iso-α-acids, are responsible for the beer bitterness [252], contributing to the beer bitter taste by around 80 % [253]. Thus, the results with good control of bitterness (C2 and C4 conditions) are consistent with the permanence of such compounds in the light beer upon its partial dealcoholization. Besides, the iso-α-acids also contribute to the microbiological stability of beer [254,255] and may have a favorable health effect on beer consumers [256,257]. Thus, the bitterness values are a positive indicator of the beer quality. However, iso-α-acids present in beer have trans/cis isomers with a ratio of about 0.4 [258]. These isomers seem to have a different contribution to these positive effects [252], the trans isomer showing the best properties in both aspects [259]. In addition, as shown in Fig. 6.3B, non-alcoholic beers in the literature have a lower retention capacity of compounds responsible for bitterness than the obtained here. This could be explained by isomer conversion from

the trans to the more stable cis, decreasing the absorbance value of bitterness. This conversion is also supported by the lower solubility in water of the trans isomer favoring the cis isomer formation [259].

Color

The beer color is mainly attributed to melanoidins, nitrogen-containing polymers formed from the Maillard reaction during the brewing [260]. Melanoidins constitute a very heterogeneous group of compounds with antioxidant capacity [261], but only a few of them have been isolated. One of them is perlolyrine [262], whose boiled temperature is around 534 °C, expecting that its loss during the dealcoholization should not be significant (OD is based on a vapor phase separation). Fig. 6.4A shows a continuous color increase as a function of the removal of ethanol in all experimental conditions studies.

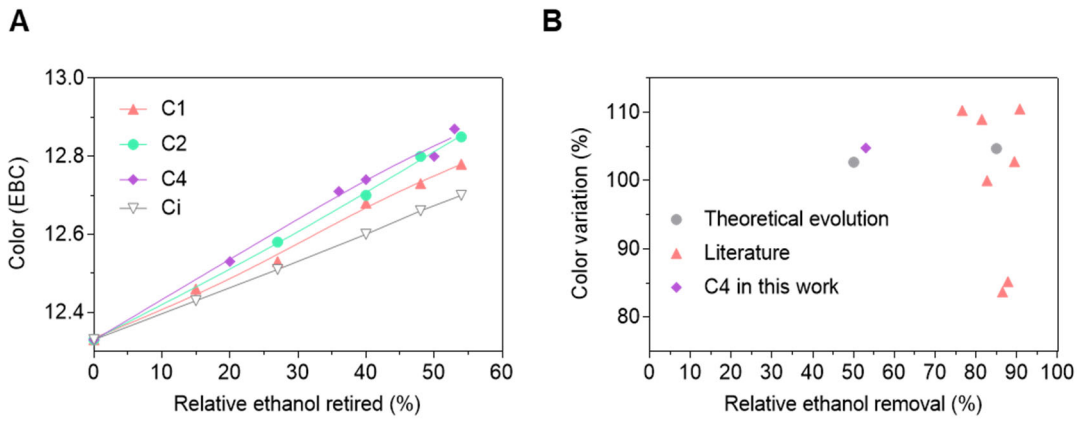

Fig. 6.4 Color in beer as a function of relative ethanol removal. A) Evolution of color from feed beer (with 12.3 EBC) under C1, C2 and C4 conditions. The "theoretical values" (Ci) correspond to the concentration increase due to the removal of ethanol. B) Relative total color value retention in partial and total dealcoholized beers obtained from different studies (Fig. S6.1). The lines are only guides to the eye.

The color increases are consistent with the retention of melanoidins, explaining the enhancement of the antioxidant activity of the light beers, discussed above. Alternatively, the increase in color could not only be due to the formation of the Maillard reaction products. In this sense, several studies concluded that the oxidative degradation of some polyphenols is responsible for the color increment observed during beer storage [261]. Unfortunately, the major issue is that this oxidative degradation not only affects the color intensity but also the correlation with the chill haze formation (i.e. a precipitation of beer polyphenols and proteins [263]) reported by several authors, leading to a decline in the beer stability properties [264]. In any event, since the relative

changes in color are small, the color increment observed here is closer to the predicted value, as shown in Fig. 6.4B. On the contrary, those beers with a lower ethanol amount (at ca. 90 % of ethanol removal) presented in Figure 4B exhibited, in general, a higher color increment than the predicted one. This can be explain by the sharper oxidation of polyphenols with a less amount of ethanol in beer [265].

6.4 Conclusions

It has been demonstrated that osmotic distillation is a feasible technology for beer partial dealcoholization using a polypropylene hollow fiber membrane module. A light beer, with 2.5 v/v% of ethanol, was produced feeding the dealcoholization plant with a Lager beer with an ethanol degree of 5.2 v/v%. The viability of the approach was adequately assessed with the typical quality parameters of the brewing industry such as pH, antioxidant activity, total carbohydrates, bitterness and color. The set of these parameters resulted a useful tool to set up the membrane soft operation conditions (mainly the low temperature of 11 °C) to achieve a better preservation of the beer quality.

Furthermore, the light beer production made possible to achieve a compromise between the decrease of the alcoholic degree and the loss of beer properties, allowing to stablished the operation conditions that limited the loss of beer components. A fed flow of 74 $mL \cdot min^{-1}$ and a volume ratio between both streams (beer and extracted water) equal to 3 allowed to obtain a light beer with quality parameters comparable to those of the original ones. This light beer showed a better quality parameters profile than total dealcoholized beers reported in literature.

6.5 Supplementary information

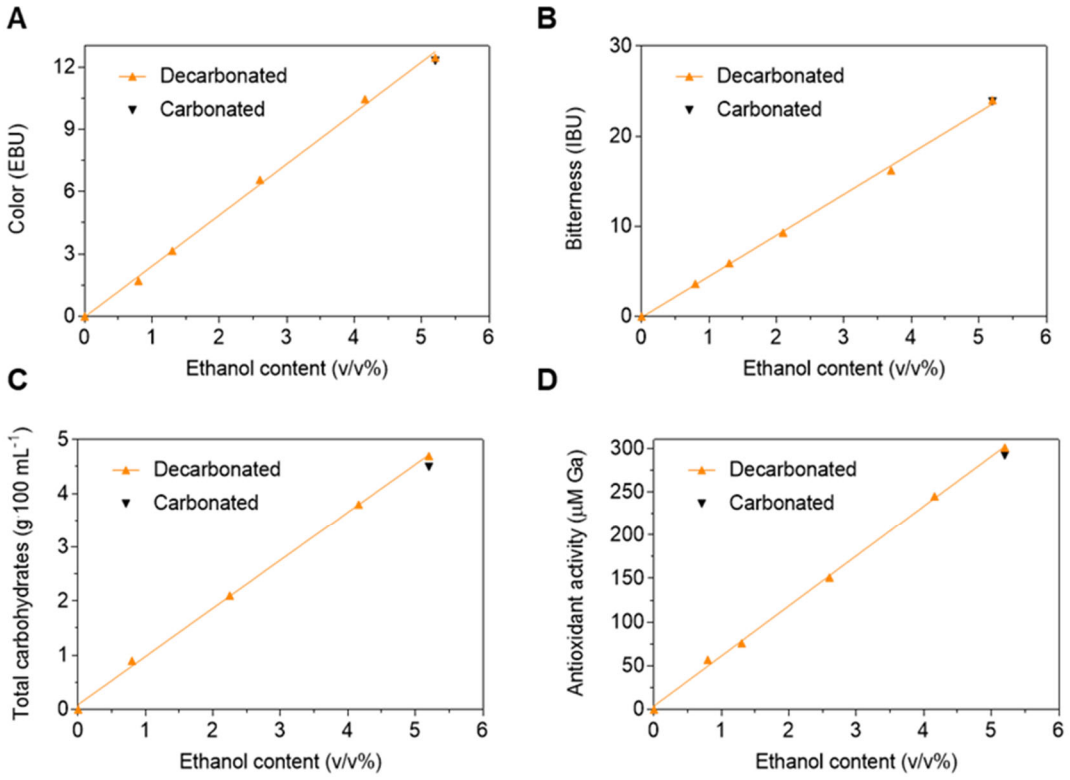

Fig. S6.1. Quality parameters analysis validation with successive lager beer dilutions.

Table S6.1. Summarize of previous studies in literature used to compare the light beer obtained.

	Quality parameters				
Ref.	pH	Antioxidant activity	Total carbohydrates	Bitterness	Color
[238]	X	X	X		X
[172]	X	X	X	X	X
[171]	X	X	X	X	X
[239]	X	X	X	X	X

CAPÍTULO 7

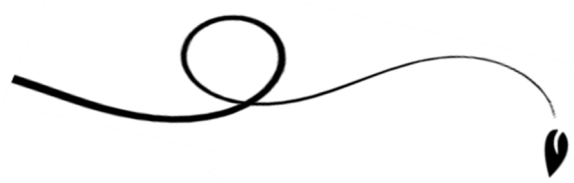

CONCLUSIONES

7 Conclusiones

1. La planta de OD puesta a punto en este trabajo, equipada con un módulo de membrana de polipropileno (PP) comercial, suministrado por 3M, presenta un comportamiento análogo trabajando con alimentaciones sintética (disolución hidroalcohólica) y real (vino). Durante el proceso, la monitorización en tiempo real por ganancia en masa de la corriente de barrido generada proporciona un control adecuado del grado de desalcoholización, favoreciendo la reproducibilidad de los resultados experimentales.

2. Del estudio de las variables de operación llevado a cabo con el módulo de membrana de PP de 3M se concluye que una relación adecuada de los volúmenes de ambas corrientes (alimentación (*Vf*) y barrido (*Vs*), con $Vf \cdot Vs^{-1} = 2$) y un caudal de alimentación óptimo (Q_f = 74 mL·min^{-1}) favorecen la transferencia de etanol. Esto disminuye el tiempo experimental requerido para alcanzar el grado de desalcoholización objetivo.

3. Se ha desarrollado un modelo teórico-empírico que incorpora la solubilidad de los componentes del vino en el material de la membrana (definida por los llamados parámetros de solubilidad de Hansen) a la expresión clásica de resistencia de una membrana, basada en el modelo llamado de *Dusty-Gas*. El modelo propuesto es capaz de predecir con éxito el comportamiento del etanol en todas las condiciones experimentales estudiadas, con un error promedio del 4,3 %, y corrige la sobreestimación de la transferencia de los alcoholes aromáticos predicha por el modelo clásico.

4. El estudio del comportamiento de hasta 25 compuestos relacionados con el aroma del vino en los diferentes ensayos de desalcoholización ha permitido correlacionar la volatilidad de cada componente y su comportamiento durante la OD. Así, se concluye que la pérdida de aromas se establece en el orden ésteres > alcoholes > ácidos, opuesto al de las respectivas volatilidades, aunque un menor tiempo de contacto del vino con la membrana disminuye el impacto general de la desalcoholización. La concentración inicial de cada aroma no afecta a su pérdida porcentual, mientras que la temperatura de operación sí que influye en el comportamiento de los ésteres derivados de ácidos grasos de cadena larga,

cuya pérdida se ha reducido en este trabajo al operar a una temperatura tan baja como 11 °C.

5. Un módulo de membrana suministrado por Zena y equipado con fibras huecas de PP de mayor tamaño de poro (0,1 µm) que el suministrado por 3M (0,03 µm) permite disminuir el tiempo de operación sin repercusión significativa sobre los parámetros estudiados en el vino desalcoholizado. Por otro lado, utilizando un módulo de fibras huecas de PVDF (fluoruro de polivinilideno) suministrado por Polymem, la gran mayoría de componentes mantuvieron sus concentraciones inalteradas tras el proceso. La mayor hidrofobia del PVDF con respecto al PP habría hecho disminuir el efecto de arrastre del etanol, así como evitado el mojado de los poros por dicho compuesto, reduciendo el impacto del proceso sobre el conjunto de aromas del vino. El rendimiento alcanzado por este módulo de membrana, en términos de retención de aromas en el vino tratado, es el más alto reportado hasta la fecha en un proceso de desalcoholización constituido por una única etapa.

6. Se ha llevado a cabo por primera vez la intensificación de la OD mediante su combinación con un proceso secuencial de PV con el fin de solucionar el problema del consumo excesivo de agua asociado a la OD. La pervaporación hidrófoba (a 60 °C con una membrana zeolítica de silicalita-1) seguida de la pervaporación hidrófila (a 75 °C con una membrana zeolítica de mordenita) ha permitido la recuperación del etanol de la corriente de barrido procedente de la desalcoholización. El agua recuperada de este proceso se ha utilizado para la OD de manera satisfactoria (es decir, produciendo la misma variación en las propiedades estudiadas del vino que si se usara agua pura), reduciendo el consumo de agua asociado a la OD prácticamente a cero. Por otra parte, se ha recuperado el 88 % del etanol extraído del vino para obtener un bioetanol >99 % en peso. Esta intensificación del proceso de OD (OD-PV_{HFB}-PV_{HFL}) permite incrementar el potencial industrial de la OD como técnica de desalcoholización.

7. El alcance de la OD se ha extendido satisfactoriamente a la cerveza, ajustando el producto de interés a las características intrínsecas de la técnica de desalcoholización (máximo grado de transferencia conocido). Se este modo se ha obtenido una cerveza parcialmente desalcoholizada (2,5 v/v%, correspondiente a la denominada *light beer*) que presenta parámetros de calidad similares a los de

la cerveza original. Las propiedades de la cerveza se han evaluado en base a los parámetros de calidad establecidos habitualmente a escala industrial (pH, amargor, concentración de carbohidratos, carácter antioxidante y color). Además, la monitorización de tales parámetros durante la desalcoholización resulta ser una herramienta útil para adaptar de manera sencilla y con garantías las condiciones experimentales establecidas previamente para el vino.

CAPÍTULO 8

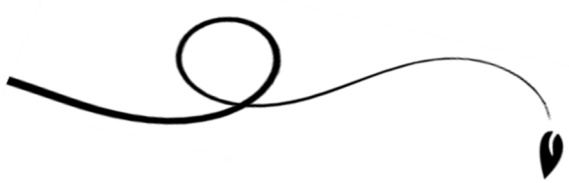

BIBLIOGRAFÍA

8 Bibliografía

[1] K.E. Trenberth, Climate change caused by human activities is happening and it already has major consequences, J. Energy Nat. Resour. Law. 36 (2018) 463–481.

[2] I.M. Held, B.J. Soden, Robust responses of the hydrological cycle to global warming, J. Clim. 19 (2006) 5686–5699.

[3] S. Manabe, Role of greenhouse gas in climate change, Tellus. 71 (2019) 1–13.

[4] G.C. Hegerl, U. Cubasch, Greenhouse gas induced climate change, Environ. Sci. Pollut. Res. 3 (1996) 99–102.

[5] T.J. Crowley, Causes of climate change over the past 1000 years, Science (80). 289 (2000) 270–277.

[6] T.R. Carter, M.L. Parry, J.H. Porter, Climatic change and future agroclimatic potential in Europe, Int. J. Climatol. 11 (1991) 251–269.

[7] J.A. Church, Climate change: How fast are sea levels rising?, Science (80). 294 (2001) 802–803.

[8] C. Henricsson, M.C. De Jesus Ferreira, K. Hedfalk, K. Elbing, C. Larsson, R.M. Bill, J. Norbeck, S. Hohmann, L. Gustafsson, Engineering of a Novel Saccharomyces cerevisiae Wine Strain with a Respiratory Phenotype at High External Glucose Concentrations, Appl. Environ. Microbiol. 71 (2005) 6185.

[9] N.A. Rayner, D.E. Parker, E.B. Horton, C.K. Folland, L. V. Alexander, D.P. Rowell, E.C. Kent, A. Kaplan, Global analyses of sea surface temperature, sea ice, and night marine air temperature since the late nineteenth century, J. Geophys. Res. Atmos. 108 (2003) 4407.

[10] O. Hoegh-Guldberg, Climate change, coral bleaching and the future of the world's coral reefs, Mar. Freshw. Res. 50 (1999) 839–866.

[11] R. Castaño-Rosa, R. Barrella, C. Sánchez-Guevara, R. Barbosa, I. Kyprianou, E. Paschalidou, N.S. Thomaidis, D. Dokupilova, J.P. Gouveia, J. Kádár, T.A. Hamed, P. Palma, Cooling Degree Models and Future Energy Demand in the Residential Sector. A Seven-Country Case Study, Sustainability 13 (2021) 2987.

[12] F. Giorgi, Climate change hot-spots, Geophys. Res. Lett. 33 (2006) 8707.

[13] M. De Castro, J. Martín-Vide, S. Alonso, The climate of Spain: past, present and scenarios for the 21st century, (2005).

[14] E. Vargas-Amelin, P. Pindado, The challenge of climate change in Spain: Water resources, agriculture and land, J. Hydrol. 518 (2014) 243–249.

[15] T. Estrela, M.A. Pérez-Martin, E. Vargas, Impacts of climate change on water resources in Spain, Hydrol. Sci. J. 57 (2012) 1154–1167.

[16] G. V. Jones, M.A. White, O.R. Cooper, K. Storchmann, Climate change and global wine quality, Clim. Change. 73 (2005) 319–343.

[17] A. Benito, I. Romero, N. Domínguez, E. García-Escudero, I. Martín, Leaf blade and petiole analysis for nutrient diagnosis in Vitis viniferaL. cv. Garnacha tinta, Aust. J. Grape Wine Res. 19 (2013) 285–298.

[18] D. Piccardo, G. Favre, O. Pascual, J.M. Canals, F. Zamora, G. González-Neves, Influence of the use of unripe grapes to reduce ethanol content and pH on the color, polyphenol and polysaccharide composition of conventional and hot macerated Pinot Noir and Tannat wines, Eur. Food Res. Technol. 245 (2019) 1321–1335.

[19] D. Piccardo, J. Gombau, O. Pascual, A. Vignault, P. Pons, J.. Canals, G. Gonzalez-

Neves, F. Zamora, Influence of two prefermentative treatments to reduce the ethanol content and pH of red wines obtained from overripe grapes, Vitis J. Grapevine. 58 (2019) 59–67.
[20] F. Zamora (2003), Elaboración y crianza del vino tinto: Aspectos científicos y prácticos. (3ª edición), Madrid: AMV Ediciones.
[21] S. Martin, R.M. Pangborn, Taste interaction of ethyl alcohol with sweet, salty, sour and bitter compounds, J. Sci. Food Agric. 21 (1970) 653–655.
[22] A.L. Robinson, S.E. Ebeler, H. Heymann, P.K. Boss, P.S. Solomon, R.D. Trengove, Interactions between wine volatile compounds and grape and wine matrix components influence aroma compound headspace partitioning, J. Agric. Food Chem. 57 (2009) 10313–10322.
[23] S. Ferrero-del-Teso, I. Arias, A. Escudero, V. Ferreira, P. Fernández-Zurbano, M.-P. Sáenz-Navajas, Effect of grape maturity on wine sensory and chemical features: The case of Moristel wines, LWT. 118 (2020) 108848.
[24] B. Pineau, J.C. Barbe, C. Van Leeuwen, D. Dubourdieu, Examples of perceptive interactions involved in specific “Red-” and “Black-berry” aromas in red wines, J. Agric. Food Chem. 57 (2009) 3702–3708.
[25] C.L. Norris, D.C. Taylor, S. Taylor, What is rogue marketing? An exploration of how hard seltzer sparked a social media phenomenon, Int. J. Wine Bus. Res. 34 (2022) 329–348.
[26] W.M. Kliewer, N.K. Dokoozlian, Leaf Area/Crop Weight Ratios of Grapevines: Influence on Fruit Composition and Wine Quality, Am. J. Enol. Vitic. 56 (2005) 170–181.
[27] A. Palliotti, S. Poni, J.G. Berrios, F. Bernizzoni, Vine performance and grape composition as affected by early-season source limitation induced with anti-transpirants in two red Vitis vinifera L. cultivars, Aust. J. Grape Wine Res. 16 (2010) 426–433.
[28] M. Stoll, M. Lafontaine, H.R. Schultz, Possibilities to reduce the velocity of berry maturation through various leaf area to fruit ratio modifications in Vitis vinifera L. Riesling, Le Progrès Agric. Vitic. 127 (2010) 68–71.
[29] C. Böttcher, K. Harvey, C.G. Forde, P.K. Boss, C. Davies, Auxin treatment of pre-veraison grape (Vitis vinifera L.) berries both delays ripening and increases the synchronicity of sugar accumulation, Aust. J. Grape Wine Res. 17 (2011) 1–8.
[30] S. Poni, M. Gatti, F. Bernizzoni, S. Civardi, N. Bobeica, E. Magnanini, A. Palliotti, Late leaf removal aimed at delaying ripening in cv. Sangiovese: physiological assessment and vine performance, Aust. J. Grape Wine Res. 19 (2013) 378–387.
[31] A. Palliotti, F. Panara, O. Silvestroni, V. Lanari, P. Sabbatini, G.S. Howell, M. Gatti, S. Poni, Influence of mechanical postveraison leaf removal apical to the cluster zone on delay of fruit ripening in Sangiovese (Vitis vinifera L.) grapevines, Aust. J. Grape Wine Res. 19 (2013) 369–377.
[32] M. Stoll, M. Bischoff-Schaefer, M. Lafontaine, S. Tittmann, J. Henschke, Impact of various leaf area modifications on berry maturation in vitis vinifera L. “Riesling,” Acta Hortic. 978 (2013) 293–300.
[33] A.K. Parker, R.W. Hofmann, C. van Leeuwen, A.R.G. Mclachlan, M.C.T. Trought, Manipulating the leaf area to fruit mass ratio alters the synchrony of total soluble solids accumulation and titratable acidity of grape berries, Aust. J. Grape Wine Res. 21 (2015) 266–276.

[34] F. Martínez de Toda, J.C. Sancha, P. Balda, Reducing the sugar and pH of the grape (vitis vinifera l. Cvs. “Grenache” and ’tempranillo’) through a single shoot trimming, Afr. J. Enol. Vitic. 34 (2017) 246-251.
[35] P. Zhang, X. Wu, S. Needs, D. Liu, S. Fuentes, K. Howell, The influence of apical and basal defoliation on the canopy structure and biochemical composition of Vitis vinifera cv. shiraz grapes and wine, Front. Chem. 5 (2017) 48.
[36] G.J. Pickering, D.A. Heatherbell, M.F. Barnes, Optimising glucose conversion in the production of reduced alcohol wine using glucose oxidase, Food Res. Int. 31 (1998) 685–692.
[37] G.J. Pickering, D.A. Heatherbell, M.F. Barnes, The Production of Reduced-Alcohol Wine Using Glucose Oxidase Treated Juice. Part I. Composition, Am. J. Enol. Vitic. 50 (1999) 291–298.
[38] E. Ruiz, M.D. Busto, S. Ramos-Gómez, D. Palacios, M.C. Pilar-Izquierdo, N. Ortega, Encapsulation of glucose oxidase in alginate hollow beads to reduce the fermentable sugars in simulated musts, Food Biosci. 24 (2018) 67–72.
[39] L. Liguori, P. Russo, D. Albanese, M. Di Matteo, Production of Low-Alcohol Beverages: Current Status and Perspectives, Food Processing for Increased Quality and Consumption, (2018) 347-382.
[40] O.J. Schelezki, K. Šuklje, P.K. Boss, D.W. Jeffery, Comparison of consecutive harvests versus blending treatments to produce lower alcohol wines from Cabernet Sauvignon grapes: Impact on wine volatile composition and sensory properties, Food Chem. 259 (2018) 196–206.
[41] O.J. Schelezki, A. Deloire, D.W. Jeffery, Substitution or dilution? Assessing pre-fermentative water implementation to produce lower alcohol Shiraz wines, Molecules. 25 (2020) 2245.
[42] B.N.E. Biyela, W.J. Du Toit, B. Divol, D.F. Malherbe, P. van Rensburg, The production of reduced-alcohol wines using Gluzyme Mono® 10.000 BG-treated grape juice, South African J. Enol. Vitic. 30 (2009) 124–132.
[43] J. Röcker, M. Schmitt, L. Pasch, K. Ebert, M. Grossmann, The use of glucose oxidase and catalase for the enzymatic reduction of the potential ethanol content in wine, Food Chem. 210 (2016) 660–670.
[44] C. Varela, D.R. Kutyna, M.R. Solomon, C.A. Black, A. Borneman, P.A. Henschke, I.S. Pretorius, P.J. Chambers, Evaluation of gene modification strategies for the development of low-alcohol-wine yeasts, Appl. Environ. Microbiol. 78 (2012) 6068–6077.
[45] N.P. Jolly, C. Varela, I.S. Pretorius, Not your ordinary yeast: non-Saccharomyces yeasts in wine production uncovered, FEMS Yeast Res. 14 (2014) 215–237.
[46] S.V. Makarytchev, T.A.G. Langrish, R.G.H. Prince, Structure and regimes of liquid film flow in spinning cone columns, Chem. Eng. Sci. 53 (1998) 1541–1550.
[47] S. V. Makarytchev, T.A.G. Langrish, D.F. Fletcher, Mass Transfer Analysis of Spinning Cone Columns Using CFD, Chem. Eng. Res. Des. 82 (2004) 752–761.
[48] S.V. Makarytchev, T.A.G. Langrish, D.F. Fletcher, Exploration of Spinning Cone Column Capacity and Mass Transfer Performance Using CFD, Chem. Eng. Res. Des. 83 (2005) 1372–1380.
[49] E. Aguera, M. Bes, A. Roy, C. Camarasa, J.M. Sablayrolles, Partial removal of ethanol during fermentation to obtain reduced-alcohol wines, Am. J. Enol. Vitic. 61 (2010) 53–60.

[50] Y.Y. Belisario-Sánchez, A. Taboada-Rodríguez, F. Marín-Iniesta, A. Iguaz-Gainza, A. López-Gómez, Aroma Recovery in Wine Dealcoholization by SCC Distillation, Food Bioprocess Technol. 5 (2012) 2529–2539.
[51] F. Huerta-Pérez, J.R. Pérez-Correa, Optimizing ethanol recovery in a spinning cone column, J. Taiwan Inst. Chem. Eng. 83 (2018) 1–9.
[52] K. Bui, R. Dick, G. Moulin, P. Galzy, A Reverse Osmosis for the Production of Low Ethanol Content Wine, Am. J. Enol. Vitic. 37 (1986) 297-300.
[53] C.E. Nielsen, Low alcohol beer by hyperfiltration route, Brew. Distill. Int. 12 (1982) 39–41.
[54] C.L. Duitschaever, J. Alba, C. Buteau, B. Allen, Riesling Wines Made From Must Concentrated by Reverse Osmosis. I. Experimental Conditions and Composition of Musts and Wines, Am. J. Enol. Vitic. 42 (1991) 19-25.
[55] R.W. Baker (2004), Membrane Technology and Applications. Chichester (UK): John Wiley & Sons, Ltd.
[56] Z. Berk, Food Process Engineering and Technology, (2018).
[57] C. Visvanathan, R. Ben Aim, K. Parameshwaran, Membrane Separation Bioreactors for Wastewater Treatment, Crit. Rev. Environ. Sci. Technol. 30 (2000) 1–48.
[58] T. Le, X. Chen, H. Dong, W. Tarpeh, A. Perea-Cachero, J. Coronas, S.M. Martin, M. Mohammad, A. Razmjou, A.R. Esfahani, N. Koutahzadeh, P. Cheng, P.R. Kidambi, M.R. Esfahani, An Evolving Insight into Metal Organic Framework-Functionalized Membranes for Water and Wastewater Treatment and Resource Recovery, Ind. Eng. Chem. Res. 60 (2021) 6869–6907.
[59] A.K. Pabby, S.S.H. Rizvi, A.M.S. Requena, eds., Handbook of Membrane Separations, CRC Press, 2008.
[60] S. Cerneaux, I. Struzyńska, W.M. Kujawski, M. Persin, A. Larbot, Comparison of various membrane distillation methods for desalination using hydrophobic ceramic membranes, J. Membr. Sci. 337 (2009) 55–60.
[61] M. Gryta, Concentration of saline wastewater from the production of heparin, Desalination. 129 (2000) 35–44.
[62] F. Cacho-Bailo, S. Catalán-Aguirre, M. Etxeberría-Benavides, O. Karvan, V. Sebastian, C. Téllez, J. Coronas, Metal-organic framework membranes on the inner-side of a polymeric hollow fiber by microfluidic synthesis, J. Memb. Sci. 476 (2015) 277–285.
[63] J.D. Perry, K. Nagai, W.J. Koros, Polymer Membranes for Hydrogen Separations, MRS Bull. 31 (2006) 745–749.
[64] P. Vandezande, L.E.M. Gevers, I.F.J. Vankelecom, Solvent resistant nanofiltration: separating on a molecular level, Chem. Soc. Rev. 37 (2008) 365–405.
[65] S. Meillon, C. Urbano, P. Schlich, Contribution of the Temporal Dominance of Sensations (TDS) method to the sensory description of subtle differences in partially dealcoholized red wines, Food Qual. Prefer. 20 (2009) 490–499.
[66] S. Meillon, C. Urbano, G. Guillot, P. Schlich, Acceptability of partially dealcoholized wines – Measuring the impact of sensory and information cues on overall liking in real-life settings, Food Qual. Prefer. 21 (2010) 763–773.
[67] R. Longo, J.W. Blackman, P.J. Torley, S.Y. Rogiers, L.M. Schmidtke, Changes in volatile composition and sensory attributes of wines during alcohol content reduction, J. Sci. Food Agric. 97 (2017) 8–16.

[68] L.M. Schmidtke, J.W. Blackman, S.O. Agboola, Production technologies for reduced alcoholic wines, J. Food Sci. 77 (2012).
[69] European council, amending Regulation (EC) No 1234/2007 establishing a common organisation of agricultural markets and on specific provisions for certain agricultural products (Single CMO Regulation), Off. J. Eur. Union. 2008 (2009) 1–56.
[70] S.L. Wee, C.T. Tye, S. Bhatia, Membrane separation process—Pervaporation through zeolite membrane, Sep. Purif. Technol. 63 (2008) 500–516.
[71] C. Brazinha, J.G. Crespo, Aroma recovery from hydro alcoholic solutions by organophilic pervaporation: Modelling of fractionation by condensation, J. Memb. Sci. 341 (2009) 109–121.
[72] J.G. Crespo, C. Brazinha, Fundamentals of pervaporation, Pervaporation, Vap. Permeat. Membr. Distill. Princ. Appl. (2015) 3–17.
[73] A. Heintz, W. Stephan, A generalized solution—diffusion model of the pervaporation process through composite membranes Part II. Concentration polarization, coupled diffusion and the influence of the porous support layer, J. Memb. Sci. 89 (1994) 153–169.
[74] J.G. Wijmans, R.W. Baker, The solution-diffusion model: a review, J. Memb. Sci. 107 (1995) 1–21.
[75] A. Ghofar, T. Kokugan, The pervaporation mechanism of dilute ethanol solution by hydrophobic porous membranes, Biochem. Eng. J. 18 (2004) 235–238.
[76] B. Bolto, M. Hoang, Z. Xie, A review of membrane selection for the dehydration of aqueous ethanol by pervaporation, Chem. Eng. Process. Process Intensif. 50 (2011) 227–235.
[77] Y. Huang, R.W. Baker, L.M. Vane, Low-energy distillation-membrane separation process, Ind. Eng. Chem. Res. 49 (2010) 3760–3768.
[78] J.H.B. Jaimes, M.E.T. Alvarez, J.V. Rojas, R.M. Filho, Pervaporation: Promissory method for the bioethanol separation of fermentation, Chem. Eng. Trans. 38 (2014) 139–144.
[79] M. Gavahian, P.E.S. Munekata, I. Eş, J.M. Lorenzo, A. Mousavi Khaneghah, F.J. Barba, Emerging techniques in bioethanol production: from distillation to waste valorization, Green Chem. 21 (2019) 1171–1185.
[80] H.O.E. Karlsson, G. Trägårdh, Applications of pervaporation in food processing, Trends Food Sci. Technol. 7 (1996) 78–83.
[81] A. Baudot, M. Marin, Pervaporation of Aroma Compounds: Comparison of Membrane Performances with Vapour-Liquid Equilibria and Engineering Aspects of Process Improvement, Food Bioprod. Process. 75 (1997) 117–142.
[82] L. Takács, G. Vatai, K. Korány, Production of alcohol free wine by pervaporation, J. Food Eng. 78 (2007) 118–125.
[83] M. Catarino, A. Ferreira, A. Mendes, Study and optimization of aroma recovery from beer by pervaporation, J. Memb. Sci. 341 (2009) 51–59.
[84] R. Castro-Muñoz, Pervaporation: The emerging technique for extracting aroma compounds from food systems, J. Food Eng. 253 (2019) 27–39.
[85] R. Castro-Muñoz, C. Conidi, A. Cassano, Membrane-based technologies for meeting the recovery of biologically active compounds from foods and their by-products, Crit. Rev. Food Sci. Nutr. 59 (2019) 2927–2948.
[86] X. Sun, G. Dang, X. Ding, C. Shen, G. Liu, C. Zuo, X. Chen, W. Xing, W. Jin, Production

of alcohol-free wine and grape spirit by pervaporation membrane technology, Food Bioprod. Process. 123 (2020) 262–273.
[87] N. García-Martín, S. Perez-Magariño, M. Ortega-Heras, C. González-Huerta, M. Mihnea, M.L. González-Sanjosé, L. Palacio, P. Prádanos, A. Hernández, Sugar reduction in musts with nanofiltration membranes to obtain low alcohol-content wines, Sep. Purif. Technol. 76 (2010) 158–170.
[88] N. García-Martín, S. Perez-Magariño, M. Ortega-Heras, C. González-Huerta, M. Mihnea, M.L. González-Sanjosé, L. Palacio, P. Prádanos, A. Hernández, Sugar reduction in white and red musts with nanofiltration membranes, Desalin. Water Treat. 27 (2011) 167–174.
[89] M. Mihnea, M.L. González-Sanjosé, M. Ortega-Heras, S. Pérez-Magariño, N. García-Martin, L. Palacio, P. Prádanos, A. Hernández, Impact of must sugar reduction by membrane applications on volatile composition of Verdejo wines, J. Agric. Food Chem. 60 (2012) 7050–7063.
[90] H. Mira, A. Guiomar, V. Geraldes, M.N. De Pinho, Membrane processing of grape must for control of the alcohol content in fermented beverages, J. Membr. Sci. Res. 4 (2017) 308–312.
[91] J. Labanda, S. Vichi, J. Llorens, E. López-Tamames, Membrane separation technology for the reduction of alcoholic degree of a white model wine, LWT - Food Sci. Technol. 42 (2009) 1390–1395.
[92] S. Banvolgyi, I. Kiss, E. Bekassy-Molnar, G. Vatai, Concentration of red wine by nanofiltration, Desalination. 198 (2006) 8–15.
[93] S. Banvolgyi, K. Savaş Bahçeci, G. Vatai, S. Bekassy, E. Bekassy-Molnar, Partial dealcoholization of red wine by nanofiltration and its effect on anthocyanin and resveratrol levels, Food Sci. Technol. Int. 22 (2016) 677–687.
[94] M. Catarino, A. Mendes, Dealcoholizing wine by membrane separation processes, Innov. Food Sci. Emerg. Technol. 12 (2011) 330–337.
[95] P.A. Hogan, R.P. Canning, P.A. Peterson, R.A. Johnson, A.S. Michaels, A new option : Osmotic distillation, Chem. Eng. Prog. 94 (1998) 49–61.
[96] M. Margallo, R. Aldaco, A. Barceló, N. Diban, I. Ortiz, A. Irabien, Life cycle assessment of technologies for partial dealcoholisation of wines, Sustain. Prod. Consum. 2 (2015) 29–39.
[97] V.D. Alves, I.M. Coelhoso, Effect of membrane characteristics on mass and heat transfer in the osmotic evaporation process, J. Memb. Sci. 228 (2004) 159–167.
[98] C.M. Hansen, Aspects of solubility, surfaces and diffusion in polymers, Prog. Org. Coatings. 51 (2004) 55–66.
[99] C.M. Hansen, 50 Years with solubility parameters - Past and future, Prog. Org. Coatings. 51 (2004) 77–84.
[100] M.H. Charles, Hansen Solubilities Parameters, Boca Ratón, 2013.
[101] L. Paseta, G. Potier, S. Abbott, J. Coronas, Using Hansen solubility parameters to study the encapsulation of caffeine in MOFs, Org. Biomol. Chem. 13 (2015) 1724–1731.
[102] C. Andecochea Saiz, S. Darvishmanesh, A. Buekenhoudt, B. Van der Bruggen, Shortcut applications of the Hansen Solubility Parameter for Organic Solvent Nanofiltration, J. Memb. Sci. 546 (2018) 120–127.
[103] N. Diban, V. Athes, M. Bes, I. Souchon, Ethanol and aroma compounds transfer study for partial dealcoholization of wine using membrane contactor, J. Memb.

Sci. 311 (2008) 136–146.
[104] N. Diban, A. Arruti, A. Barceló, M. Puxeu, A. Urtiaga, I. Ortiz, Membrane dealcoholization of different wine varieties reducing aroma losses. Modeling and experimental validation, Innov. Food Sci. Emerg. Technol. 20 (2013) 259–268.
[105] R. Ferrarini, G.M. Ciman, F. Camin, S. Bandini, C. Gostoli, Variation of oxygen isotopic ratio during wine dealcoholization by membrane contactors: Experiments and modelling, J. Memb. Sci. 498 (2016) 385–394.
[106] M.T. Lisanti, A. Gambuti, A. Genovese, P. Piombino, L. Moio, Partial Dealcoholization of Red Wines by Membrane Contactor Technique: Effect on Sensory Characteristics and Volatile Composition, Food Bioprocess Technol. 6 (2013) 2289–2305.
[107] L. Liguori, P. Russo, D. Albanese, M. Di Matteo, Evolution of quality parameters during red wine dealcoholization by osmotic distillation, Food Chem. 140 (2013) 68–75.
[108] B. Fedrizzi, E. Nicolis, F. Camin, E. Bocca, C. Carbognin, M. Scholz, P. Barbieri, F. Finato, R. Ferrarini, Stable Isotope Ratios and Aroma Profile Changes Induced Due to Innovative Wine Dealcoholisation Approaches, Food Bioprocess Technol. 7 (2014) 62–70.
[109] A. Gabelman, S.T. Hwang, Hollow fiber membrane contactors, J. Memb. Sci. 159 (1999) 61–106.
[110] E. Curcio, E. Drioli, Membrane distillation and related operations - A review, Sep. Purif. Rev. 34 (2005) 35–86.
[111] T.K.˚ Udelová, E. Bartuli, A. Strunga, J. Hvožd'a, M. Dohnal, Fully Polymeric Distillation Unit Based on Polypropylene Hollow Fibers, Polymers (Basel). 13 (2021) 1031.
[112] P. Russo, L. Liguori, O. Corona, D. Albanese, M. Di Matteo, L. Cinquanta, Combined Membrane Process for Dealcoholization of Wines: Osmotic Distillation and Reverse Osmosis, Chem. Eng. Trans. 75 (2019) 7–12.
[113] C.M. Salgado, E. Fernández-Fernández, L. Palacio, F.J. Carmona, A. Hernández, P. Prádanos, Application of pervaporation and nanofiltration membrane processes for the elaboration of full flavored low alcohol white wines, Food Bioprod. Process. 101 (2017) 11–21.
[114] D.T. Pham, V.J. Stockdale, D. Wollan, D.W. Jeffery, K.L. Wilkinson, Compositional Consequences of Partial Dealcoholization of Red Wine by Reverse Osmosis-Evaporative Perstraction, Molecules. 24 (2019) 1404.
[115] D.-T. Pham, R. Ristic, V.J. Stockdale, D.W. Jeffery, J. Tuke, K. Wilkinson, Influence of partial dealcoholization on the composition and sensory properties of Cabernet Sauvignon wines, Food Chem. 325 (2020) 126869.
[116] A.M. Jordão, A. Vilela, F. Cosme, From Sugar of Grape to Alcohol of Wine: Sensorial Impact of Alcohol in Wine, Beverages. 1 (2015) 292–310.
[117] W. Kujawski, M. Gierszewska-Druiyńska, J. Warczok, C. Güell, Application of pervaporation and osmotic membrane distillation to the regeneration of spent solutions from the osmotic food dehydration, Polish J. Chem. Technol. 11 (2009) 41–45.
[118] F.E. Sam, T.Z. Ma, R. Salifu, J. Wang, Y.M. Jiang, B. Zhang, S.Y. Han, Techniques for dealcoholization of wines: Their impact on wine phenolic composition, volatile composition, and sensory characteristics, Foods. 10 (2021) 2498.

[119] Reglamento (CE) No 606/2009, de 10 de julio de 2009, que fija determinadas disposiciones de aplicación del Reglamento (CE) no 479/2008 del Consejo en lo relativo a las categorías de productos vitícolas, las prácticas enológicas y las restricciones aplicables, Diario Oficial de la Unión Europea L nº 193, de 24 de julio de 2009.
[120] A. Escudero, B. Gogorza, M.A. Melús, N. Ortín, J. Cacho, V. Ferreira, Characterization of the Aroma of a Wine from Maccabeo. Key Role Played by Compounds with Low Odor Activity Values, J. Agric. Food Chem. 52 (2004) 3516–3524.
[121] V. Ferreira, N. Ortín, A. Escudero, R. López, J. Cacho, Chemical characterization of the aroma of Grenache rosé wines: aroma extract dilution analysis, quantitative determination, and sensory reconstitution studies, J. Agric. Food Chem. 50 (2002) 4048–4054.
[122] G. Donadini, S. Porretta, Uncovering patterns of consumers' interest for beer: A case study with craft beers, Food Res. Int. 91 (2017) 183–198.
[123] The Brewers of Europe (2020), The Contribution made by Beer to the European Economy: EU Report - March 2020.
[124] H.Q. Yeo, S.-Q. Liu, An overview of selected specialty beers: developments, challenges and prospects, Int. J. Food Sci. Technol. 49 (2014) 1607–1618.
[125] R. Mateo-Gallego, S. Pérez-Calahorra, I. Lamiquiz-Moneo, V. Marco-Benedí, A. Bea, A. Fumanal, A. Prieto-Martín, M. Laclaustra, A. Cenarro, C. F, Effect of an alcohol-free beer enriched with isomaltulose and a resistant dextrin on insulin resistance in diabetic patients with overweight or obesity, Clin. Nutr. 39 (2020) 475–483.
[126] L. Montanari, O. Marconi, H. Mayer, P. Fantozzi, Production of alcohol-free beer, Beer Heal. Dis. Prev. (2008) 61–75.
[127] T. Brányik, D.P. Silva, M. Baszczyňski, R. Lehnert, J.B. Almeida E Silva, A review of methods of low alcohol and alcohol-free beer production, J. Food Eng. 108 (2012) 493–506.
[128] C.M. Galanakis, Emerging technologies for the production of nutraceuticals from agricultural by-products: A viewpoint of opportunities and challenges, Food Bioprod. Process. 91 (2013) 575–579.
[129] C.M. Galanakis, Separation of functional macromolecules and micromolecules: From ultrafiltration to the border of nanofiltration, Trends Food Sci. Technol. 42 (2015) 44–63.
[130] A. Cassano, C. Conidi, R. Ruby-Figueroa, R. Castro-Muñoz, Nanofiltration and Tight Ultrafiltration Membranes for the Recovery of Polyphenols from Agro-Food By-Products, Int. J. Mol. Sci. 19 (2018).
[131] L. Colen, J. Swinnen, Economic Growth, Globalisation and Beer Consumption, J. Agric. Econ. 67 (2016) 186–207.
[132] S. Malfliet, K. Goiris, G. Aerts, L. de Cooman, Analytical-Sensory Determination of Potential Flavour Deficiencies of Light Beers, J. Inst. Brew. 115 (2009) 49–63.
[133] M.P. McCarthy, M.J. Best, R.A. Betts, Climate change in cities due to global warming and urban effects, Geophys. Res. Lett. 37 (2010) L09705.
[134] B.B. Hansen, V. Grøtan, I. Herfindal, A.M. Lee, The Moran effect revisited: spatial population synchrony under global warming, Ecography (Cop.). 43 (2020) 1591–1602.

[135] N.H. Mermelstein (2000, 1 de noviembre). Removing Alcohol from Wine, Food Technology Magazine 54. Recuperado de: https://www.ift.org/news-and-publications/food-technology-magazine/issues/2000/november/columns/processing
[136] F. Zamora, Las manoproteínas; origen e interés enológico, Enólogos. 39 (2005) 28–31.
[137] J. Drappier, C. Thibon, A. Rabot, L. Geny-Denis, Relationship between wine composition and temperature: Impact on Bordeaux wine typicity in the context of global warming—Review, Crit. Rev. Food Sci. Nutr. 59 (2019) 14–30.
[138] OIV, International Organisation of Vine and wine (OIV). OIV Rules and implications concerning reduction of alcohol levels. Alcohol level reduction in Wine. Oenoviti International Network. 1st International Symposium. ISVV, Villenave d'Ornon, France., (2013).
[139] P. Godden, E. Wilkes, D. Johnson, Trends in the composition of Australian wine 1984-2014, Aust. J. Grape Wine Res. 21 (2015) 741–753.
[140] J. Wang, X. Zhang, L. Su, H. Li, L. Zhang, J. Wei, Global warming effects on climate zones for wine grape in Ningxia region, China, Theor. Appl. Climatol. 140 (2020) 1527–1536.
[141] M.C. Goldner, M.C. Zamora, P. Di Leo Lira, H. Gianninoto, A. Bandoni, Effect of ethanol level in the perception of aroma attributes and the detection of volatile compounds in red wine, J. Sens. Stud. 24 (2009) 243–257.
[142] M. Rosell, U. de Faire, M.L. Hellénius, Low prevalence of the metabolic syndrome in wine drinkers - Is it the alcohol beverage or the lifestyle?, Eur. J. Clin. Nutr. 57 (2003) 227–234.
[143] S. Dequin, J.-L. Escudier, M. Bely, J. Noble, W. Albertin, I. Masneuf-Pomarède, P. Marullo, J.-M. Salmon, J.M. Sablayrolles, How to adapt winemaking practices to modified grape composition under climate change conditions, OENO One. 51 (2017) 205–214.
[144] M.A. Olego, F. Visconti, M.J. Quiroga, J.M. de Paz, E. Garzón-Jimeno, Assessing the effects of soil liming with dolomitic limestone and sugar foam on soil acidity, leaf nutrient contents, grape yield and must quality in a mediterranean vineyard, Spanish J. Agric. Res. 14 (2016) 1102.
[145] M. Catarino, A. Mendes, L.M. Madeira, A. Ferreira, Alcohol removal from beer by reverse osmosis, in: Sep. Sci. Technol., 2007: pp. 3011–3027.
[146] O. Corona, L. Liguori, D. Albanese, M. Di Matteo, L. Cinquanta, P. Russo, Quality and volatile compounds in red wine at different degrees of dealcoholization by membrane process, Eur. Food Res. Technol. 245 (2019) 2601–2611.
[147] R. Prasad, K.K. Sirkar, Dispersion-free solvent extraction with microporous hollow-fiber modules, AIChE J. 34 (1988) 177–188.
[148] K.H. Keller, T.R. Stein, A two-dimensional analysis of porous membrane transport, Math. Biosci. 1 (1967) 421–437.
[149] L. Liguori, P. Russo, D. Albanese, M. Di Matteo, Effect of Process Parameters on Partial Dealcoholization of Wine by Osmotic Distillation, Food Bioprocess Technol. 6 (2013) 2514–2524.
[150] C. Ortega, R. Lopez, J. Cacho, V. Ferreira, Fast analysis of important wine volatile compounds Development and validation of a new method based on gas chromatographic-flame ionisation detection analysis of dichloromethane

microextracts, J. Chromatogr. A. (2001) 205–214.
[151] L. Liguori, D. Albanese, A. Crescitelli, M. Di Matteo, P. Russo, Impact of dealcoholization on quality properties in white wine at various alcohol content levels, J. Food Sci. Technol. 56 (2019) 3707–3720.
[152] S. Bocquet, F. Gascons Viladomat, C. Muvdi Nova, J. Sanchez, V. Athes, I. Souchon, Membrane-based solvent extraction of aroma compounds: Choice of configurations of hollow fiber modules based on experiments and simulation, J. Memb. Sci. 281 (2006) 358–368.
[153] S. Shen, S.E. Kentish, G.W. Stevens, Shell-side mass-transfer performance in hollow-fiber membrane contactors, Solvent Extr. Ion Exch. 28 (2010) 817–844.
[154] R.H. Perry (2001), Perry's Chemical Engineers' Handbook. 7th ed., New York: McGraw Hill.
[155] A. Baudot, J. Floury, H.E. Smorenburg, Liquid-liquid extraction of aroma compounds with hollow fiber contactor, AIChE J. 47 (2001) 1780–1793.
[156] C.M. Hansen, Polymer additives and solubility parameters, Prog. Org. Coatings. 51 (2004) 109–112.
[157] S. Varavuth, R. Jiraratananon, S. Atchariyawut, Experimental study on dealcoholization of wine by osmotic distillation process, Sep. Purif. Technol. 66 (2009) 313–321.
[158] P. Czekaj, F. López, C. Güell, Membrane fouling by turbidity constituents of beer and wine: characterization and prevention by means of infrasonic pulsing, J. Food Eng. 49 (2001) 25–36.
[159] J.-C. Ruf (2010), The implementation of the OIV standards at the international level and in the framework of innovation in the wine sector. Organisation Internationale de la Vigne et du Vin.
[160] D. Thompson (2016), Lower Alcohol Wines a Multi-market Perspective. Wine Intelligence Report Brochure.
[161] R. Golan, Y. Gepner, I. Shai, Wine and Health–New Evidence, Eur. J. Clin. Nutr. 72 (2019) 55–59.
[162] M. Mehta, S. Satsangi, A. Duseja, S. Taneja, R.K. Dhiman, Y. Chawla, Can Alcoholic Liver Disease and Nonalcoholic Fatty Liver Disease Co-Exist?, J. Clin. Exp. Hepatol. 7 (2017) 121–126.
[163] I. Baik, C. Shin, Prospective study of alcohol consumption and metabolic syndrome, Am. J. Clin. Nutr. 87 (2008) 1455–1463.
[164] C.C. Chen, W.Y. Lin, C.I. Li, C.S. Liu, T.C. Li, Y.T. Chen, C.W. Yang, M.P. Chang, C.C. Lin, The association of alcohol consumption with metabolic syndrome and its individual components: The Taichung community health study, Nutr. Res. 32 (2012) 24–29.
[165] A.J. Saliba, L.A. Ovington, C.C. Moran, Consumer demand for low-alcohol wine in an Australian sample, Int. J. Wine Res. 5 (2013) 1–8.
[166] C. Puglisi, R. Ristic, J. Saint, K. Wilkinson, Evaluation of Spinning Cone Column Distillation as a Strategy for Remediation of Smoke Taint in Juice and Wine, Molecules. 27 (2022) 8096.
[167] M. Gil, S. Estévez, N. Kontoudakis, F. Fort, J.M. Canals, F. Zamora, Influence of partial dealcoholization by reverse osmosis on red wine composition and sensory characteristics, Eur. Food Res. Technol. 237 (2013) 481–488.
[168] A. Gambuti, A. Rinaldi, M.T. Lisanti, R. Pessina, L. Moio, Partial dealcoholisation of

red wines by membrane contactor technique: Influence on colour, phenolic compounds and saliva precipitation index, Eur. Food Res. Technol. 233 (2011) 647–655.
[169] D. Mangindaan, K. Khoiruddin, I.G. Wenten, Beverage dealcoholization processes: Past, present, and future, Trends Food Sci. Technol. 71 (2018) 36–45.
[170] J. Esteras-Saz, Ó. de la Iglesia, C. Peña, A. Escudero, C. Téllez, J. Coronas, Theoretical and practical approach to the dealcoholization of water-ethanol mixtures and red wine by osmotic distillation, Sep. Purif. Technol. 270 (2021) 118793.
[171] L. Liguori, G. De Francesco, P. Russo, G. Perretti, D. Albanese, M. Di Matteo, Production and characterization of alcohol-free beer by membrane process, Food Bioprod. Process. 94 (2015) 158–168.
[172] L. Liguori, G. De Francesco, P. Russo, D. Albanese, G. Perretti, M. Di Matteo, Quality improvement of low alcohol craft beer produced by evaporative pertraction, Chem. Eng. Trans. 43 (2015) 13–18.
[173] P. Russo, L. Liguori, D. Albanese, A. Crescitelli, M. Di Matteo, Investigation of osmotic distillation technique for beer dealcoholization, Chem. Eng. Trans. 32 (2013) 1735–1740.
[174] R. Thanedgunbaworn, R. Jiraratananon, M.H. Nguyen, Vapour Transport Mechanism in Osmotic Distillation Process, Int. J. Food Eng. 5 (2009).
[175] M. Gryta, Influence of polypropylene membrane surface porosity on the performance of membrane distillation process, J. Memb. Sci. 287 (2007) 67–78.
[176] Y. Lu, S. Sathasivam, J. Song, C.R. Crick, C.J. Carmalt, I.P. Parkin, Robust self-cleaning surfaces that function when exposed to either air or oil, Science (80-.). 347 (2015) 1132–1135.
[177] M. Rezaei, D.M. Warsinger, J.H. Lienhard V, M.C. Duke, T. Matsuura, W.M. Samhaber, Wetting phenomena in membrane distillation: Mechanisms, reversal, and prevention, Water Res. 139 (2018) 329–352.
[178] K. Boussu, B. Van der Bruggen, A. Volodin, J. Snauwaert, C. Van Haesendonck, C. Vandecasteele, Roughness and hydrophobicity studies of nanofiltration membranes using different modes of AFM, J. Colloid Interface Sci. 286 (2005) 632–638.
[179] P. Bulejko, An analysis on energy demands in airborne particulate matter filtration using hollow-fiber membranes, Energy Reports. 7 (2021) 2727–2736.
[180] M. Breniaux, L. Zeng, F. Bayrounat, R. Ghidossi, Gas transfer management by membrane contactors in an oenological context: Influence of operating parameters and membrane materials, Sep. Purif. Technol. 227 (2019) 115733.
[181] T. Brozova, M. Raudensky, Determination of surface wettability of polymeric hollow fibres, J. Elastomers Plast. 50 (2018) 737–746.
[182] H.W. Pilone, B. F. & Berg, Some factors affecting tartrate stability in wine., Am. J. EnoL Vitic. 16 (1965) 195–211.
[183] X. Tian, L. Cheng, Y. Yan, H. Liu, W. Zhao, Q. Guo, An improved solution to estimate relative permeability in tight oil reservoirs, J. Pet. Explor. Prod. Technol. 5 (2015) 305–314.
[184] R. Thanedgunbaworn, R. Jiraratananon, M.H. Nguyen, Mass and heat transfer analysis in fructose concentration by osmotic distillation process using hollow fibre module, J. Food Eng. 78 (2007) 126–135.

[185] P. Xu, T.W. Coyle, L. Pershin, J. Mostaghimi, From lotus effect to petal effect: Tuning the water adhesion of non-wetting rare earth oxide coatings, J. Eur. Ceram. Soc. 40 (2020) 1692–1702.
[186] Z. Zhang, X. Wu, L. Wang, B. Zhao, J. Li, H. Zhang, Wetting mechanism of a PVDF hollow fiber membrane in immersed membrane contactors for CO 2 capture in the presence of monoethanolamine, RSC Adv. 7 (2017) 13451–13457.
[187] M. Ma, Y. Mao, M. Gupta, K.K. Gleason, G.C. Rutledge, Superhydrophobic Fabrics Produced by Electrospinning and Chemical Vapor Deposition, Macromolecules. 38 (2005) 9742–9748.
[188] Z.-Q. Dong, X. Ma, Z.-L. Xu, W.-T. You, F. Li, Superhydrophobic PVDF–PTFE electrospun nanofibrous membranes for desalination by vacuum membrane distillation, Desalination. 347 (2014) 175–183.
[189] D. Song, B. Song, H. Hu, X. Du, P. Du, C.-H. Choi, J.P. Rothstein, Effect of a surface tension gradient on the slip flow along a superhydrophobic air-water interface, Phys. Rev. Fluids. 3 (2018) 033303.
[190] Jun Ying Tan, Wei Lun Ang, Abdul Wahab Mohammad, Hydrophobic polyvinylidene fluoride membrane modified with silica nanoparticles and silane for succinic acid purification using osmotic distillation process, J. Kejuteraan. 33 (2021) 89–101.
[191] R. Sander, Compilation of Henry's law constants (version 4.0) for water as solvent, Atmos. Chem. Phys. 15 (2015) 4399–4981.
[192] B. Pineau, J.C. Barbe, C. Van Leeuwen, D. Dubourdieu, Which impact for beta-damascenone on red wines aroma?, J. Agric. Food Chem. 55 (2007) 4103–4108.
[193] L.M. Schmidtke, J.W. Blackman, S.O. Agboola, Production Technologies for Reduced Alcoholic Wines, J. Food Sci. 77 (2012) R25–R41.
[194] G. De Francesco, O. Marconi, V. Sileoni, G. Freeman, E.G. Lee, S. Floridi, G. Perretti, Influence of the dealcoholisation by osmotic distillation on the sensory properties of different beer types, J. Food Sci. Technol. 58 (2021) 1488–1498.
[195] A. Cassano, C. Conidi, E. Drioli, A Comprehensive Review of Membrane Distillation and Osmotic Distillation in Agro-Food Applications, J. Membr. Sci. Res. 6 (2020) 304–318.
[196] P. Garcìla-Herreros, J.M. Goìmez, I.D. Gil, G. Rodriìguez, Optimization of the design and operation of an extractive distillation system for the production of fuel grade ethanol using glycerol as entrainer, Ind. Eng. Chem. Res. 50 (2011) 3977–3985.
[197] S. Karimi, R.R. Karri, M. Tavakkoli Yaraki, J.R. Koduru, Processes and separation technologies for the production of fuel-grade bioethanol: a review, Environ. Chem. Lett. 19 (2021) 2873–2890.
[198] M. Balat, Potential alternatives to edible oils for biodiesel production – A review of current work, Energy Convers. Manag. 52 (2011) 1479–1492.
[199] B.D. Solomon, J.R. Barnes, K.E. Halvorsen, Grain and cellulosic ethanol: History, economics, and energy policy, Biomass and Bioenergy. 31 (2007) 416–425.
[200] M.N. Salimi, S.E. Lim, A.H.M. Yusoff, M.F. Jamlos, Conversion of rice husk into fermentable sugar by two stage hydrolysis, J. Phys. Conf. Ser. 908 (2017) 012056.
[201] M. Irfan, M. Nadeem, Q. Syed, Ethanol production from agricultural wastes using Sacchromyces cervisae, 45 (2014) 457–465.
[202] S.B. Jamaldheen, P.B. Saynik, V.S. Moholkar, A. Goyal, Fermentation and pyrolysis

of Finger millet straw: Significance of hydrolysate composition for ethanol production and characterization of bio-oil, Bioresour. Technol. Reports. 13 (2021) 100630.
[203] K.M. Harinikumar, R.L. Kudahettige-Nilsson, A. Devadas, M. Holmgren, A. Sellstedt, Bioethanol production from four abundant Indian agricultural wastes, Biofuels. 11 (2020) 607–613.
[204] Y. Ai, S. Feng, Y. Wang, J. Lu, M. Sun, H. Hu, Z. Hu, R. Zhang, P. Liu, H. Peng, Y. Wang, L. Cao, T. Xia, L. Peng, Integrated genetic and chemical modification with rice straw for maximum bioethanol production, Ind. Crops Prod. 173 (2021) 114133.
[205] Ó.J. Sánchez, C.A. Cardona, Trends in biotechnological production of fuel ethanol from different feedstocks, Bioresour. Technol. 99 (2008) 5270–5295.
[206] R.J. Bothast, M.A. Schlicher, Biotechnological processes for conversion of corn into ethanol, Appl. Microbiol. Biotechnol. 67 (2005) 19–25.
[207] G. Fischer, S. Prieler, H. van Velthuizen, G. Berndes, A. Faaij, M. Londo, M. de Wit, Biofuel production potentials in Europe: Sustainable use of cultivated land and pastures, Part II: Land use scenarios, Biomass and Bioenergy. 34 (2010) 173–187.
[208] E.B. Belal, Bioethanol production from rice straw residues, Braz J Microbiol. 44 (2013) 225–234.
[209] S. Banerjee, R. Sen, R.A. Pandey, T. Chakrabarti, D. Satpute, B.S. Giri, S. Mudliar, Evaluation of wet air oxidation as a pretreatment strategy for bioethanol production from rice husk and process optimization, Biomass and Bioenergy. 33 (2009) 1680–1686.
[210] J.C. Solarte-Toro, J.M. Romero-García, J.C. Martínez-Patiño, E. Ruiz-Ramos, E. Castro-Galiano, C.A. Cardona-Alzate, Acid pretreatment of lignocellulosic biomass for energy vectors production: A review focused on operational conditions and techno-economic assessment for bioethanol production, Renew. Sustain. Energy Rev. 107 (2019) 587–601.
[211] C.A. Cardona Alzate, O.J. Sánchez Toro, Energy consumption analysis of integrated flowsheets for production of fuel ethanol from lignocellulosic biomass, Energy. 31 (2006) 2447–2459.
[212] V. Van Hoof, L. Van den Abeele, A. Buekenhoudt, C. Dotremont, R. Leysen, Economic comparison between azeotropic distillation and different hybrid systems combining distillation with pervaporation for the dehydration of isopropanol, Sep. Purif. Technol. 37 (2004) 33–49.
[213] P.D. Chapman, T. Oliveira, A.G. Livingston, K. Li, Membranes for the dehydration of solvents by pervaporation, J. Memb. Sci. 318 (2008) 5–37.
[214] C.L. Hsueh, J.F. Kuo, Y.H. Huang, C.C. Wang, C.Y. Chen, Separation of ethanol-water solution by poly(acrylonitrile-co-acrylic acid) membranes, Sep. Purif. Technol. 41 (2005) 39–47.
[215] S.H. Chen, R.M. Liou, C.S. Hsu, D.J. Chang, K.C. Yu, C.Y. Chang, Pervaporation separation water/ethanol mixture through lithiated polysulfone membrane, J. Memb. Sci. 193 (2001) 59–67.
[216] J. Coronas, J. Santamaría, Separations Using Zeolite Membranes, Sep. Purif. Rev. 28 (1999) 127–177.
[217] T.C. Bowen, R.D. Noble, J.L. Falconer, Fundamentals and applications of pervaporation through zeolite membranes, J. Memb. Sci. 245 (2004) 1–33.

[218] A.J. Toth, A. Andre, E. Haaz, P. Mizsey, New horizon for the membrane separation: Combination of organophilic and hydrophilic pervaporations, Sep. Purif. Technol. 156 (2015) 432–443.
[219] A. Andre, T. Nagy, A.J. Toth, E. Haaz, D. Fozer, J.A. Tarjani, P. Mizsey, Distillation contra pervaporation: Comprehensive investigation of isobutanol-water separation, J. Clean. Prod. 187 (2018) 804–818.
[220] F.U. Nigiz, N. Durmaz Hilmioglu, Anhydrous fuel ethanol production by a combined hydrophobic–hydrophilic pervaporation system, Energy Sources, Part A Recover. Util. Environ. Eff. 38 (2016) 3348–3353.
[221] M. Omidali, A. Raisi, A. Aroujalian, Separation and purification of isobutanol from dilute aqueous solutions by a hybrid hydrophobic/hydrophilic pervaporation process, Chem. Eng. Process. Process Intensif. 77 (2014) 22–29.
[222] Y. Morigami, M. Kondo, J. Abe, H. Kita, K. Okamoto, The first large-scale pervaporation plant using tubular-type module with zeolite NaA membrane, Sep. Purif. Technol. 1–3 (2001) 251–260.
[223] L. Qiu, I. Kumakiri, K. Tanaka, X. Chen, H. Kita, Effect of seed crystal size on the properties of silicalite-1 membranes synthesized in a fluoride containing medium, J. Chem. Eng. Japan. 50 (2017) 345–350.
[224] M.H. Zhu, S.L. Xia, X.M. Hua, Z.J. Feng, N. Hu, F. Zhang, I. Kumakiri, Z.H. Lu, X.S. Chen, H. Kita, Rapid preparation of acid-stable and high dehydration performance mordenite membranes, Ind. Eng. Chem. Res. 53 (2014) 19168–19174.
[225] I. Kumakiri, K. Hashimoto, Y. Nakagawa, Y. Inoue, Y. Kanehiro, K. Tanaka, H. Kita, Application of FAU zeolite membranes to alcohol/acrylate mixture systems, Catal. Today. 236 (2014) 86–91.
[226] J.J. Rodríguez-Bencomo, C. Muñoz-González, I. Andújar-Ortiz, P.J. Martín-Álvarez, M.V. Moreno-Arribas, M.Á. Pozo-Bayón, Assessment of the effect of the non-volatile wine matrix on the volatility of typical wine aroma compounds by headspace solid phase microextraction/gas chromatography analysis, J. Sci. Food Agric. 91 (2011) 2484–2494.
[227] P. Peng, Y. Lan, L. Liang, K. Jia, Membranes for bioethanol production by pervaporation, Biotechnol. Biofuels. 14 (2021) 1–33.
[228] M.H. Zhu, Z.J. Feng, X.M. Hua, H. long Hu, S.L. Xia, N. Hu, Z. Yang, I. Kumakiri, X.S. Chen, H. Kita, Application of a mordenite membrane to the esterification of acetic acid and alcohol using sulfuric acid catalyst, Microporous Mesoporous Mater. 233 (2016) 171–176.
[229] K.I. Okamoto, H. Kita, K. Horii, K. Tanaka, M. Kondo, Zeolite NaA Membrane: Preparation, Single-Gas Permeation, and Pervaporation and Vapor Permeation of Water/Organic Liquid Mixtures, Ind. Eng. Chem. Res. 40 (2000) 163–175.
[230] R.W. Baker, J.G. Wijmans, Y. Huang, Permeability, permeance and selectivity: A preferred way of reporting pervaporation performance data, J. Memb. Sci. 348 (2010) 346–352.
[231] C. Abels, F. Carstensen, M. Wessling, Membrane processes in biorefinery applications, J. Memb. Sci. 444 (2013) 285–317.
[232] R.D. Offeman, C.N. Ludvik, Poisoning of mixed matrix membranes by fermentation components in pervaporation of ethanol, J. Memb. Sci. 367 (2011) 288–295.
[233] Ó. de la Iglesia, R. Mallada, M. Menéndez, J. Coronas, Continuous zeolite

membrane reactor for esterification of ethanol and acetic acid, Chem. Eng. J. 131 (2007) 35–39.
[234] V. Poznyak, D. Rekve (Eds.) (2018), Global status report on alcohol and health 2018. Geneva: World Health Organization (OMS).
[235] I. Nascimento, L. Calado, M.E. Duncan, B. Trindade, L. Sphaier, V. Silva, F. Peixoto, Interference in beer bitterness measurements caused by polymer tubes, J. Food Eng. 275 (2020) 109879.
[236] S.S. Nielsen, Total Carbohydrate by Phenol-Sulfuric Acid Method, Food Anal. Lab. Man. (2017) 137–141.
[237] P.A.R. Tafulo, R.B. Queirós, C.M. Delerue-Matos, M.G.F. Sales, Control and comparison of the antioxidant capacity of beers, Food Res. Int. 43 (2010) 1702–1709.
[238] G. De Francesco, G. Freeman, E. Lee, O. Marconi, G. Perretti, Effects of operating conditions during low-alcohol beer production by osmotic distillation, J. Agric. Food Chem. 62 (2014) 3279–3286.
[239] L. Liguori, G. De Francesco, P. Russo, G. Perretti, D. Albanese, M. Di Matteo, Quality Attributes of Low-Alcohol Top-Fermented Beers Produced by Membrane Contactor, Food Bioprocess Technol. 9 (2016) 191–200.
[240] R.S. Jackson, Postfermentation Treatments and Related Topics, in: Wine Sci., Elsevier, 2008: pp. 418–519.
[241] J.L. Fernandez, W.J. Simpson, Measurement and prediction of the susceptibility of lager beer to spoilage by lactic acid bacteria, J. Appl. Bacteriol. 78 (1995) 419–425.
[242] g Li, F. Liu, Changes in Organic Acids during Beer Fermentation, J. Am. Soc. Brew. Chem. 73 (2015) 275–279.
[243] R. Petrucci, P. Di Matteo, A.P. Sobolev, L. Liguori, D. Albanese, N. Proietti, M. Bortolami, P. Russo, Impact of Dealcoholization by Osmotic Distillation on Metabolic Profile, Phenolic Content, and Antioxidant Capacity of Low Alcoholic Craft Beers with Different Malt Compositions, J. Agric. Food Chem. 69 (2021) 4816–4826.
[244] M. Bartoszek, J. Polak, An electron paramagnetic resonance study of antioxidant properties of alcoholic beverages, Food Chem. 132 (2012) 2089–2093.
[245] H. Zhao, W. Chen, J. Lu, M. Zhao, Phenolic profiles and antioxidant activities of commercial beers, Food Chem. 119 (2010) 1150–1158.
[246] D. Ceccaroni, V. Sileoni, O. Marconi, G. De Francesco, E.G. Lee, G. Perretti, Specialty rice malt optimization and improvement of rice malt beer aspect and aroma, LWT. 99 (2019) 299–305.
[247] B. Vanderhaegen, H. Neven, H. Verachtert, G. Desdelinckx, The chemistry of beer aging – a critical review, Food Chem. 95 (2006) 357–381.
[248] M. Jurková, P. Čejka, K. Štěrba, J. Olšovská, Determination of Total Carbohydrate Content in Beer Using Its Pre-column Enzymatic Cleavage and HPLC-RI, Food Anal. Methods. 7 (2014) 1677–1686.
[249] L.C. Nogueira, F. Silva, I.M.P.L.V.O. Ferreira, L.C. Trugo, Separation and quantification of beer carbohydrates by high-performance liquid chromatography with evaporative light scattering detection, J. Chromatogr. A. 1065 (2005) 207–210.
[250] M. Li, J. Du, K. Zhang, Profiling of carbohydrates in commercial beers and their

influence on beer quality, J. Sci. Food Agric. 100 (2020) 3062–3070.
[251] A. Hollnagel, L.W. Kroh, 3-Deoxypentosulose: An α-Dicarbonyl Compound Predominating in Nonenzymatic Browning of Oligosaccharides in Aqueous Solution, J. Agric. Food Chem. 50 (2002) 1659–1664.
[252] D. De Keukeleire, Fundamentals of beer and hop chemistry, Quim. Nova. 23 (2000) 108–112.
[253] D. De Keukeleire, J. Vindevogel, R. Szücs, P. Sandra, The history and analytical chemistry of beer bitter acids, Trends Anal. Chem. 11 (1992) 275–280.
[254] C.A. Blanco, A. Rojas, D. Nimubona, Effects of acidity and molecular size on bacteriostatic properties of beer hop derivates, Trends Food Sci. Technol. 18 (2007) 144–149.
[255] L.A. Hazelwood, M.C. Walsh, J.T. Pronk, J.-M. Daran, Involvement of Vacuolar Sequestration and Active Transport in Tolerance of Saccharomyces cerevisiae to Hop Iso-α-Acids, Appl. Environ. Microbiol. 76 (2010) 318–328.
[256] M. Ponticelli, D. Russo, I. Faraone, C. Sinisgalli, F. Labanca, L. Lela, L. Milella, The Promising Ability of Humulus lupulus L. Iso-α-acids vs. Diabetes, Inflammation, and Metabolic Syndrome: A Systematic Review, Molecules. 26 (2021) 954.
[257] J.-L. Zhao, Y.-J. Chen, J. Yu, Z.-Y. Du, Q. Yuan, Y.-R. Sun, X. Wu, Z.-Q. Li, X.-H. Wu, J. Hu, R. Xie, ISO-alpha-acids improve the hematoma resolution and prevent peri-hematoma inflammations by transforming microglia via PPARgamma-CD36 axis in ICH rats, Int. Immunopharmacol. 83 (2020) 106396.
[258] G. Haseleu, D. Intelmann, T. Hofmann, Structure determination and sensory evaluation of novel bitter compounds formed from β-acids of hop (Humulus lupulus L.) upon wort boiling, Food Chem. 116 (2009) 71–81.
[259] A.J. Laurent, N. Bindslev, V. Vukojević, L. Terenius, Iso-α-acids in Nonalcoholic and Alcoholic Beer Stimulate Growth of Neuron-like SH-SY5Y Cells and Neuroepithelial Stem Cells, ACS Bio Med Chem Au. 1 (2021) 11–20.
[260] E. Langner, W. Rzeski, Biological Properties of Melanoidins: A Review, Int. J. Food Prop. 17 (2014) 344–353.
[261] A. Martinez-Gomez, I. Caballero, C.A. Blanco, Phenols and Melanoidins as Natural Antioxidants in Beer. Structure, Reactivity and Antioxidant Activity, Biomolecules. 10 (2020) 400.
[262] C. Nagai, K. Noda, A. Kirihara, Y. Tomita, M. Murata, A Low-Molecular Weight Maillard Pigment from Beer was Identified as Perlolyrine, a Maillard Reaction Product from Tryptophan, Food Sci. Technol. Res. 25 (2019) 81–88.
[263] Y. Wang, L. Ye, Haze in Beer: Its Formation and Alleviating Strategies, from a Protein–Polyphenol Complex Angle, Foods. 10 (2021) 3114.
[264] K.J. Siebert, Effects of Protein−Polyphenol Interactions on Beverage Haze, Stabilization, and Analysis, J. Agric. Food Chem. 47 (1999) 353–362.
[265] M. Simon, S. Collin, Why Oxidation Should Be Still More Feared in NABLABs: Fate of Polyphenols and Bitter Compounds, Beverages. 8 (2022) 61.